2020

Magnetic ionic liquids in applications of nucleic acid analysis: Sequence-specific extraction of DNA and preservation solvents of RNA

Chenghui Zhu
Iowa State University

Magnetic ionic liquids in applications of nucleic acid analysis: Sequence-specific extraction of DNA and preservation solvents of RNA

by

Chenghui Zhu

A thesis submitted to the graduate faculty

in partial fulfillment of the requirements for the degree of

MASTER OF SCIENCE

Major: Analytical Chemistry

Program of Study Committee:
Jared L. Anderson, Major Professor
Robbyn K. Anand
Marit Nilsen-Hamilton

The student author, whose presentation of the scholarship herein was approved by the program of study committee, is solely responsible for the content of this thesis. The Graduate College will ensure this thesis is globally accessible and will not permit alterations after a degree is conferred.

Iowa State University

Ames, Iowa

2020

TABLE OF CONTENTS

Page

ACKNOWLEDGMENTS

I would like to thank my committee chair, Anderson Jared Lee, and my committee members, Anand Robbyn Kimberly and Nilsen-Hamilton Marit, for their guidance and support throughout the course of this research.

In addition, I would also like to thank my friends, colleagues, the department faculty and staff for making my time at Iowa State University a wonderful experience. I would like to thank my previous and current group members: He Nan, Kevin Clark, María José Trujillo-Rodríguez, Israel Donizéti de Souza, Idaira Pacheco-Fernández, Jakub Šulc, Ester Peris García, Jiwoo An, Stephen Pierson, Xiong Ding, Deepak Chand, Marcelino Verona, Miranda Emaus, Ashley Bowers, Qamar Farooq, Gabriel Odugbesi, Han Chen, Philip Eor, Nabeel Abbasi, Derek Eitzmann, Victoria Zeger, Shu-An Hsieh, and Donghyun Ryoo for their consistent help and suggestions, and making my time at Iowa State University a wonderful journey.

Last but not least, I would like to thank my parents for their love and support. I want to also offer my appreciation to those who were willing to participate in my surveys and observations, without whom, this thesis would not have been possible.

ABSTRACT

The selective extraction and accumulation of specific deoxyribonucleic acid (DNA) fragments is required for targeted nucleic acid analysis in order to minimize interferences from samples with abundant heterogeneous sequences. In addition, it is essential to isolate and preserve nucleic acid from biological sample containing numerous compounds such as endonucleases prior to sample analysis. Very recently, ionic liquid (IL) and magnetic ionic liquid (MIL) based materials have shown significant promise in the area of biological sample preparation and separation. In this thesis, various types of ILs and MILs are exhaustively descripted and utilized for two applications: 1) sequence-specific extraction of DNA and 2) RNA preservation.

Functionalized oligonucleotide probes named as ion-tagged oligonucleotides (ITOs) and disubstituted ion-tagged oligonucleotides (DTOs) that hybridize with complementary DNA targets can be subsequently captured by a hydrophobic MIL support. The ITO- and DTO-MIL system is investigated for sequence-specific extraction of DNA in a relatively low concentration within multiple sample matrices such as blood and plasma. This particle- and aggregation-free extraction method is highly potential and beneficial for analysis based on microfluidic devices.

In addition, RNA samples obtained from yeast cells can be extracted and preserved by several MILs simultaneously. RNA remains the high quantity and structural integrity within MILs at room temperature. Moreover, specific MILs can be used to reduce ribonuclease A (RNase A) degradation of RNA. This RNA preservation method reveals multiple advantages including energy-saving and equipment-independent which makes it applicable to in-field RNA sample preparation.

Keywords: magnetic ionic liquid, ion-tagged oligonucleotide, sequence-specific extraction, magnetic beads, high performance liquid chromatography, polymerase chain reaction, ribonuclease A, reverse transcription, agarose gel electrophoresis.

CHAPTER 1. GENERAL INTRODUCTION

1.1 A Brief Introduction of Ionic Liquids and Magnetic Ionic Liquids

Following the discovery of ionic liquids (ILs) over a century ago, IL-based materials have been shown to exhibit encouraging advance in chemical sciences including nucleic acid analysis.[1,2] ILs are organic molten salts that possess melting points at or below 100 °C. Due to their tunable cation and anion structures,[3,4] ILs possess a number of advantageous physicochemical properties including relatively low vapor pressure at ambient temperatures, high thermal stability, wide electrochemical window, and different solvation properties.[5] Conventional ILs such as 1-alkyl-3-methylimidazolium hexafluorophosphate ($[C_nMIM^+][PF_6^-]$) or the same cation paired with bis[(trifluoromethyl)sulfonyl]imide ($[NTf_2^-]$) anion are widely used as extraction solvents in various liquid phase microextraction.[6] Recently, ILs have been explored as solvents in nucleic acid applications based on their ability to interact with a variety of biomolecules.[7,8] For instance, Wang and coworkers took the advantage of the 1-butyl-3-methylimidazolium hexafluorophosphate ($[BMIM^+][PF_6^-]$) IL to extract deoxyribonucleic acid (DNA) from aqueous solution.[1] In a more recent study, Freire and co-workers developed a nucleic acid preservation method in which ribonucleic acid (RNA) was extracted and preserved by cholinium L-lysinate ([Ch][Lys]) IL.[10]

Magnetic ionic liquids (MILs) are a subclass of ILs that incorporate paramagnetic centers in their chemical structures. MILs also have been the subject of intensified interest in numerous analytical applications due to their similar physicochemical properties to conventional ILs as well as the strong response to external magnetic fields.[11,12] For instance, our group investigated the MIL applications in performing DNA extraction,[11] supporting polymerase chain reaction (PCR),[13] and preserving DNA from degradation.[14] The development of MILs for nucleic acid

analysis has aroused great research interest due to their properties outperforming conventional materials. Unlike ferrofluids that are prone to aggregation and sedimentation, MILs exist as neat magnetic solvents. MILs also exhibit low volatility and circumventing the need for stabilizing organic solvents that are often employed in ferrofluids to prevent particle agglomeration.[15] Some of the common chemical structures of ILs and MILs can be seen in Figure 1.1.

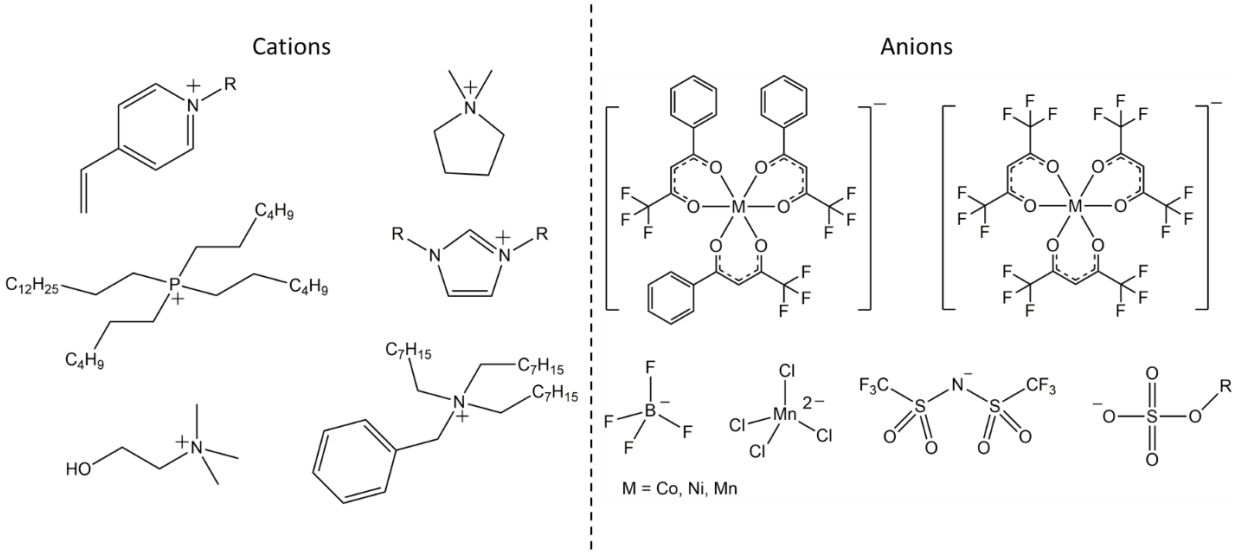

Figure 1.1 Common cations and anions used in ILs and MILs.

1.2 A Brief Introduction of Nucleic Acid Analysis

Nucleic acids are biopolymers that have fundamental implications on the biochemical processes of every living organism. DNA and RNA have the unique ability to pair with its complementary sequence by Watson–Crick hydrogen bonding, which can be widely exploited to construct DNA-material conjugates for chemical, biological, and medical applications. The applications of nucleic acid analysis have included DNA-based therapeutics,[16] identification of DNA biomarkers in blood,[17] and understanding gene-disease relationships.[18]

Although numbers of technologies have been developed for nucleic acid sequencing and analysis, the detection of specific DNA sequences remains a significant challenge due to the

interfering background signal in bioanalytical assays caused by untargeted sequences.[19,20] Moreover, nucleic acid in biological samples such as blood and plasma may contain numerous compounds including proteins and lipids. Biomolecular techniques such as quantitative polymerase chain reaction (qPCR), quantitative reverse transcription polymerase chain reaction (qRT-PCR), and Northern Blot analysis require sufficiently pure analytes to prevent the inefficiency of analysis.[21-24] In certain conditions, preservation steps before in-lab analysis are critical for nucleic acid collected in the field.[25] Conventional techniques such as lyophilization, formalin fixed paraffin-embedded tissues (FFPE), and diethylpyrocarbonate (DEPC) pretreatment suffer from drawbacks including the requirements of specialized equipment, multiple tedious steps, or a high amount of energy.[26-30]

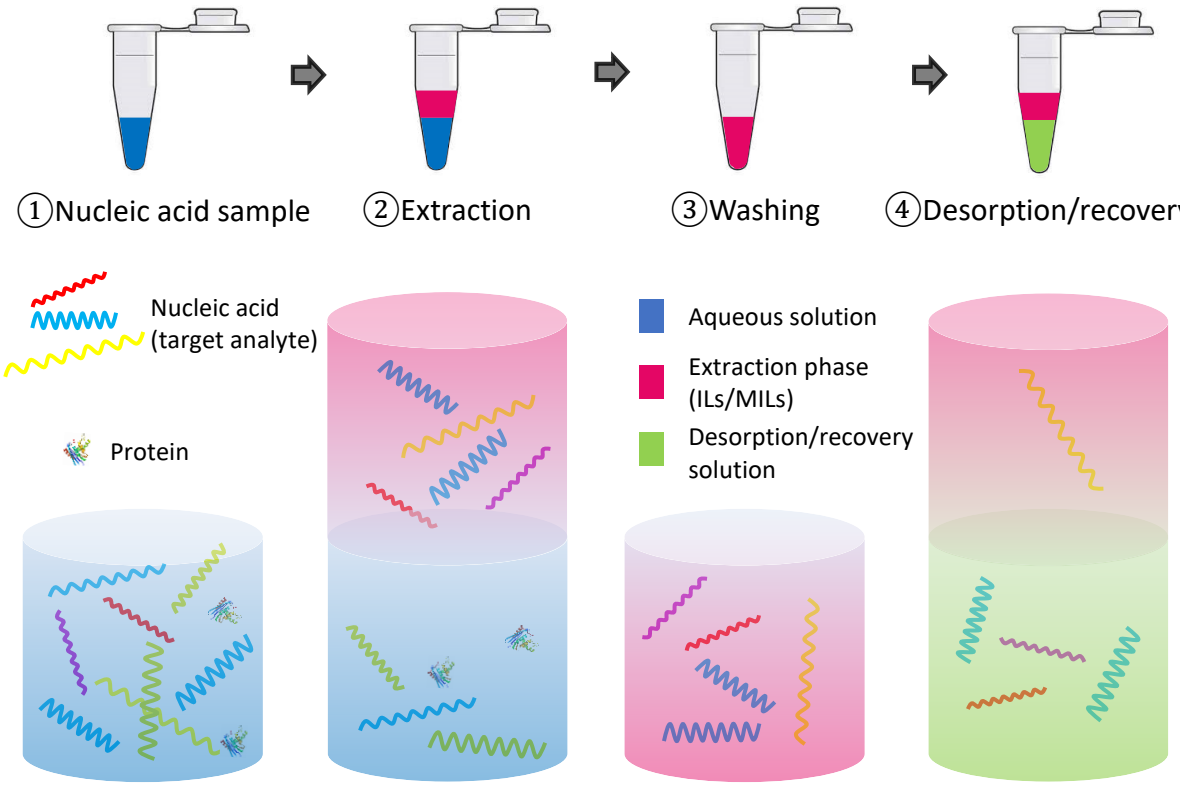

Figure 1.2 Schematic of a LLE procedure using ILs or MILs.

In order to ameliorate the conventional DNA or RNA analysis methods, several MILs and ILs have been studied in plenty of fields including genomic analysis, pharmaceutical industry, and microextraction. ILs and MILs can be highly beneficial for liquid-liquid extraction (LLE) with advantages such as high efficiency and simple operation. A general process of LLE can be seen in Figure 1.2.

1.3 Organization of the Thesis

The main goal of this thesis is to extend the use of novel ILs and MILs to nucleic acid sample preparation and extraction areas, and in combination with detection techniques including liquid chromatography, qPCR, and gel electrophoresis. According to this objective, the thesis has been divided into the following chapters:

Chapter 2 describes a sequence-specific DNA extraction method by incorporating ion-tagged oligonucleotide (ITO) or disubstituted ion-tagged oligonucleotide (DTO) probes with MIL supports. The ITO or DTO probes can be customized with different oligonucleotides to capture specific target sequences. This “particle-free” method reveals an effective extraction by taking the advantage of the high loading efficiency between probes and supports. A series of ITO and DTO probes was synthesized through thiol-ene “click” reactions and investigated for their target-capture capabilities. In addition, a commercial approach using biotinylated probes and magnetic beads was studied as a comparison.

Chapter 3 describes the ITO/DTO-MIL system with advanced ITO/DTO probes, MIL supports, and optimized extraction conditions. Various combinations between probes and supports were tested and compared. Furthermore, this sequence-specific DNA extraction method was applied to several complex sample matrices including diluted plasma and diluted blood. The femtomolar level of target DNA sequences was successfully isolated and preconcentrated from a biological sample containing high amounts of proteins and background DNA.

Chapter 4 describes a combined approach of extraction and preservation of RNA by MIL solvents. Yeast total RNA can be extracted and preserved by different MILs in a single-step procedure. RNA preserved by MILs remained the structural integrity after a 15 day storage period at room temperature. The ribonuclease A (RNase A) degradation of RNA can be significantly reduced within a few of MILs. Moreover, the partitioning of RNA and MILs was investigated to elucidate the preservation mechanism and the recovery efficiency.

Chapter 5 provides a summary of all research projects.

1.4 References

(1) Pedro, A. Q.; Pereira, P.; Quental, M. J.; Carvalho, A. P.; Santos, S. M.; Queiroz, J. A.; Sousa, F.; Freire, M. G. Cholinium-Based Good's Buffers Ionic Liquids as Remarkable Stabilizers and Recyclable Preservation Media for Recombinant Small RNAs. *ACS Sustain. Chem. Eng.* **2018**, *6* (12), 16645–16656.

(2) Mondal, D.; Sharma, M.; Mukesh, C.; Gupta, V.; Prasad, K. Improved Solubility of DNA in Recyclable and Reusable Bio-Based Deep Eutectic Solvents with Long-Term Structural and Chemical Stability. *Chem. Commun.* **2013**, *49* (83), 9606–9608.

(3) Brown, P.; Butts, C. P.; Eastoe, J.; Padrón Hernández, E.; Machado, F. L. D. A.; De Oliveira, R. J. Dication Magnetic Ionic Liquids with Tuneable Heteroanions. *Chem. Commun.* **2013**, *49* (27), 2765–2767.

(4) Santos, E.; Albo, J.; Irabien, A. Magnetic Ionic Liquids: Synthesis, Properties and Applications. *RSC Adv.* **2014**, *4* (75), 40008–40018.

(5) Hallett, J. P.; Welton, T. Room-Temperature Ionic Liquids: Solvents for Synthesis and Catalysis. 2. *Chem. Rev.* **2011**, *111* (5), 3508–3576.

(6) An, J.; Trujillo-Rodríguez, M. J.; Pino, V.; Anderson, J. L. Non-Conventional Solvents in Liquid Phase Microextraction and Aqueous Biphasic Systems. *J. Chromatogr. A* **2017**, *1500*, 1–23.

(7) Fujita, K.; MacFarlane, D. R.; Forsyth, M. Protein Solubilising and Stabilising Ionic Liquids. *Chem. Commun.* **2005**, *70* (38), 4804–4806.

(8) Chandran, A.; Ghoshdastidar, D.; Senapati, S. Groove Binding Mechanism of Ionic Liquids: A Key Factor in Long-Term Stability of DNA in Hydrated Ionic Liquids? *J. Am. Chem. Soc.* **2012**, *134* (50), 20330–20339.

(9) Wang, J. H.; Cheng, D. H.; Chen, X. W.; Du, Z.; Fang, Z. L. Direct Extraction of Double-Stranded DNA into Ionic Liquid 1-Butyl-3-Methylimidazolium Hexafluorophosphate and Its Quantification. *Anal. Chem.* **2007**, *79* (2), 620–625.

(10) Quental, M. V.; Pedro, A. Q.; Pereira, P.; Sharma, M.; Queiroz, J. A.; Coutinho, J. A. P.; Sousa, F.; Freire, M. G. Integrated Extraction-Preservation Strategies for RNA Using Biobased Ionic Liquids. *ACS Sustain. Chem. Eng.* **2019**, *7* (10), 9439–9448.

(11) Clark, K. D.; Nacham, O.; Yu, H.; Li, T.; Yamsek, M. M.; Ronning, D. R.; Anderson, J. L. Extraction of DNA by Magnetic Ionic Liquids: Tunable Solvents for Rapid and Selective DNA Analysis. *Anal. Chem.* **2015**, *87* (3), 1552–1559.

(12) Pierson, S. A.; Nacham, O.; Clark, K. D.; Nan, H.; Mudryk, Y.; Anderson, J. L. Synthesis and Characterization of Low Viscosity Hexafluoroacetylacetonate-Based Hydrophobic Magnetic Ionic Liquids. *New J. Chem.* **2017**, *41* (13), 5498–5505.

(13) Clark, K. D.; Yamsek, M. M.; Nacham, O.; Anderson, J. L. Magnetic Ionic Liquids as PCR-Compatible Solvents for DNA Extraction from Biological Samples. *Chem. Commun.* **2015**, *51* (94), 16771–16773.

(14) Clark, K. D.; Sorensen, M.; Nacham, O.; Anderson, J. L. Preservation of DNA in Nuclease-Rich Samples Using Magnetic Ionic Liquids. *RSC Adv.* **2016**, *6* (46), 39846–39851.

(15) Genc, S.; Derin, B. Synthesis and Rheology of Ferrofluids: A Review. *Curr. Opin. Chem. Eng.* **2014**, *3*, 118–124.

(16) Juliano, R. L.; Ming, X.; Nakagawa, O. The Chemistry and Biology of Oligonucleotide Conjugates. *Acc. Chem. Res.* **2012**, *45* (7), 1067–1076.

(17) Gormally, E.; Caboux, E.; Vineis, P.; Hainaut, P. Circulating Free DNA in Plasma or Serum as Biomarker of Carcinogenesis: Practical Aspects and Biological Significance. *Mutat. Res. - Rev. Mutat. Res.* **2007**, *635* (2–3), 105–117.

(18) Sophie, J.; Christophe, M.; Jean, T.; Gerard, L.; Helene, M.; Francoise, F.; Xavier, N.; Jerome, E.; Francois, V. Relationships between Staphylococcus Aureus Genetic Background, Virulence Factors, Agr Groups (Alleles), and Human Disease. *Infect. Immun.* **2002**, *70* (2), 631–641.

(19) Albert, T. J.; Molla, M. N.; Muzny, D. M.; Nazareth, L.; Wheeler, D.; Song, X.; Richmond, T. A.; Middle, C. M.; Rodesch, M. J.; Packard, C. J.; et al. Direct Selection of Human Genomic Loci by Microarray Hybridization. *Nat. Methods* **2007**, *4* (11), 903–905.

(20) Porreca, G. J.; Zhang, K.; Li, J. B.; Xie, B.; Austin, D.; Vassallo, S. L.; LeProust, E. M.; Peck, B. J.; Emig, C. J.; Dahl, F.; et al. Multiplex Amplification of Large Sets of Human Exons. *Nat. Methods* **2007**, *4* (11), 931–936.

(21) Condon, C. Maturation and Degradation of RNA in Bacteria. *Curr. Opin. Microbiol.* **2007**, *10* (3), 271–278.

(22) Zhiguo, W.; Baofeng, Y. *MicroRNA Expression Detection Methods*; **2010**; Vol. 91.

(23) Smith, M. T.; Wilding, K. M.; Hunt, J. M.; Bennett, A. M.; Bundy, B. C. The Emerging Age of Cell-Free Synthetic Biology. *FEBS Lett.* **2014**, *588* (17), 2755–2761.

(24) Hatzimanikatis, V.; Choe, L. H.; Lee, K. H. Proteomics: Theoretical and Experimental Considerations. *Biotechnol. Prog.* **1999**, *15* (3), 312–318.

(25) Murphy, M. A.; Waits, L. P.; Kendall, K. C.; Wasser, S. K.; Higbee, J. A.; Bogden, R. An Evaluation of Long-Term Preservation Methods for Brown Bear (Ursus Arctos) Faecal DNA Samples. *Conserv. Genet.* **2002**, *3* (4), 435–440.

(26) Naddeo, M.; Vitagliano, L.; Russo, A.; Gotte, G.; D'Alessio, G.; Sorrentino, S. Interactions of the Cytotoxic RNase A Dimers with the Cytosolic Ribonuclease Inhibitor. *FEBS Lett.* **2005**, *579* (12), 2663–2668.

(27) Farragher, S. M.; Tanney, A.; Kennedy, R. D.; Paul Harkin, D. RNA Expression Analysis from Formalin Fixed Paraffin Embedded Tissues. *Histochem. Cell Biol.* **2008**, *130* (3), 435–445.

(28) Koopmans, M.; Monroe, S. S.; Coffield, L. M.; Zaki, S. R. Optimization of Extraction and PCR Amplification of RNA Extracts from Paraffin-Embedded Tissue in Different Fixatives. *J. Virol. Methods* **1993**, *43* (2), 189–204.

(29) Wolf, B.; Lesnaw, J. A.; Reichmann, M. E. A Mechanism of the Irreversible Inactivation of Bovine Pancreatic Ribonuclease by Diethylpyrocarbonate: A General Reaction of Diethylpyrocarbonate with Proteins. *Eur. J. Biochem.* **1970**, *13* (3), 519–525.

(30) Fedorcsák, I.; Ehrenberg, L. Effects of Diethyl Pyrocarbonate and Methyl Methanesulfonate on Nucleic Acids and Nucleases. *Acta Chemica Scandinavica*. **1966**, pp 107–112.

CHAPTER 2. MAXIMIZING ION-TAGGED OLIGONUCLEOTIDE LOADING ON MAGNETIC IONIC LIQUID SUPPORTS FOR THE SEQUENCE-SPECIFIC EXTRACTION OF NUCLEIC ACIDS

Kevin D. Clark[†], Chenghui Zhu, and Jared L. Anderson

Department of Chemistry, Iowa State University, Ames, Iowa 50011, United States

[†] Beckman Institute of Advanced Science and Technology, University of Illinois at Urbana-Champaign, Urbana, Illinois 61801, United States

Modified from a manuscript published in *Anal. Chem.* **2019**, 91, 5945−5952

2.1 Abstract

Targeted nucleic acid analysis requires the highly selective extraction of desired DNA fragments in order to minimize interferences from samples with abundant heterogeneous sequences. We previously reported a method based on functionalized oligonucleotide probes known as ion-tagged oligonucleotides (ITOs) that hybridize with complementary DNA targets for subsequent capture using a hydrophobic magnetic ionic liquid (MIL) support. Although the ITO-MIL approach enriched specific DNA sequences in quantities comparable to a commercial magnetic bead-based method, the modest affinity of the ITO for the hydrophobic MIL limited the yield of DNA targets, particularly when stringent wash conditions were applied to remove untargeted DNA. Here, we report the synthesis and characterization of a series of ITOs in which functional groups were installed within the cation and anion components of the tag moiety in order to facilitate loading of the ITO to the MIL support phase. In addition to hydrophobic interactions, we demonstrate that π−π stacking and fluorophilic interactions can be exploited for loading oligonucleotide probes onto MILs. Using a disubstituted ion-tagged oligonucleotide (DTO) possessing two linear C_8 groups, nearly quantitative loading of the probe onto the MIL

support was achieved. The enhanced stability of the DTO within the MIL solvent permitted successive wash steps without the loss of the DNA target compared to a monosubstituted ITO with a single C_8 group that was susceptible to increased loss of analyte. Furthermore, the successful capture of a 120 bp KRAS fragment from human plasma samples followed by real-time quantitative polymerase chain reaction (qPCR) amplification is demonstrated.

2.2 Introduction

Despite the importance of DNA as a biological repository for genetic information, the vast majority of nucleic acid sequences are not targeted in molecular diagnostics applications. For example, mutant populations of cell-free DNA that indicate malignancy can be as low as 0.01% abundance of the wild-type sequence in human plasma.[1] Major advances in nucleic acid sequencing and detection technologies have provided a rapid means to routinely characterize thousands of samples per day, but the detection of specific DNA sequences such as single-nucleotide polymorphisms remains a significant challenge due to high levels of untargeted nucleic acids that increase the background signal in bioanalytical assays.[2,3] In order to overcome this bottleneck in nucleic acid analysis, sample preparation methods that capture and enrich specific DNA sequences must be developed.

The most popular approaches for the enrichment of specific nucleic acid sequences are based on magnetic beads or particles coated with streptavidin. Biotinylated oligonucleotide probes that exhibit a high affinity toward streptavidin can be designed to capture DNA targets via base-pairing interactions. After a washing step to remove interfering DNA molecules, the extracted nucleic acid targets can be released for downstream analysis. Successive washes may improve the purity of the nucleic acid recovered from the magnetic beads but often result in lower analyte yields.[4,5] Moreover, the tendency of interferences from the sample matrix to nonspecifically adsorb to the magnetic support material often requires an additional step

involving the use of bovine serum albumin (BSA) in the workflow to pacify or block the surface. Contemporary magnet-based DNA capture methods are also limited by aggregation of the solid bead/particle support material, resulting in lower capture efficiencies and the clogging of liquid handling devices.[6-9] Such particle aggregates are particularly unwanted if downstream bioanalysis is to be performed within a microfluidic device possessing narrow channels that can be easily obstructed.

An ideal magnetic support material for DNA extraction would possess the following features: 1) mitigate or eliminate aggregation behavior, 2) exhibit low nonspecific extraction of untargeted DNA and interferences (like proteins), and 3) possess high affinity toward decorated oligonucleotide probe molecules. In contrast to conventional magnetic supports, magnetic ionic liquids (MILs) are paramagnetic molten salts comprised of organic/inorganic cations and anions with melting points at or below 100 °C.[10,11] Physicochemical properties of MILs including viscosity, hydrophobicity, magnetic susceptibility, and solvation behavior can be readily tuned by judicious selection/functionalization of the cation and anion structures.[12-14] The liquid nature of MILs represents a key advantage over solid magnetic substrates that suffer from particle agglomeration, making these solvents ideal for biomolecule sample preparation applications that interface with downstream bioassays. MILs based on Fe(III),[15] Co(II),[16] and Ni(II) anion complexes were recently shown to provide high enrichment factors for a variety of DNA fragments and, in some cases, were directly coupled to polymerase chain reaction (PCR) and real-time quantitative PCR (qPCR) for rapid detection and quantification of extracted nucleic acids in the MIL phase.[17,18] The particle- and aggregation-free extraction of specific DNA sequences has also been demonstrated using a Mn(II)-based hydrophobic MIL as a paramagnetic liquid support material.[19] By appending amphiphilic alkylimidazolium groups to synthetic

oligonucleotides, the probe molecules partitioned to the MIL support via simple hydrophobic interaction and facilitated the capture of complementary DNA sequences via Watson−Crick base pairing. Moreover, the affinity of the ion-tagged oligonucleotide (ITO) probes for the hydrophobic MIL support was highly dependent on the chemical structure of the bioconjugate where longer alkyl groups (e.g., octyl) in the ITO resulted in enhanced partitioning to the MIL phase.

Although the previously described MIL-ITO approach provided similar sequence-specific DNA extraction yields to a commercial magnetic bead-based method,[19] the modest affinities (ca. 50% loading efficiency) of the ITO probe for the MIL support limited the technique in three important ways: 1) since fewer probe molecules partitioned to the MIL support, a lower capacity for target DNA was observed, 2) ITO probes with lower affinity for the MIL are more readily desorbed upon successive washing of the MIL phase to improve sample purity/selectivity for DNA targets, and 3) interferences in complex samples (e.g., cell lysate) resulted in decreased extraction yields by competing with the ITO probe for sorption to the MIL. Here, we report a series of ITOs with unique ion tag structures, elucidating the structural components of the tag moiety that result in improved affinities of the synthetic probe for the MIL support. In addition to modifying the ITO cation structure, fluorophilic anions (e.g., bis-[(trifluoromethyl)sulfonyl]imide [NTf_2^-]) and amphiphilic anions were paired with imidazolium cations for enhanced partitioning to the MIL support. We investigated a cyclic disulfide-modified oligonucleotide starting material for the preparation of disubstituted ion-tagged oligonucleotides (DTOs) that provided loading efficiencies greater than 95% onto the MIL support, furnishing an extraction phase capable of recovering a 10-fold greater quantity of target nucleic acid compared to monosubstituted ITOs. The stability of the ITO- and DTO-MIL

interactions was studied under stringent hybridization conditions, ultimately revealing that DTOs provided superior recoveries of target DNA sequences from samples containing interfering nucleotide sequences. As demonstrated herein, the structural tunability of both the cation and anion components of the ion tag greatly expands the modes of intermolecular interactions between ITO probes and MIL supports, facilitating high-efficiency DNA extraction and guiding the design of future ITOs.

2.3 Experimental Section

2.3.1 Reagents and Materials

Acetonitrile (99.9%), LC-MS grade acetonitrile (≥ 99.9%), hexane, mixture of isomers (≥ 98.5%), ethylenediaminetetraacetic acid (EDTA, 99.4% ~ 100.06%), triethylamine (TEA, ≥ 99.5%), magnesium chloride (99.0% ~ 102.0%), 1-bromooctane, ammonium persulfate (APS, ≥ 98%)), sodium octylsulfate (≥ 95%), and plasma from human were purchased from Sigma Aldrich (St. Louis, MO, USA). Ethyl ether (≥ 99%) was purchased from Avantor (Center Valley, PA, USA). Allylimidazole (99%) was purchased from Alfa Aesar (Ward Hill, MA, USA). 1,1,1,5,5,5-Hexafluoroacetylacetone (99%) and 4,4,4-trifluoro-1-phenyl-1,3-butanedione (99%) were purchased from ACROS organics (Morris, NJ, USA). Tris(hydroxymethyl)aminomethane (ultra pure), tris(hydroxymethyl)aminomethane hydrochloride (≥ 99.0%), urea (≥ 99%) and boric acid (≥ 99.5%) were purchased from RPI (Mount Prospect, IL, USA). Tris(2-carboxyethyl)phosphine (TCEP) was purchased from Soltec Ventures (Beverly, MA, USA). Sodium hydroxide, sodium chloride, M-270 Streptavidin coated Dynabeads, SYBR Green I nucleic acid gel stain, dimethylsulfoxide (DMSO), acetic acid, and ammonium hydroxide were purchased from Fisher Scientific (Fair Lawn, NJ, USA). Tetramethylethylenediamine (TEMED), 40% acrylamide and bis-acrylamide solution 29:1, and SsoAdvanced Universal SYBR Green Supermix and a KRAS, human PrimePCR™ SYBR green

assay including template and primers (120 bp amplicon) were purchased from Bio-Rad Laboratories (Hercules, CA, USA). Dithiolated, biotinylated, and unmodified oligonucleotides and primers were purchased from Integrated DNA Technologies (Coralville, IA, USA). The oligonucleotide probe sequence used for extraction of the KRAS target was 5'- TTG AAC TAG CAA TGC CTG TG -3'.

2.3.2 Synthesis of MILs

The trihexyl(tetradecyl)phosphonium manganese(II) hexafluoroacetylacetonate ($[P_{66614}^+][Mn(hfacac)_3^-]$) MIL and the trihexyl(tetradecyl)phosphonium manganese(II) 4,4,4-trifluoro-1-phenyl-1,3-butanedionate ($[P_{66614}^+][Mn(Phtfacac)_3^-]$) MILs were synthesized using a similar approach to previously reported procedures[20-22] and their chemical structures are shown in Figure A1a,b of Appendix A. Synthesis procedures the MILs used in this study are described in the Supporting Information. The products were characterized using ESI-TOFMS in both positive and negative ion modes (Figures A3-A6).

2.3.3 Synthesis and Characterization of ITOs and DTOs

Allylimidazolium salts were synthesized as previously reported.[19,23,24] The ITO and DTO structures investigated herein are shown in Table 2.1 and were synthesized according to published procedures.[19] Briefly, 4 nmol of a 20-mer thiolated oligonucleotide (for ITO synthesis) or 2 nmol of a 20-mer oligo with a terminal cyclic disulfide (for DTO synthesis) were reduced using 40 nmol of tris(2-carboxyethyl)phosphine (TCEP). The thiolated oligo was then transferred to a UV transparent 96-well microplate along with 400 nmol of an allyl-functionalized imidazolium salt for a final solution composition of 30% (v/v) ACN. The reaction well was sealed with optically transparent tape, purged with N_2, and placed beneath a handheld UV lamp set to 365 nm output for 1-2 h. The ITOs or DTOs were separated from unreacted starting material using denaturing polyacrylamide gel electrophoresis (PAGE). Product bands were

Table 2.1 Effect of ITO and DTO structure on hybridization, loading, and target capture performance.

Oligonucleotide (20-mer)	Structure	Melting Temp (°C)	Loading Efficiency[a] (%, n=3)	Loading Capacity[b] (pmol μL^{-1}, n=3)	Target Capture Cq[c]
Untagged	3'- HO—DNA -5'	75	10 ± 3	7 ± 2	35.35 ± 0.6
[ABIM$^+$][Br$^-$]-ITO	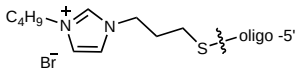	75	12 ± 3	8 ± 2	36.01 ± 0.5
[ABIM$^+$][NTf$_2^-$]-ITO	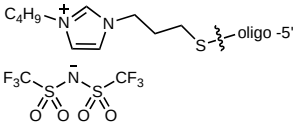	67	40 ± 4	25 ± 2	na[d]
[ABIM$^+$][OS$^-$]-ITO	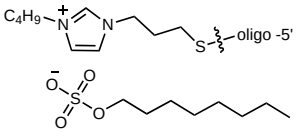	75	45 ± 2	28 ± 1	28.2 ± 1.1
[ABIM$^+$] [PFBS$^-$]-ITO	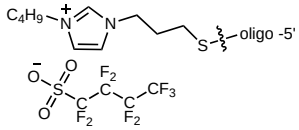	70	35 ± 5	22 ± 3	na[d]
[AOIM$^+$][OS$^-$]-ITO	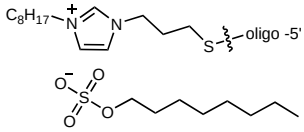	75	74 ± 4	46 ± 2	26.1 ± 0.3
[AOIM$^+$][Br$^-$]-ITO	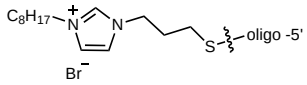	72	48 ± 4	31 ± 3	25.67 ± 1.3
[ADIM$^+$][Br$^-$]-ITO	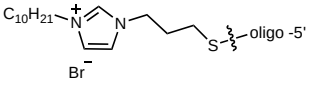	76	75 ± 5	47 ± 3	24.7 ± 2.3
[AOIM$^+$]$_2$[Br$^-$]-DTO	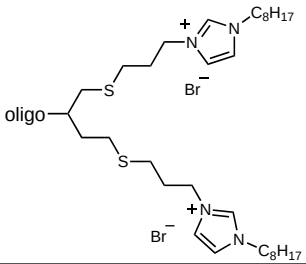	73	95 ± 4	57 ± 2	24.3 ± 1.1

[a] Conditions: concentration of ITO: 8 ng μL^{-1}; hydrophobic MIL: [P_{66614}^+][$Mn(hfacac)_3^-$]; MIL volume: 1 µL; sample volume: 50 µL; extraction time: 10 min; quantification method: anion-exchange HPLC with UV detection at 260 nm.
[b] Conditions: same as *a*. MIL density = 1.4 mg μL^{-1}
[c] Conditions: amount of ITO: 1.69 pmol; amount of target: 169 fmol of 261 bp DNA target; MIL volume: 1 µL; sample volume: 50 µL; extraction time: 10 min; desorption time: 10 min at 90 °C quantification method: qPCR.
[d] Not applicable. Extractions were not performed coupled with qPCR due to comparatively low loading efficiencies.

excised, crushed, and eluted with Milli-Q water overnight. The ITOs or DTOs were characterized by reversed-phase ion-pair LC-TOFMS (see Figures A7, A8, A12 for details).

2.3.4 Sequence-Specific DNA Capture Using MILs and ITO or DTO Probes

For DNA extraction, ITOs or DTOs were added to a 25 mM NaCl solution containing 0.169 fmol of 261 bp DNA target at various probe:target ratios. For experiments testing probe selectivity, 0.169 fmol of a DNA sequence (complement, 1 nt, or 2 nt mismatch to the ITOs probe) was also added to solution. The probes and DNA targets were annealed by heating at 90 °C for 5 min followed by cooling of the solution to 37 °C for 5 min. A 1 µL aliquot of MIL support was then added to the solution and incubated at 37 °C for 10 min to extract the ITO- or DTO-target duplex. The sample solution was decanted, and the MIL phase was washed using 50 µL of deionized water. Extracted DNA targets were desorbed from the MIL phase in 50 µL of deionized water at 90 °C for 10 min. A 1 µL aliquot of desorption solution was analyzed by qPCR amplification.

2.3.5 Loading Efficiency of ITO or DTO Probes onto the MIL Support

The ITO and DTO stability within the MIL phase was tested using HPLC for direct detection of the probe molecules. For these experiments, a liquid phase microextraction technique was used in which a 1 µL aliquot of hydrophobic MIL support was immersed in a 50 µL solution containing 60 pmol (400 ng) of ITO or DTO for 10 min at room temperature. A 20 µL aliquot of the aqueous layer was then removed for injection onto an Agilent 1260 HPLC with a variable wavelength detector (Santa Clara, CA, USA) and separated on a 35 mm × 4.6 mm i.d. × 2.5 µm TSKgel DEAENPR anion exchange column with a 5 mm × 4.6 mm i.d.× 5 µm TSKgel DEAE-NPR guard column (Tosoh Bioscience, King of Prussia, PA). Mobile phase A consisted of 20 mM Tris-HCl (pH 8), and mobile phase B was 1 M NaCl and 20 mM Tris-HCl (pH 8).

DNA was detected at 260 nm, and the amount of DNA recovered from the MIL phase was determined using an external calibration curve.

2.3.6 qPCR Amplification

Each qPCR reaction mix was 19 µL which contains 4.6 µL of deionized water, 2.6 µL of 50 mM $MgCl_2$, 1 µL of DMSO, 0.8 µL of 10 µM forward and reverse primers, and 10 µL of SsoAdvanced Universal SYBR Green Supermix (2x). The forward and reverse primers for qPCR amplification of the 261 bp target sequence were 5′- CAC GCT TAC ATT CAC GCC CT -3′ and 5′- CGA GCG TCC CAA AAC CTT CT -3′. For all reactions, 1 µL of the template DNA was added to the 19 µL of the qPCR reaction mix. For amplification of the 120 bp KRAS target, the reaction mix included 4.4 µL of water, 10 µL of SsoAdvanced Supermix, 1 µL of primer mix, 2.6 µL of 50 mM $MgCl_2$, 1 µL of DMSO, and 1 µL of template DNA. The primers from the KRAS, human PrimePCR assay kit were used without further purification. Amplification was performed using a Bio-Rad CFX96 Touch Real-Time PCR Detection System or Bio-Rad CFX Connect Real-Time PCR Detection System. The thermal program used for all qPCR assays included an initial denaturation step of 95.0 °C for 5 min followed by 40 cycles consisting of 95.0 °C for 10 s and 64.0 °C for 30 s. A five-point external calibration curve was used to determine the amplification efficiency and quantify extracted nucleic acid.

2.4 Results and Discussion

2.4.1 Design of ITOs for Enhanced Loading Efficiency onto MIL Supports

The extraction of specific DNA sequences is highly dependent on facilitating strong interactions between the oligonucleotide probe and the support phase. Contemporary methods rely on noncovalent interactions between biotin labels and streptavidin-coated magnetic bead/particles, but these materials often suffer from agglomeration processes that diminish extraction performance. As described in our previous work, we employed a magnetic liquid

support and ITO probes to circumvent the drawbacks of solid particle supports while maintaining a high yield of target DNA sequences.[19] Since the studied ITOs possessed alkyl chain lengths ranging from methyl to octyl, the probes exhibited limited affinity for the hydrophobic MIL support (ca. 50% ITO loading efficiency). In order to improve the partitioning of ITOs to the MIL support, we synthesized a series of ITOs possessing one or more of the following properties: longer alkyl groups in the cation, amphiphilic anions, fluorophilic anions, and multiple ion tag moieties. Initially, we focused on the synthesis of alkylimidazolium tags with longer carbon chains (C_{10} and C_{16}). However, reaction mixtures containing the amphiphilic 1-allyl-3-hexadecylimidazolium bromide ($[AHIM^+][Br^-]$) salt resulted in the precipitation of the thiolated nucleic acid starting material due to the alkylimidazolium group exhibiting surfactant properties and forming aggregates with DNA.[25] This phenomenon was not observed when using 1-allyl-3-decylimidazolium bromide ($[ADIM^+][Br^-]$) or any other alkylimidazolium salts with shorter chain lengths.

In order to determine the influence of the longer alkyl chain on partitioning to the MIL phase, the ITO product generated from reaction with the $[ADIM^+][Br^-]$ salt was subjected to liquid phase microextraction using the $[P_{66614}^+][Mn(hfacac)_3^-]$ MIL support as the extraction solvent. As shown in Table 2.1, a loading efficiency of 75 ± 5% was observed for the $[ADIM^+][Br^-]$-ITO, compared to a 48 ± 4% loading efficiency of the 1-allyl-3-octylimidazolium bromide ($[AOIM^+][Br^-]$)-ITO, with an unmodified oligonucleotide probe providing 10 ± 3% under the same conditions.[19] This result is likely due to the increased hydrophobic interactions between the C_{10} alkyl chain and the hydrophobic MIL support.

Given that dispersive interactions primarily govern the partitioning of the ITO to the MIL phase and yet the longer chain alkylimidazolium salts tended to precipitate the oligo starting

material, ITOs were synthesized to include hydrophobic groups in the anion as well. Allyl-bearing imidazolium salts were prepared with octylsulfate anions via metathesis reaction between the bromide form of the imidazolium salt and sodium octylsulfate.[26] As shown in Table 2.1, a loading efficiency of 45 ± 2% was observed for the 1-allyl-3-butylimidazolium octylsulfate ([$ABIM^+$][OS^-])-ITO. The loading efficiency was a substantial increase from the [Br^-] analog, which exhibited a loading efficiency of 12 ± 3%. In addition to amphiphilic anions, fluorine-rich anions were also imparted to the tag moiety of the ITO in an effort to capitalize on fluorophilic interactions with the fluorinated ligands of the MIL support (i.e., hfacac). Allylimidazolium salts with either [NTf_2^-] or [$PFBS^-$] anions were prepared by metathesis reactions and subsequently studied for their ability to partition to the hydrophobic MIL. When paired with the [$ABIM^+$] cation in the ITO structure, both [NTf_2^-] and [$PFBS^-$] anions contributed to higher ITO loading efficiency (40 ± 4% and 35 ± 5%, respectively) compared to the [Br^-] form of the ITO (ca. 12%). Since the [OS^-] anion appeared to have the greatest influence on loading efficiency, an ITO with the [$AOIM^+$] cation and [OS^-] anion components was synthesized. A significantly higher affinity for the MIL phase was observed for the [$AOIM^+$][OS^-]-ITO, resulting in a loading efficiency of 74 ± 4%. These results strongly suggest that the anion component of the ITO plays an important role in facilitating binding of the ITO probe to the MIL support and could be used for further optimization of probe-support affinity.

Because the noncovalent labeling of the ITO probe with an additional alkyl moiety (i.e., [OS^-] anions) provided enhanced loading efficiency, the covalent attachment of another alkyl group of the same length would also be expected to improve affinity toward the MIL. A dithiolated oligonucleotide starting material was employed as a means to introduce two ion-tags with C_8 alkyl groups into the same probe structure via covalent linkage. The structure of the

resulting $[AOIM^+]_2[Br^-]$-DTO is shown in Table 2.1. The loading efficiency was investigated under the same conditions used for the ITO probes and revealed nearly quantitative capture (95 ± 4%) of the $[AOIM^+]_2[Br^-]$-DTO by the hydrophobic $[P_{66614}^+][Mn(hfacac)_3^-]$ MIL.

Apart from hydrophobic interactions that facilitate loading onto the MIL support, ion tags with benzylimidazolium groups ($[ABzIM^+][Br^-]$-ITO) were coupled with the $[P_{66614}^+][Mn(Phtfacac)_3^-]$ MIL support which possesses phenyl groups within the anion component in order to investigate the effect of π–π stacking on loading efficiency. The structures of the $[P_{66614}^+][Mn(Phtfacac)_3^-]$ MIL and the $[ABzIM^+][Br^-]$-ITO are shown in Figures A1b and A2, respectively. The loading efficiency and selectivity were tested using either a benzyl or C_8-tagged oligo coupled with either the $[P_{66614}^+][Mn(Phtfacac)_3^-]$ MIL or the $[P_{66614}^+][Mn(hfacac)_3^-]$ MIL to account for nonspecific interactions (i.e., hydrophobic interactions) that may also contribute to loading efficiency of the aromatic tag and/or MIL support. As shown in Table A1 of Appendix A, no differences in extraction efficiency were observed for the benzyl-tagged oligo and an unlabeled oligo using the $[P_{66614}^+][Mn(Phtfacac)_3^-]$ MIL support. However, duplexes generated from the $[ABzIM^+][Br^-]$-ITO and its complementary sequences were extracted with substantially higher efficiency (40 ± 3%) than untagged duplexes (1 ± 1%), indicating the feasibility of utilizing π-stacking interactions for sequence specific DNA capture.

2.4.2 Binding Affinity and Durability of ITO-MIL Interactions

In order to determine whether high loading efficiency was correlated to better retention of probe molecules within the MIL support solvent, the desorption of either ITOs or DTO from the MIL after successive wash steps commonly employed to remove untargeted DNA in sequence-specific extraction procedures was tested. Similar to the procedures shown in Figure 2.1b and c, the $[AOIM^+][Br^-]$-ITO or $[AOIM^+]_2[Br^-]$-DTO was loaded onto the MIL support and subsequently immersed in a solution containing complementary 20 mer DNA. The probes and

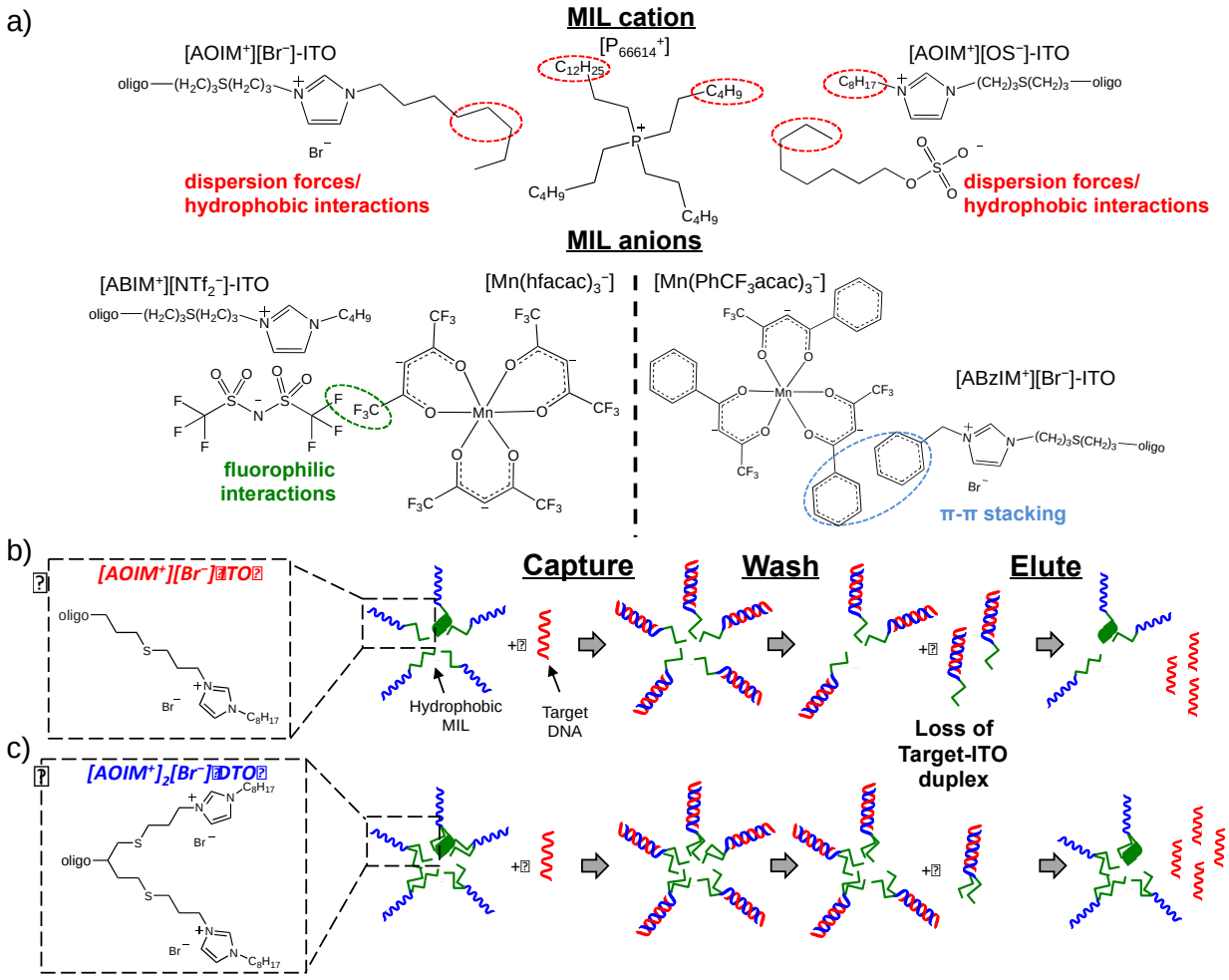

Figure 2.1 (a) Chemical structures of the MILs used in this study and examples of the intermolecular interactions between the cation/anion components of the ion tag and the MIL support that govern ITO loading efficiency. Schematic showing the sequence-specific DNA extraction procedure using the hydrophobic $[P_{66614}^{+}][Mn(hfacac)_3^{-}]$ MIL and the (b) mono-substituted $[AOIM^{+}][Br^{-}]$-ITO or (c) di-substituted $[AOIM^{+}]_2[Br^{-}]$-DTO.

targets were annealed and then washed with 25 mM NaCl at 40 °C for 10 min, and the aqueous phase was removed for anion-exchange HPLC analysis. Figure 2.2a shows chromatograms obtained for the ITO (red trace) or DTO (blue trace) experiments. As indicated by the area of the later eluting peak, 2.7 ± 0.6-fold more probe-target duplex was desorbed from the MIL support when the $[AOIM^{+}][Br^{-}]$-ITO was used to capture the DNA target. These findings are in good

agreement with the results obtained for the loading efficiency data (Table 2.1) and show a positive correlation between loading efficiency and stability of the ITO-MIL interactions.

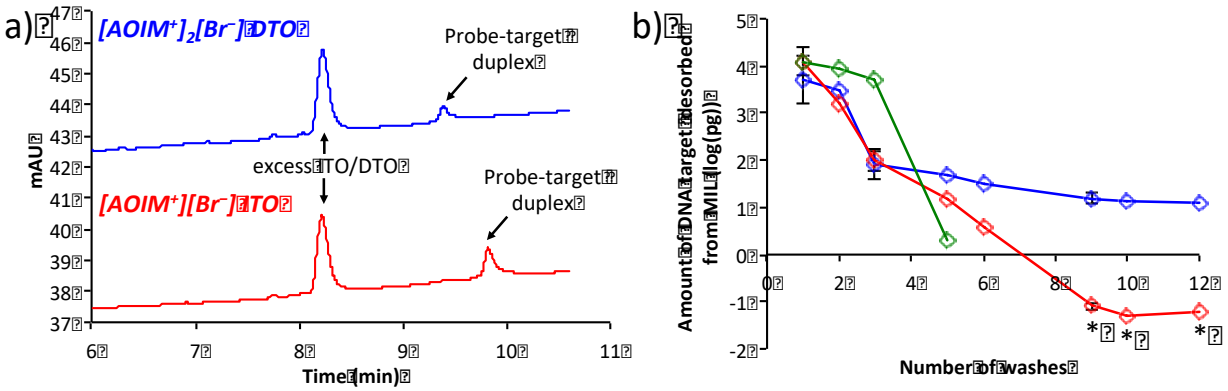

Figure 2.2 (a) HPLC quantification of the loss of target-ITO duplex from the MIL support after loading a solution containing 60 pmol of duplex onto the MIL and subsequently heating the sample at 37 ˚C for 10 min in 25 mM NaCl solution. (b) 0.169 pmol (ca. 2.7×10^4 pg) of 261 bp DNA target from aqueous solution using probes substituted with one (red trace) or two (blue trace) [$AOIM^+$][Br^-] groups, or an unmodified probe sequence (green trace). The asterisk indicates that the data were outside the range of the calibration curve and were extrapolated to obtain these values.

Many relevant nucleic acid targets are much longer sequences than the initially studied 20 mer and may potentially impact the partitioning behavior of the probe-target duplex from the MIL support. The affinity between the ITOs and DTOs for the MIL was also tested following the capture of a model 261 bp DNA sequence. For these experiments, a procedure similar to Figure 2.1b and c was employed, using qPCR amplification to detect very small quantities of nucleic acid desorbed from the MIL. After extraction of a solution containing 0.169 pmol of target using either ITO, DTO, or an unmodified oligonucleotide as hybridization probes, the MIL phase was subjected to successive washes with 25 mM NaCl at 37 °C in order to maintain base pairing within the probe-target duplex. Wash fractions were collected for qPCR analysis until no detectable target DNA remained, or the amount of desorbed target DNA from wash to wash remained constant. As shown in Figure 2.2b, the amount of DNA target desorbed from the MIL

decreased after the first three wash steps when using either the ITO or DTO. The initial rapid decrease in DNA target desorption was also observed when using unmodified oligonucleotide probes, indicating that the phenomenon is due to the release of DNA nonspecifically extracted by the MIL support. It is important to note that a greater amount of untagged probe-target duplex was initially released from the MIL phase than for ITO- or DTO-target duplexes, likely due to weaker interactions between the untagged probe and MIL support. Moreover, no DNA was detected for any subsequent washes for the sample extracted using the unmodified oligonucleotide probe. After 9 wash steps, the amount of DNA target released by the $[AOIM^+][Br^-]$-ITO was lower than the limit of quantification. However, the $[AOIM^+]_2[Br^-]$-DTO continued to release a small amount of DNA target into the subsequent wash solutions and retained a detectable amount of DNA target for up to 12 successive washes. These results indicate that the DTO is retained within the MIL phase longer and may be subjected to more rigorous washing or hybridization conditions than the monosubstituted ITO.

2.4.3 Distinguishing Double- and Single-Nucleotide Variants Using ITOs with MIL-Based Capture and Comparison to a Commercial Magnetic Bead-Based Method

Single-nucleotide polymorphisms are the most common type of alteration to genomic DNA and are widely recognized to provide meaningful diagnostic information for numerous diseases. These modifications are invariably colocalized with high levels of background nucleic acids that differ by a single base pair. The selectivity of the ITO and DTO probes for complementary sequences and mismatched sequences was initially tested using melt curve analysis. As shown in Table 2.1 and Figures A9 and A10, the Tm value of the $[AOIM^+]_2[Br^-]$-DTO probe and complement was comparable to the monosubstituted $[AOIM^+][Br^-]$-ITO, indicating little influence of the second alkyl chain on hybridization behavior. Similarly, both ITO and DTO showed only minor melt curve features for the 1 and 2 nt mismatches, compared

to the more prominent and higher melting temperature peaks observed for the unmodified oligonucleotide probe (Figure A11). For $[AOIM^+][OS^-]$, a slightly higher melting temperature with the complementary sequence was observed compared to the unmodified oligo probe, while ITOs with $[NTf_2^-]$ and $[PFBS^-]$ anions resulted in much lower melting temperatures (Table 2.1). Although ITOs with $[NTf_2^-]$ and $[PFBS^-]$ anions showed minimal peaks for 1 and 2 nt mismatches, the melt curves were very broad (ca. 20 °C), indicating noncanonical base pairing or nonspecific interactions.[27] For this reason, we focused on the DTO and $[AOIM^+][Br^-]$-ITOs for extraction applications.

Cell-free nucleic acid biomarkers in plasma cover a wide range of concentrations from no detectable amount to 1000 ng μL^{-1} with the average concentration near 200 ng μL^{-1}.[28,29] Due to the presence of highly similar interfering DNA, low abundance target DNA sequences are particularly challenging to detect. As shown in Table A2, the MIL-based extraction conditions were optimized for low target concentrations, resulting in a 5:1 ratio of probe:target sequence (0.845 fmol of DTO) and 1 μL of MIL. Next, the extraction selectivities of the $[AOIM^+]_2[Br^-]$-DTO and $[AOIM^+][Br^-]$-ITO were studied by spiking a 3.4 pM (0.027 ng μL^{-1}) solution of 261 bp target DNA with interfering sequences (20 mers) with either 0, 1, or 2 nt mismatches to the 20 mer probes. The samples were then subjected to extraction using the procedures shown in Figures 2.1b and c. Extractions were also performed using a commercial method based on magnetic beads according to the manufacturers instructions. As shown in Table 2.2, the ITO and DTO methods exhibited superior extraction performance compared to the magnetic bead-based approach when single nucleotide variants were added to solution. These findings are likely due to higher nonspecific DNA extraction observed for magnetic beads when compared to the $[P_{66614}^+][Mn(hfacac)_3^-]$ MIL support.[19]

Table 2.2 Quantification cycle (Cq) values for sequence specific DNA extraction using DTO, ITO, or magnetic bead-based methods obtained from qPCR amplification.

Extraction method	DNA target + 20 mer comp (n=3)	DNA target + 20 mer 1 nt mismatch (n=3)	DNA target + 20 mer 2 nt mismatch (n=3)	DNA target (n=3)
Dynabeads M-270[a]	32.98 ± 0.46	32.52 ± 0.26	31.31 ± 0.64	31.23 ± 0.06
$[AOIM^+]_2[Br^-]$[b]	30.51 ± 0.84	29.30 ± 1.16	31.59 ± 0.10	28.29 ± 0.19
$[AOIM^+][Br^-]$[b]	31.29 ± 1.06	30.58 ± 0.34	30.07 ± 0.94	30.36 ± 0.65

[a]Extraction conditions: biotinlayted probe: 16.9 fmol; dynabeads M-270: 1.3 µg; 261 bp DNA target: 0.169 fmol; DTO $[AOIM^+]_2[Br^-]$: 0.845 fmol; ITO $[AOIM^+][Br^-]$: 16.9 fmol. Interfering sequences were all spiked at 1:1 mole ratio to target.
[b]261 bp DNA target were first hybridized in 50 µL 25 mM NaCl solution from 90 °C for 5 min to 37 °C for 5 min. 1 µL of MIL: $[P_{66614}^+][Mn(hfacac)_3^-]$ was added in the middle of the solution after hybridization. The extraction was performed for 10 min at room temperature. The 261 bp DNA target were desorbed with 50 µL of 25 mM NaCl at 37 °C for 10 min.

2.4.4 Sequence-Specific DNA Capture from Bacterial Cell Lysate and Human Plasma Using DTO Probes and MIL Support

In order to investigate the influence of a complex sample matrix on the performance of the DTO-based DNA capture method, approximately 1×10^6 *E. coli* cells were lysed by ultrasonication, and the crude lysate was spiked with target DNA. Two approaches were studied for sequence-specific DNA extraction: 1) a hybridize-first method where the probe and target are hybridized prior to capture by the MIL support and 2) a load-first method where the DTO probe is first loaded onto the MIL support and subsequently used for extraction of target DNA. For both methods, the optimal ratio of DTO:target (5:1) was used. Figure 2.3 shows that when the hybridize-first method was employed for the extraction of 0.3 ng of target DNA from the crude cell lysate, a Cq value of approximately 33 was obtained using the DTO probe. However, a much lower Cq value (23.5 ± 0.2) was observed for the load-first method, indicating an approximate 1000-fold increase in the amount of DNA recovered compared to the hybridize-first method. The observation that greater quantities of DNA target were recovered using the load-first method

may be due to nonspecific interactions between the alkyl chains of the DTO and lipophilic components of the cell lysate that compete with the hydrophobic MIL. Figure 2.3 also shows a similar trend for the monosubstituted [AOIM$^+$][Br$^-$]-ITO, albeit less pronounced due to the ITO possessing one fewer C_8 alkyl group.

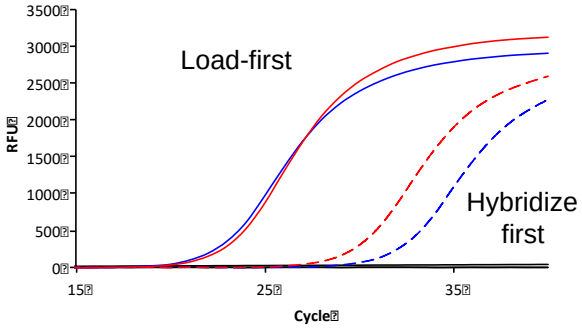

Figure 2.3 qPCR amplification of 261 bp DNA target isolated from *E. coli* cell lysate using the ITO-MIL approach either in hybridize first (dashed lines) or load first (solid lines) mode. Samples spiked with 0.3 ng of target were subjected to each mode using either the monosubstituted [AOIM$^+$][Br$^-$]-ITO (red traces) or the disubstituted [AOIM$^+$]$_2$[Br$^-$]-DTO (blue traces).

The detection of cell-free nucleic acids in human plasma has diagnostic and prognostic potential for a variety of cancers.[28] Although it is an appealing alternative to conventional tissue biopsies, plasma samples contain proteins and globulins that inhibit the direct PCR amplification of DNA targets.[30] The extraction performance of the DTO-MIL method was investigated in human plasma samples spiked with 6 fmol of a 120 bp fragment from a known oncogene, KRAS, as the DNA target. The MIL and DTO-based method was also compared to an approach using commercially available streptavidin-coated magnetic beads and biotinylated oligonucleotides (20-mer) complementary to the KRAS fragment. Prior to extraction, samples were diluted 10-fold in order to minimize the nonspecific extraction due to matrix interferences. As shown in Figure 2.4, the diluted plasma sample resulted in diminished extraction efficiency

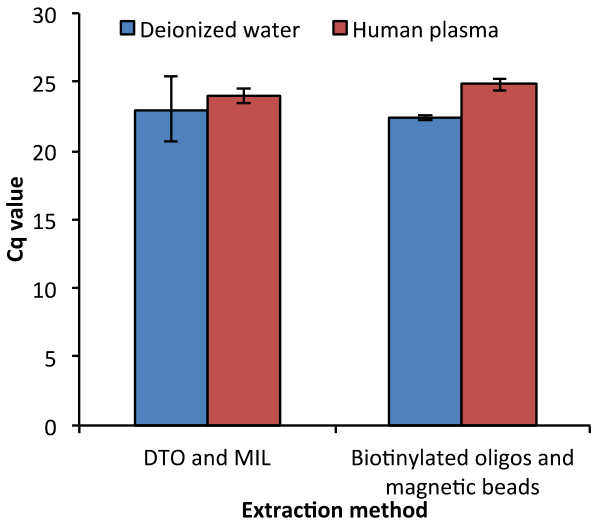

Figure 2.4 Comparison of sequence-specific DNA capture methods for aqueous solution and human plasma samples. A 120 bp fragment of human KRAS gene was extracted using either commercially available magnetic beads and biotinylated oligo probes or the DTO-MIL method and subjected to qPCR amplification.

for the DTO-MIL method compared an aqueous DNA solution, likely due to competing interactions between matrix components and the MIL. A similar trend was observed for the magnetic bead-based approach, which exhibited little to no difference in Cq values (24.82 ± 0.45) when compared to the DTO-MIL method (23.97 ± 0.60) for the extraction of KRAS fragment from plasma.

2.5 Conclusions

The analysis of specific DNA sequences invariably requires a selective sample preparation procedure that eliminates or dramatically reduces the quantity of untargeted biomolecules from the sample. The recognition of target DNA using ITOs coupled with MIL-based capture represents a powerful approach for the enrichment of specific DNA sequences. In order to capitalize on the selectivity and high DNA target yields afforded by the ITO-MIL method, we investigated a series of ITO probes with various hydrophobic and fluorophilic functional groups in the cation and anion moieties of the ion tag. The best performing probe

possessed two alkyl groups (C_8) that facilitated dense loading of the DTO onto the MIL support. When applied for the capture of specific DNA sequences from aqueous solution, the high affinity of the DTO for the MIL support allowed for more stringent wash conditions than a monosubstituted ITO ([AOIM$^+$][Br$^-$]-ITO). Furthermore, the DTO-MIL system was capable of extracting target DNA from solutions containing single nucleotide variants with higher DNA yields than a commercial magnetic bead-based approach. The DTO-based method also selectively extracted DNA from crude bacterial cell lysate, demonstrating the tolerance of the sample preparation method toward interferences in complex samples.

2.6 Acknowledgments

The authors acknowledge Miranda N. Emaus for her assistance in experiments involving the extraction of KRAS fragment from plasma. J.L.A. acknowledges funding from the Chemical Measurement and Imaging Program at the National Science Foundation (CHE-1709372).

2.7 References

(1) Diehl, F.; Li, M.; Dressman, D.; He, Y.; Shen, D.; Szabo, S.; Diaz, L. A.; Goodman, S. N.; David, K. A.; Juhl, H.; et al. Detection and Quantification of Mutations in the Plasma of Patients with Colorectal Tumors. *Proc. Natl. Acad. Sci. U. S. A.* **2005**, *102* (45), 16368–16373.

(2) Albert, T. J.; Molla, M. N.; Muzny, D. M.; Nazareth, L.; Wheeler, D.; Song, X.; Richmond, T. A.; Middle, C. M.; Rodesch, M. J.; Packard, C. J.; et al. Direct Selection of Human Genomic Loci by Microarray Hybridization. *Nat. Methods* **2007**, *4* (11), 903–905.

(3) Porreca, G. J.; Zhang, K.; Li, J. B.; Xie, B.; Austin, D.; Vassallo, S. L.; LeProust, E. M.; Peck, B. J.; Emig, C. J.; Dahl, F.; et al. Multiplex Amplification of Large Sets of Human Exons. *Nat. Methods* **2007**, *4* (11), 931–936.

(4) Yang, H.; Qu, L.; Wimbrow, A. N.; Jiang, X.; Sun, Y. Rapid Detection of Listeria Monocytogenes by Nanoparticle-Based Immunomagnetic Separation and Real-Time PCR. *Int. J. Food Microbiol.* **2007**, *118* (2), 132–138.

(5) Sista, R.; Hua, Z.; Thwar, P.; Sudarsan, A.; Srinivasan, V.; Eckhardt, A.; Pollack, M.; Pamula, V. Development of a Digital Microfluidic Platform for Point of Care Testing. *Lab Chip* **2008**, *8* (12), 2091–2104.

(6) Davis, J. A.; Inglis, D. W.; Morton, K. J.; Lawrence, D. A.; Huang, L. R.; Chou, S. Y.; Sturm, J. C.; Austin, R. H. Deterministic Hydrodynamics: Taking Blood Apart. *Proc. Natl. Acad. Sci. U. S. A.* **2006**, *103* (40), 14779–14784.

(7) Fan, Z. H.; Mangru, S.; Granzow, R.; Heaney, P.; Ho, W.; Dong, Q.; Kumar, R. Dynamic DNA Hybridization on a Chip Using Paramagnetic Beads. *Anal. Chem.* **1999**, *71* (21), 4851–4859.

(8) Liu, D.; Liang, G.; Zhang, Q.; Chen, B. Detection of Mycobacterium Tuberculosis Using a Capillary-Array Microsystem with Integrated DNA Extraction, Loop-Mediated Isothermal Amplification, and Fluorescence Detection. *Anal. Chem.* **2013**, *85* (9), 4698–4704.

(9) Lund-Olesen, T.; Dufva, M.; Hansen, M. F. Capture of DNA in Microfluidic Channel Using Magnetic Beads: Increasing Capture Efficiency with Integrated Microfluidic Mixer. *J. Magn. Magn. Mater.* **2007**, *311*, 396–400.

(10) Clark, K. D.; Nacham, O.; Purslow, J. A.; Pierson, S. A.; Anderson, J. L. Magnetic Ionic Liquids in Analytical Chemistry: A Review. *Anal. Chim. Acta* **2016**, *934*, 9–21.

(11) Santos, E.; Albo, J.; Irabien, A. Magnetic Ionic Liquids: Synthesis, Properties and Applications. *RSC Adv.* **2014**, *4* (75), 40008–40018.

(12) Brown, P.; Butts, C. P.; Eastoe, J.; Padrón Hernández, E.; Machado, F. L. D. A.; De Oliveira, R. J. Dication Magnetic Ionic Liquids with Tuneable Heteroanions. *Chem. Commun.* **2013**, *49* (27), 2765–2767.

(13) Nacham, O.; Clark, K. D.; Yu, H.; Anderson, J. L. Synthetic Strategies for Tailoring the Physicochemical and Magnetic Properties of Hydrophobic Magnetic Ionic Liquids. *Chem. Mater.* **2015**, *27* (3), 923–931.

(14) Nan, H.; Peterson, L.; Anderson, J. L. Evaluating the Solvation Properties of Metal-Containing Ionic Liquids Using the Solvation Parameter Model. *Anal. Bioanal. Chem.* **2018**, *410* (19), 4597–4606.

(15) Clark, K. D.; Nacham, O.; Yu, H.; Li, T.; Yamsek, M. M.; Ronning, D. R.; Anderson, J. L. Extraction of DNA by Magnetic Ionic Liquids: Tunable Solvents for Rapid and Selective DNA Analysis. *Anal. Chem.* **2015**, *87* (3), 1552–1559.

(16) Peng, X.; Clark, K. D.; Ding, X.; Zhu, C.; Varona, M.; Emaus, M. N.; An, J.; Anderson, J. L. Coupling Oligonucleotides Possessing a Poly-Cytosine Tag with Magnetic Ionic Liquids for Sequence-Specific DNA Analysis. *Chem. Commun.* **2018**, *54* (73), 10284–10287.

(17) Clark, K. D.; Yamsek, M. M.; Nacham, O.; Anderson, J. L. Magnetic Ionic Liquids as PCR-Compatible Solvents for DNA Extraction from Biological Samples. *Chem. Commun.* **2015**, *51* (94), 16771–16773.

(18) Emaus, M. N.; Clark, K. D.; Hinners, P.; Anderson, J. L. Preconcentration of DNA Using Magnetic Ionic Liquids That Are Compatible with Real-Time PCR for Rapid Nucleic Acid Quantification. *Anal. Bioanal. Chem.* **2018**, *410* (17), 4135–4144.

(19) Clark, K. D.; Varona, M.; Anderson, J. L. Ion-Tagged Oligonucleotides Coupled with a Magnetic Liquid Support for the Sequence-Specific Capture of DNA. *Angew. Chemie - Int. Ed.* **2017**, *56* (26), 7630–7633.

(20) Mehdi, H.; Binnemans, K.; Van Hecke, K.; Van Meervelt, L.; Nockemann, P. Hydrophobic Ionic Liquids with Strongly Coordinating Anions. *Chem. Commun.* **2010**, *46* (2), 234–236.

(21) Zhang, P.; Gong, Y.; Lv, Y.; Guo, Y.; Wang, Y.; Wang, C.; Li, H. Ionic Liquids with Metal Chelate Anions. *Chem. Commun.* **2012**, *48* (17), 2334–2336.

(22) Pierson, S. A.; Nacham, O.; Clark, K. D.; Nan, H.; Mudryk, Y.; Anderson, J. L. Synthesis and Characterization of Low Viscosity Hexafluoroacetylacetonate-Based Hydrophobic Magnetic Ionic Liquids. *New J. Chem.* **2017**, *41* (13), 5498–5505.

(23) Zhao, F.; Meng, Y.; Anderson, J. L. Polymeric Ionic Liquids as Selective Coatings for the Extraction of Esters Using Solid-Phase Microextraction. *J. Chromatogr. A* **2008**, *1208* (1–2), 1–9.

(24) Wasserscheid, P.; Van Hal, R.; Bösmann, A. 1-n-Butyl-3-Methylimidazolium ([Bmim]) Octylsulfate - An Even “greener” Ionic Liquid. *Green Chem.* **2002**, *4* (4), 400–404.

(25) Dias, R.; Mel’nikov, S.; Lindman, B.; Miguel, M. G. DNA Phase Behavior in the Presence of Oppositely Charged Surfactants. *Langmuir* **2000**, *16* (24), 9577–9583.

(26) Morrissey, S.; Pegot, B.; Coleman, D.; Garcia, M. T.; Ferguson, D.; Quilty, B.; Gathergood, N. Biodegradable, Non-Bactericidal Oxygen-Functionalised Imidazolium Esters: A Step towards “greener” Ionic Liquids. *Green Chem.* **2009**, *11* (4), 475–483.

(27) Maeda, Y.; Nunomura, K.; Ohtsubo, E. Differential Scanning Calorimetric Study of the Effect of Intercalators and Other Kinds of DNA-Binding Drugs on the Stepwise Melting of Plasmid DNA. *J. Mol. Biol.* **1990**, *215* (2), 321–329.

(28) Schwarzenbach, H.; Hoon, D. S. B.; Pantel, K. Cell-Free Nucleic Acids as Biomarkers in Cancer Patients. *Nat. Rev. Cancer* **2011**, *11* (6), 426–437.

(29) Kelley, S. O. What Are Clinically Relevant Levels of Cellular and Biomolecular Analytes? *ACS Sensors* **2017**, *2* (2), 193–197.

(30) Al-Soud, W. A.; Jönsson, L. J.; Rådström, P. Identification and Characterization of Immunoglobulin G in Blood as a Major Inhibitor of Diagnostic PCR. *J. Clin. Microbiol.* **2000**, *38* (1), 345–350.

CHAPTER 3. SELECTIVE HYBRIDIZATION AND CAPTURE OF *KRAS* DNA FROM PLASMA AND BLOOD USING ION-TAGGED OLIGONUCLEOTIDE PROBES COUPLED TO MAGNETIC IONIC LIQUIDS

Miranda N. Emaus, Chenghui Zhu, Jared L. Anderson

Department of Chemistry, Iowa State University, Ames, Iowa 50011, United States

Modified from a manuscript published in *Anal. Chim. Acta* **2020**, 1094, 1-10

3.1 Abstract

Detection of circulating tumor DNA (ctDNA) presents several challenges due to single-nucleotide polymorphisms and large amounts of background DNA. Previously, we reported a sequence-specific DNA extraction procedure utilizing functionalized oligonucleotides called ion-tagged oligonucleotides (ITOs) and disubstituted ion-tagged oligonucleotides (DTOs). ITOs and DTOs are capable of hybridizing to complementary DNA for subsequent capture by a magnetic ionic liquid (MIL) through hydrophobic interactions, π-π stacking, and fluorophilic interactions. However, the performance of the ITOs and DTOs in complex sample matrices has not yet been evaluated. In this study, we compare the amount of *KRAS* DNA extracted using ITO and DTOs from saline, 2-fold diluted plasma, 10-fold diluted plasma, and 10-fold diluted blood. We demonstrate that ITO/DTO-MIL extraction is capable of selectively preconcentrating DNA from diluted plasma and blood without additional sample preparation steps. In comparison, streptavidin-coated magnetic beads were unable to selectively extract DNA from 10-fold diluted plasma and 10-fold diluted blood without additional sample clean-up steps. Significantly more DNA could be extracted from 2-fold diluted plasma and 10-fold diluted blood matrices using the DTO probes compared to the ITO probes, likely due to stronger interactions between the probe and MIL. The ability of the DTO-MIL method to selectively preconcentrate small concentrations

of DNA from complex biological matrices suggests that this method could be beneficial for ctDNA analysis.

3.2 Introduction

Circulating tumor DNA (ctDNA) is fragmented tumor-derived DNA found in blood originating from tumor cells that have undergone apoptosis or necrosis.[1] Detection of ctDNA from blood has massive potential to supplement or replace invasive tissue biopsies for cancer diagnosis, treatment, and the monitoring of residual disease.[2] However, during the early stages of cancer or after cancer treatment, ctDNA fragments are present in low amounts relative to wild-type DNA with mutation abundances potentially less than 0.01%.[3] Large amounts of background DNA can mask low abundance mutant fragments causing false negative results.[2] Furthermore, ctDNA fragments are prone to single-nucleotide polymorphisms (SNPs).[4] The *KRAS* gene is particularly prone to SNPs, typically around codon 12 and 13 in exon 2, which can impair the guanosine triphosphatase activity of the KRAS protein resulting in cellular proliferation.[5,6] The presence of certain *KRAS* SNPs have also been correlated to the success of anti-EGFR therapy making it crucial to distinguish SNPs from wild-type DNA.[7,8] Therefore, ctDNA analysis requires sequence-specific detection in order to distinguish low concentrations of SNPs from complex matrices.

There are several polymerase chain reaction (PCR) methods for sequence-specific amplification and detection.[2,9] However, large amounts of background DNA may result in false positives due to mishybridization or mask target DNA fragments.[10] Wild-type DNA can be co-amplified with ctDNA when using similar primer sets. PCR blockers, such as peptide nucleic acids (PNAs) or locked nucleic acids (LNAs), can limit amplification of wild-type DNA.[11-13] However, PNAs and LNAs are expensive, and their ability to discriminate between the wild-type and mutant fragments rely heavily on the positioning and sequence of the probe.[14,15] Co-

amplification at lower denaturation temperature (COLD) PCR can also limit co-amplification of wild-type DNA by carefully optimizing the annealing temperature to ensure that wild-type DNA remains a duplex during the annealing and extension step.[16] While COLD-PCR is useful for selectively amplifying known and unknown mutations, the critical temperature of the mutant fragment must be lower than the wild-type DNA for selective amplification, which prevents approximately 30% of all mutations from being detected.[17] In addition, all PCR methods require highly pure DNA for amplification to occur, and blood and plasma components such as IgG or hemoglobin can inhibit PCR.[18,19] Therefore, sequence-specific DNA extraction step is needed in order to limit the co-extraction of non-target DNA and PCR inhibitors.

Sequence-specific DNA extractions can supplement PCR amplification by preventing large amounts of background DNA from contaminating the reaction. Commercial methods for such extractions often rely on streptavidin-coated magnetic beads and biotinylated oligonucleotides.[1,20,21] Target DNA can be captured using streptavidin-coated magnetic beads due to streptavidin's exceptional affinity for biotin ($K_d = 4 \times 10^{-14}$ M).[22] However, streptavidin-coated magnetic beads are prone to aggregation and sedimentation, which can reduce extraction efficiencies and clog microfluidic devices.[23,24] Other sequence-specific extraction methods include the use of oligonucleotide-modified monoliths; however, these procedures can currently achieve picomolar detection limits where most ctDNA fragments are present at femtomolar concentrations or lower.[25-27] Oleoyl-modified oligonucleotides have also been used for sequence-specific DNA extractions. DNA can be selectively hybridized to the oleoyl-modified oligonucleotide and be contained within reverse micelles of diauroylphosphatidylcholine and 1-hexanol.[28] It was demonstrated that over 60% of the target DNA was extracted using the oleoyl-modified oligonucleotides whereas only 6% and 4% of the 1 nt and 2 nt mismatch fragments,

respectively, were extracted. However, a lengthy extraction step (i.e., 3 h) is required to form the reverse micelles as significant agitation can disrupt the interface between the aqueous and organic phases. In addition, this method has never been used to extract clinically-relevant concentrations of ctDNA nor has it been applied to a complex matrix.

A recent and promising alternative to commercial sequence-specific DNA extraction approaches is the use of magnetic ionic liquids (MILs).[29] MILs are a subclass of ionic liquids (ILs) that contain a paramagnetic component in either the cation or anion allowing them to be dispersed as droplets and be rapidly collected using an external magnet.[30,31] Hydrophobic manganese(II)-based MILs, in particular, have been found to poorly extract DNA with extraction efficiencies less than 2%.[29,32,33] A series of DNA extraction probes termed ion-tagged oligonucleotides (ITOs) have been designed to contain an imidazolium headgroup that interacts with a manganese(II)-based MIL solvent support through hydrophobic interactions, π-π stacking, and fluorophilic interactions.[29,34] Recent efforts have focused on improving loading of the ITO-DNA duplex to the MIL support though the use of disubstituted ion-tagged oligonucleotides (DTOs), which contain two imidazolium headgroups capable of interacting with the MIL through hydrophobic interactions.[34] Another recent study developed a dispersive ITO-MIL method that drastically decreased the sample preparation time by dispersing the MIL using a vortex and incorporating DNA-enriched MIL into the qPCR buffer, allowing for a 19-fold enrichment of target DNA.[33]

Despite significantly higher loading efficiencies associated with the DTO, both the ITO and DTO probes extract similar amounts of DNA under optimized extraction conditions.[34] However, it still remains unclear as to whether the DTO and ITO probes exhibit similar DNA extraction performances from complex matrices such as plasma and whole blood. In addition,

there has been little optimization of the desorption step in the ITO/DTO-MIL procedure, as previous methods have relied on either a time-consuming 10 min desorption step at 90 °C or desorption of DNA during qPCR amplification, which is restricted by the temperature program and buffer conditions required for PCR.[29,33-35] This study examines the sequence-specific extraction of *KRAS* DNA from 10-fold diluted plasma, 2-fold diluted plasma, and 10-fold diluted whole blood using both ITO and DTO probes. In addition, the desorption time and ionic strength of the desorption solution were optimized to ensure maximum recovery of target DNA from the MIL. The ITO/DTO-MIL method was found to be selective when performing extractions from saline (154 mM NaCl), 10-fold diluted plasma, 2-fold diluted plasma, and 10-fold diluted blood. However, the DTO probes were significantly more advantageous in extractions from 2-fold diluted plasma and 10-fold diluted whole blood whereas the ITO probes extracted more DNA from saline compared to DTOs. These results suggest that the DTO-MIL procedure is highly versatile and capable of selectively preconcentrating femtomolar levels of target DNA from very complex samples that contain high amounts of protein and background DNA whereas the ITO probe excels when performing extraction from samples with elevated ionic strength.

3.3 Methods and materials

3.3.1 Materials and Reagents

Ammonium hydroxide (28-30% solution in water), 1,1,1,5,5,5-hexafluoroacetylacetone (99%), 1-phenyl-4,4,4-trifluoro-1,3-butanedione (99%), and trioctylamine (97%) were purchased from Acros Organics (Morris Plains, NJ, USA). Manganese(II) chloride tetrahydrate (98.0-101.0%) was purchased from Alfa Aesar (Ward Hill, MA, USA). Anhydrous diethyl ether (99.0%) was purchased from Avantor Performance Materials Inc. (Center Valley, PA, USA). Trihexyl(tetradecyl)phosphonium chloride (97.7%) was purchased from Strem Chemicals (Newburyport, MA, USA). Ammonium persulfate (APS) (≥98.0%), allyl bromide,

ethylenediaminetetraacetic acid (EDTA) (99.4-100.06%), 1-bromooctane (99%), benzylimidazole (99%), triethylamine (≥99.5%), sodium octylsulfate ([OS^-]) (>95%), Tween 20, LC-MS grade acetonitrile (ACN) (≥99.9%), lyophilized plasma from human (4% trisodium citrate), potassium hexafluorophosphate ([PF_6^-]) (≥99%), and magnesium chloride hexahydrate (99.0-102.0%) were purchased from Sigma-Aldrich (St. Louis, MO, USA). SYBR Green I (10,000x) was purchased from Life Technologies (Carlsbad, CA, USA). Proteinase K was purchased from New England Biolabs (Ipswich, MA, USA). Tris(hydroxymethyl)aminomethane (Tris) hydrochloride (HCl), urea (>99%) and tris(2-carboxyethyl)phosphine (TCEP) (>98%) were purchased from P212121 (Ypsilanti, MI, USA). SsoAdvanced Universal SYBR Green Supermix (2x), 40% acrylamide, bis-acrylamide solution 29:1, tetramethylethylenediamine (TEMED), and *KRAS*, a human PrimePCR™ SYBR green assay (120 base pair amplicon), were purchased from Bio-Rad Laboratories (Hercules, CA, USA). Cyclic disulfide-modified, thiol-modified, biotinylated, and unmodified oligonucleotides were purchased from Integrated DNA Technologies (Coralville, IA, USA). PCR caps, tube strips, sodium chloride, fresh human whole blood, and Dynabeads Steptavidin M – 270 magnetic beads were purchased from Thermo Fisher Scientific (Waltham, MA, USA). Neodymium rod (0.66 T) and cylinder magnets (0.9 T) were purchased from K&J Magnetics (Pipersville, PA, USA). Deionized water (18.2 MΩ cm), obtained from a Milli-Q water purification system, was used to prepare all aqueous solutions (Millipore, Bedford, MA, USA).

3.3.2 Synthesis and characterization of DTOs, ITOs, and MILs

The trihexyl(tetradecyl)phosphonium ([P_{66614}^+]) tris(hexafluoroacetylaceto)manganate(II) ([$Mn(hfacac)_3^-$]), [P_{66614}^+] tris(phenyltrifluoroacetylacetomanganate(II)) ([$Mn(Phtfacac)_3^-$]), trioctylbenzylammonium ([N_{888Bz}^+]) [$Mn(hfacac)_3^-$], and [N_{888Bz}^+] bis(hexafluoroacetylaceto)phenyltrifluoroacetylacetomanganate(II) ([$Mn(hfacac)_2(Phtfacac)^-$])

MILs were synthesized and characterized as previously reported.[33,36-38] MIL structures are shown in Figure 3.1. When not in use, all four MILs were stored at room temperature in a desiccator.

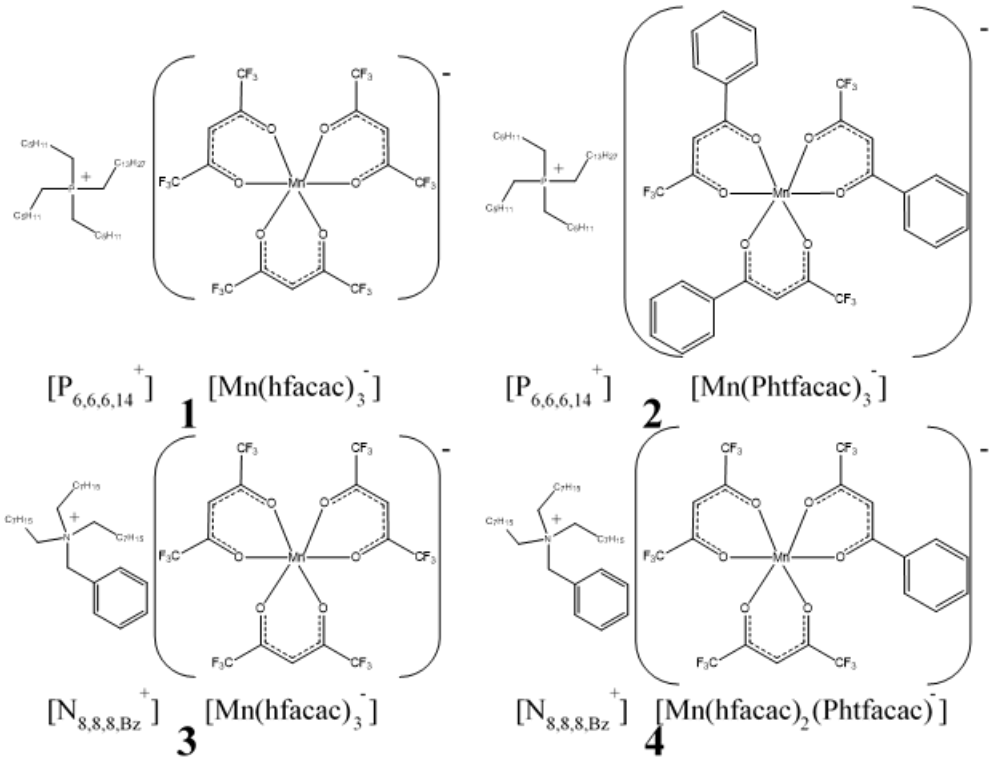

Figure 3.1 Chemical structures of the (1) $[P_{66614}^{+}][Mn(hfacac)_3^{-}]$, (2) $[P_{66614}^{+}][Mn(Phtfacac)_3^{-}]$, (3) $[N_{888Bz}^{+}][Mn(hfacac)_3^{-}]$, and (4) $[N_{888Bz}^{+}][Mn(hfacac)_2(Phtfacac)^{-}]$ MILs examined in this study.

The 1-allyl-3-octylimidazolium bromide ($[AOIM^{+}][Br^{-}]$), 1-allyl-3-decylimidazolium bromide ($[ADIM^{+}][Br^{-}]$), and 1-allyl-3-benzyllimidazolium bromide ($[ABzIM^{+}][Br^{-}]$) ILs were synthesized as previously reported.[29] In addition, all ITOs and DTOs were also synthesized as previously reported.[29,34] Briefly, 4 nmol of the thiol-modified oligonucleotide or 2 nmol of the cyclic disulfide-modified oligonucleotide was reduced using 40 nmol of TCEP. Subsequently, 400 nmol of either the $[AOIM^{+}][Br^{-}]$, $[ADIM^{+}][Br^{-}]$, or $[ABzIM^{+}][Br^{-}]$ salt (30% v/v ACN) was reacted with the reduced oligonucleotide under nitrogen (N_2) at 365 nm UV light for approximately 120 min. A NotePal X-slim Cooler Master (New Taipei City, Taiwan) was used

to cool the reaction to prevent solvent evaporation. The product was isolated using polyacrylamide gel electrophoresis (PAGE) and recovered by crushing the gel and eluting with water.

ITOs and DTOs were characterized using reversed-phase ion-pair liquid chromatography coupled to time-of-flight mass spectrometry (TOF-MS) on an Agilent 1260 Infinity high performance liquid chromatograph (HPLC) with a diode array detector coupled to an Agilent 6230B TOF mass spectrometer with an electrospray source. ITOs and DTOs were separated on a 50 mm × 2.1 mm i.d. × 1.8 mm particle size Zorbax Extend C_{18} column purchased from Agilent Technologies (Santa Clara, CA, USA). Mobile phase A contained 5 mM triethylammonium acetate (pH 7.4) and mobile phase B was ACN. The column was equilibrated for 20 min at 0.2 mL min^{-1} at 5% B. Gradient separation of ITO products was performed using the following program: 5% B from 0 to 5 min, increased from 5% to 19.4% B from 5 to 17 min, increased 19.4 − 35% B from 17 to 18 min, held at 35% B from 18 to 20 min, increased 35% B to 100% B from 20 to 30 min, and held at 100% B from 30 to 33 min. After each separation, the column was equilibrated at 5% B for 7 min prior to subsequent injections. The LC eluent was diverted to waste for the first 8 min to prevent non-volatile imidazolium salts and urea from entering the mass spectrometer. Nebulizing gas was set to 35 psi, and the drying gas (N_2) flow rate was 9 L min^{-1} at 350 °C using a capillary voltage of 4000 V. Spectra were acquired from 100 to 3000 m/z with a scan rate of 1 spectrum sec^{-1}. ITO and DTO structures are shown in Figure 3.2. The extracted ion chromatograms and mass spectra of the $[AOIM^+]_2$-*KRAS* 2$[Br^-]$, $[ADIM^+]_2$-*KRAS* 2$[Br^-]$, and $[ABzIM^+]_2$-*KRAS* 2$[Br^-]$ DTOs are shown in Figure B1 (Appendix B).

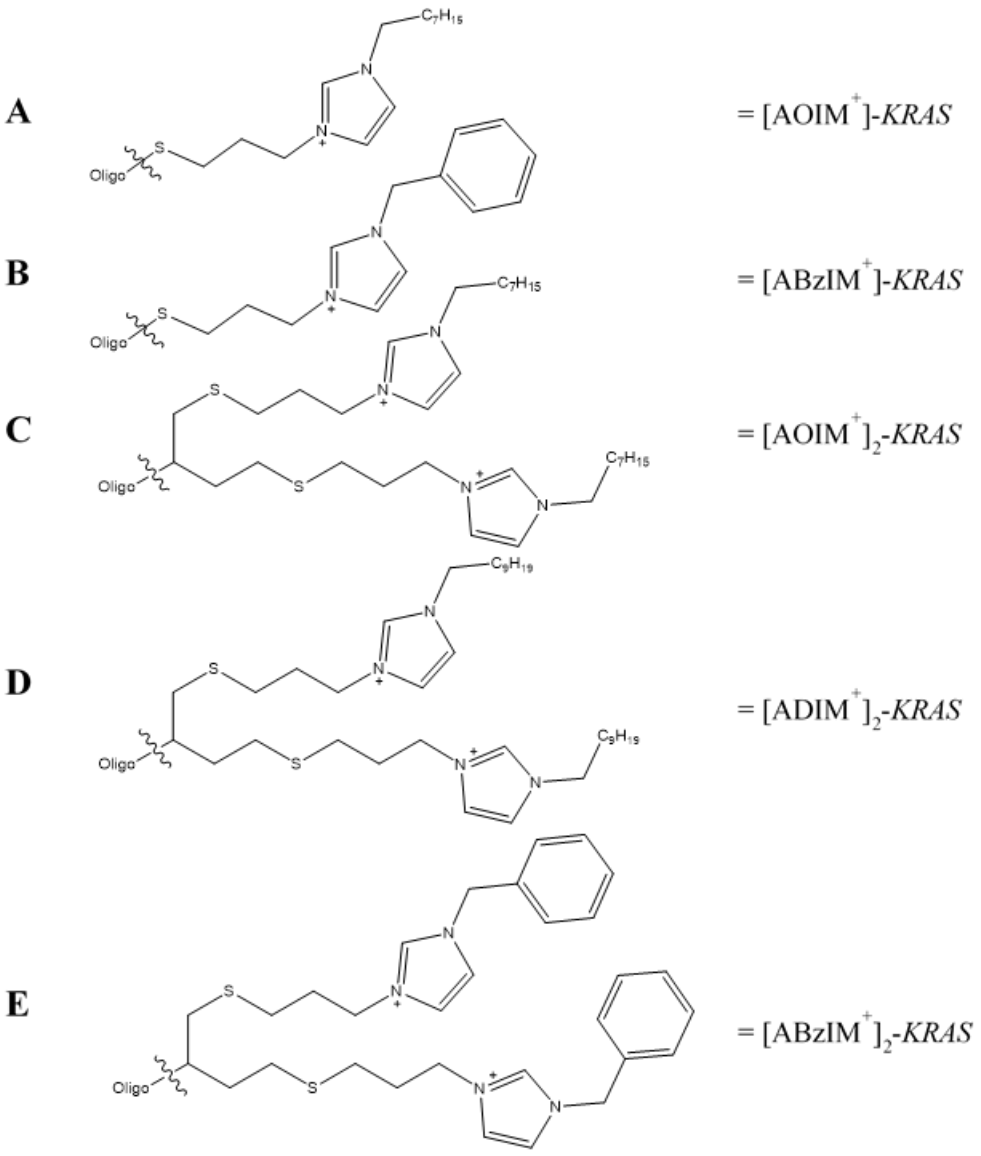

Figure 3.2 Chemical structures of the imidazolium-based ion tags associated with the (A-B) ITOs and (C-E) DTOs examined in this study.

3.3.3 Loading efficiency of ITOs and DTOs to the hydrophobic MIL

The stability of the interaction between the ITO/DTO-DNA duplex and MIL was determined by anion exchange chromatography using an Agilent 1260 HPLC with variable wavelength detection. First, 2 ppm of the DNA extraction probe was hybridized with 2 ppm of its complementary sequence in 25 mM NaCl by heating at 90 °C for 5 min then cooling to 4 °C

for 5 min. The ITO/DTO-DNA duplex was incubated for 10 min at room temperature with 1 µL of MIL. After this, 20 µL of the aqueous solution was injected onto a 35 mm × 4.6 mm i. d. × 2.5 µm TSKgel DEAE-NPR anion exchange column with a 5 mm × 4.6 mm i. d. × 5 µm TSKgel DEAE-NPR guard column from Tosoh Bioscience (King of Prussia, PA). Mobile phase A consisted of 20 mM Tris-HCl (pH 8) and mobile phase B was 20 mM Tris-HCl and 1 M NaCl (pH 8). The column was equilibrated with mobile phase A at 0.5 mL min^{-1} for 20 min prior to injection. Gradient elution was performed with the following program: increased from 0 to 50% B from 0 to 10 min, increased to 100% B from 10 min to 15 min, held at 100% B from 15 min to 20 min, decreased to 0% B from 20 min to 22 min, held at 0% B from 22 min to 30 min.

3.3.4 qPCR conditions

Quantitative PCR (qPCR) was achieved using 1x Sso Supermix and 1x PrimePCR assay mix with a final volume of 20 µL. Addition of 0.3 µL $[P_{66614}^+][Mn(hfacac)_3^-]$ MIL to the qPCR buffer required 1x Sso Supermix and 1x PrimePCR assay mix, 4 mM EDTA, and an additional 1x SYBR Green I to relieve inhibition caused by the MIL. Direct MIL-qPCR amplification using the $[N_{888Bz}^+][Mn(hfacac)_3^-]$ MIL required 1x Sso Supermix and 1x PrimePCR assay mix, additional 6.25 mM $MgCl_2$, 4 mM EDTA, and an additional 0.4x SYBR Green I. A 20 µL qPCR containing 0.3 µL of the $[N_{888Bz}^+][Mn(hfacac)_2(Phtfacac)^-]$ MIL required 1x Sso Supermix and 1x PrimePCR assay mix, an additional 2.5 mM $MgCl_2$, 2 mM EDTA, and an additional 1x SYBR Green I. Amplification was achieved on a Bio-rad CFX 96 qPCR using the following cycling protocol: 2 min initial denaturation at 95 °C followed by 40 cycles comprised of a 5 s denaturation step at 95 °C, a 30 s annealing step at 60 °C, and an optical detection step. Quantification cycles (Cq) were determined using the Bio-Rad CFX Maestro software. A standard curve was constructed for the *KRAS* template, as shown in Figure B2, and used to determine the amount of target extracted using the ITO-MIL procedure. Enrichment factors (E_f)

were determined using Equation 3.1 where C_{MIL} is the amount of DNA extracted by 0.3 µL of MIL and C_{std} is the amount of DNA present in a 0.3 µL of the solution prior to the extraction.

$$E_f = \frac{C_{MIL}}{C_{std}} \quad \text{Equation 3.1}$$

3.3.5 Extraction of target DNA

Static extractions were used to selectively extract high concentrations of target DNA using previously published methods, with slight modifications.[29,34] Briefly, 7.2×10^7 copies μL^{-1} (112 pM) of target DNA was hybridized to either 3.6×10^8 copies μL^{-1} of DTO or 7.2×10^8 copies μL^{-1} of ITO by heating the solution at 90 °C for 5 min to denature double-stranded DNA followed by cooling to 4 °C for 5 min. After hybridization, 1 µL of MIL was added to the sample for 10 min at room temperature. Subsequently, the MIL was washed with water to remove non-specifically adsorbed DNA and inhibitors from the surface of the MIL. Target DNA was subsequently desorbed in 50 µL of 25−400 mM NaCl at 90 °C for 1−10 min.

Dispersive extractions were achieved using the previously optimized method with a DTO probe to target ratio of 5:1 and ITO probe to target ratio of 10:1.[33,34] Briefly, 4, 6, or 8 µL of the $[N_{888Bz}^+][Mn(hfacac)_2(Phtfacac)^-]$, $[N_{888Bz}^+][Mn(hfacac)_3^-]$, and $[P_{66614}^+][Mn(hfacac)_3^-]$ MILs, respectively, were dispersed in a 1 mL solution containing 2×10^4 copies μL^{-1} (33 fM) of *KRAS* DNA using a vortex (Barnstead International, Dubuque, IA). After a 1 or 3 min dispersion, the MIL was collected using a 0.66 T rod magnet, and 0.3 µL of the recovered MIL was added to qPCR buffer.

Extractions using the M−270 streptavidin-coated magnetic beads were performed as recommended by the manufacturer. Prior to every extraction, 10 µg of magnetic beads were washed three times with 5 mM Tris-HCl, 0.5 mM EDTA, and 1 M NaCl (pH 7.5). All DNA

extractions consisted of 10:1 biotinylated probe to target ratio in 25 mM NaCl. The sample was initially heated at 90 °C for 5 min then cooled to 4 °C for 5 min to anneal the biotinylated probe to the target. Samples were subsequently agitated at 60 rpm or 250 rpm for extractions of 7.2×10^7 and 2×10^4 copies μL^{-1} *KRAS*, respectively, on an orbital shaker for 10 min to disperse the beads and minimize sedimentation. The beads were collected using a 0.9 T magnet and washed three times with a solution consisting of 5 mM Tris-HCl, 0.5 mM EDTA, and 1 M NaCl (pH 7.5). DNA was desorbed from the beads in 20 µL water by heating to 90 °C for 10 min.

Target *KRAS* DNA was spiked into plasma and whole blood matrices. Plasma samples were diluted using water whereas whole blood was diluted in saline in order to prevent settling of cellular debris prior to the extraction. The amount of total genomic DNA in whole blood was determined using the QIAmp DNA mini-prep kit following procedures suggested by the manufacturer.

3.3.6 Statistical analysis

The Student *t*-test was used to determine whether the DTO or ITO probe was extracting significantly more DNA. Selectivity was also determined using the Student *t*-test by comparing the extractions with and without a DNA extraction probe. Probability values (p-values) were determined from the *t*-test results, and a significance level of 0.05 was chosen. Therefore, if the p-value is less than 0.05, the two data sets were considered statistically different.

3.4 Results and discussion

3.4.1 Synthesis of novel DTO probes

Since ITO and DTO probes can interact with the MIL through hydrophobic interactions, incorporation of longer alkyl chain substituents within the probe would be expected to improve the amount of DNA loaded to the MIL. Previously, an $[AOIM^+][Br^-]$ ITO specific to a 261 bp DNA sequence was capable of achieving a modest loading efficiency of 48 ± 4% with the

$[P_{66614}^{+}][Mn(hfacac)_3^{-}]$ MIL; however, increasing the alkyl chain by just two carbons significantly improved the loading efficiency to 75 ± 5%.[34] In this study, a novel DTO containing two decyl-imidazolium headgroups was synthesized to further improve the loading efficiency of the probe to the MIL. Attempts to synthesize a DTO with alkyl chains longer than ten carbon atoms resulted in the allylimidazolium cation reacting with only one of the two thiol groups, as shown using MS (Figure B3). The incomplete reaction maybe due to the imidazolium salt exhibiting surfactant-like properties and forming aggregates with the cyclic disulfide-modified oligonucleotide.[39]

In order to identify the optimum ITO and DTO for loading target DNA to the MIL, the loading efficiency of four ITOs and seven DTOs to three hydrophobic MILs was studied, as shown in Figure 3.3. The $[AOIM^{+}]$-*KRAS* $[PF_6^{-}]$ ITO (56.94 ± 1.61%) provided the highest loading efficiency to the $[P_{66614}^{+}][Mn(hfacac)_3^{-}]$ MIL whereas there was no significant difference in loading efficiencies observed for the $[ADIM^{+}]_2$-*KRAS* 2$[Br^{-}]$ (87.65 ± 2.21%) and $[ADIM^{+}]_2$-*KRAS* 2$[OS^{-}]$ DTOs (83.56 ± 5.06%). For the $[N_{888Bz}^{+}][Mn(hfacac)_3^{-}]$ MIL, the $[ABzIM^{+}]$-*KRAS* $[Br^{-}]$ ITO (65.94 ± 9.55%) produced the highest loading and there was no significant difference in loading for the $[ADIM^{+}]_2$-*KRAS* $[Br^{-}]$ (86.28 ± 4.39%), $[ADIM^{+}]_2$-*KRAS* $[PF_6^{-}]$ (94.28 ± 2.47%), and $[ABzIM^{+}]_2$-*KRAS* $[Br^{-}]$ DTOs (89.2 ± 2.68%). Based on the Student *t*-test, there was no significant advantage in loading of the DNA extraction probe to the $[N_{888Bz}^{+}][Mn(hfacac)_2(Phtfacac)^{-}]$ MIL using either the $[AOIM^{+}]_2$-*KRAS* 2$[Br^{-}]$ (56.91 ± 7.67%) or $[ADIM^{+}]_2$-*KRAS* 2$[Br^{-}]$ DTOs (60.83 ± 3.95%). Among the ITOs and DTOs examined, the $[ABzIM^{+}]$-*KRAS* $[Br^{-}]$ ITO (53.69 ± 2.27%) produced the highest loading efficiency using the $[N_{888Bz}^{+}][Mn(hfacac)_2(Phtfacac)^{-}]$ MIL.

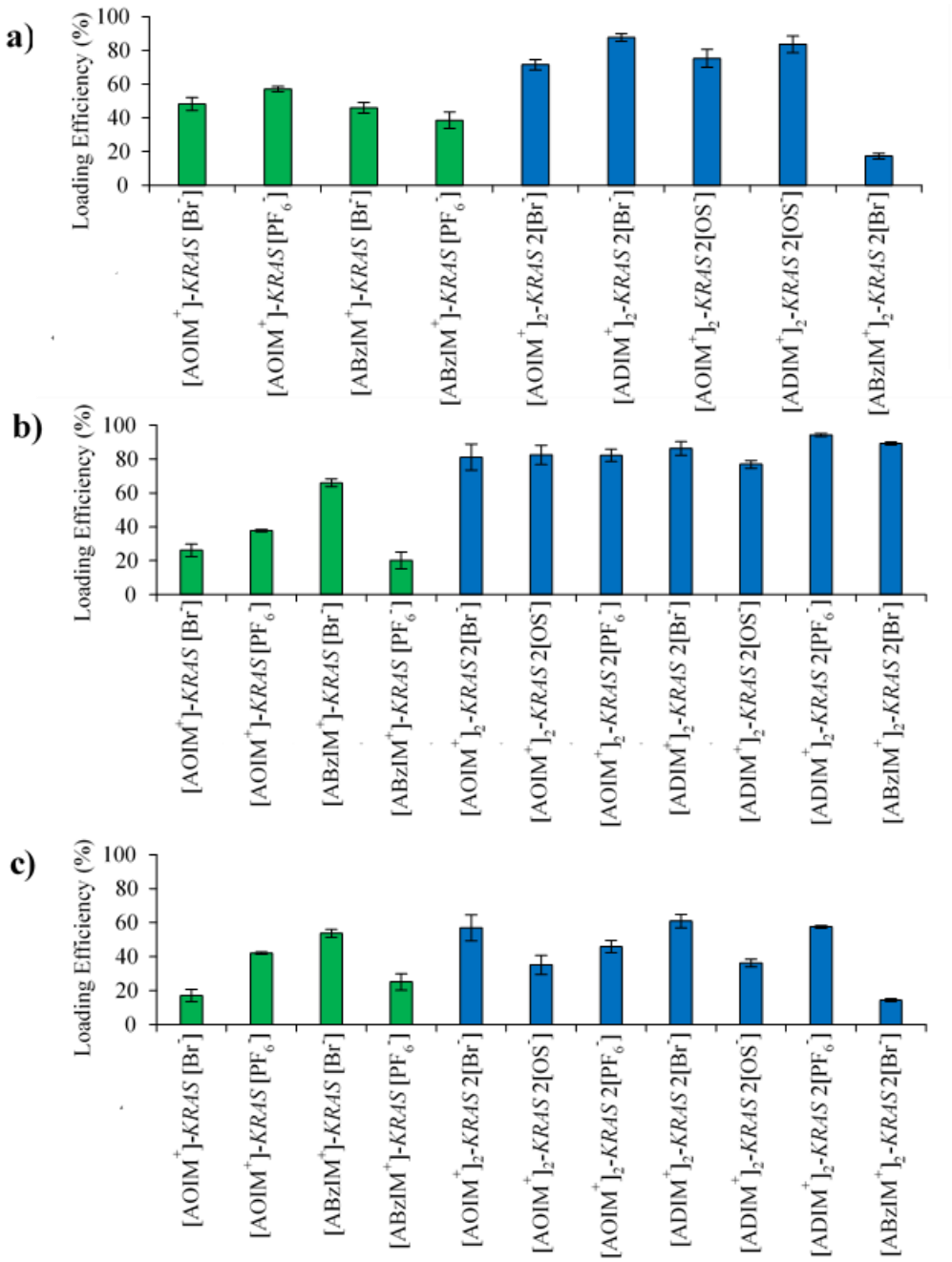

Figure 3.3 Loading efficiencies of the ITO and DTO probes to the (a) $[P_{66614}^{+}][Mn(hfacac)_3^{-}]$, (b) $[N_{888Bz}^{+}][Mn(hfacac)_3^{-}]$ and (c) $[N_{888Bz}^{+}][Mn(hfacac)_2(Phtfacac)^{-}]$ MILs. ITO or DTO concentration: 2 ng μL^{-1}; *KRAS* complement: 2 ng μL^{-1}; NaCl concentration: 25 mM; sample volume: 60 µL; MIL volume: 1 µL; extraction time: 10 min.

It was previously reported that ITOs containing the $[OS^{-}]$ anion exhibited superior loading to the MIL solvent compared to $[Br^{-}]$, bis[(trifluoromethyl)sulfonyl]imide, or

perfluorobutanesulfonate anions suggesting that the anion plays an important role in facilitating the capture of the ITO by the MIL.[34] Therefore, replacing the [Br^-] anion within the DTO structure with the amphiphilic [OS^-] anion should improve the loading of the DTO probe to the MIL. However, introducing the [OS^-] anion to the DTO did not significantly improve the loading efficiency. Utilizing the [PF_6^-] anion to facilitate fluorophilic interactions between the DTO and MIL also did not improve the loading of the probe to the MIL. These results suggest that the anion component of the DTO plays a less important role in facilitating interactions between the DTO and the MIL compared to the ITO probe. Interestingly, the [$ABzIM^+$]$_2$-*KRAS* 2[Br^-] DTO showed relatively low loading to the [P_{66614}^+][$Mn(Phtfacac)_3^-$] (17.21 ± 1.70%) and [N_{888Bz}^+][$Mn(hfacac)_2(Phtfacac)^-$] (14.23 ± 0.91%) MILs. The [$ABzIM^+$]$_2$-*KRAS* 2[Br^-] DTO was effective at loading to the [N_{888Bz}^+][$Mn(hfacac)_3^-$] MIL and the [$ABzIM^+$]-*KRAS* [Br^-] ITO exhibited the highest loading efficiencies for the [N_{888Bz}^+][$Mn(hfacac)_3^-$] and [N_{888Bz}^+][$Mn(hfacac)_2(Phtfacac)^-$] MILs. These results suggest that exploiting π-π stacking interactions with the DTOs is effective when the aromatic moieties are only in the cation.

3.4.2 Distinguishing SNPs from target DNA using ITO and DTO probes

In blood plasma samples, especially with late stage cancer patients, there are large amounts of non-target background DNA fragments (ranging from 0 to 100 pM) that can potentially be coextracted.[27] In addition, ctDNA fragments are prone to SNPs and require great care to ensure that only the desired sequence is detected. To evaluate the effect interfering DNA has on the annealing of target DNA to the extraction probe, extractions from samples containing 7.2×10^7 copies μL^{-1} of 20 nt complement, 1 nt mismatch, or 2 nt mismatch fragments (i.e., 1:1 ratio with target DNA) were performed using the [P_{66614}^+][$Mn(hfacac)_3^-$] MIL and streptavidin coated magnetic beads. Without interfering fragments present, the [$ADIM^+$]$_2$-*KRAS* 2[Br^-] and [$ADIM^+$]$_2$-*KRAS* 2[OS^-] DTOs extracted the most DNA (target capture Cq of 21.13 ± 0.30 and

21.28 ± 0.05, respectively). The addition of a 20 nt complementary sequence to the sample resulted in a higher target capture Cq indicating that less of the 120 bp target was extracted, as shown in Figure B4. These results suggest that the complementary fragment competed with the 120 bp amplicon for the probe causing lower DNA recoveries. The addition of either 1 or 2 nt mismatch fragments to the sample solution did not significantly increase the target capture Cq when using the $[AOIM^+]_2$-*KRAS* $[PF_6^-]$, $[ABzIM^+]$-*KRAS* $[Br^-]$, $[AOIM^+]_2$-*KRAS* 2$[Br^-]$, $[AOIM^+]_2$-*KRAS* 2$[OS^-]$, $[ADIM^+]_2$-*KRAS* 2$[Br^-]$, and $[ADIM^+]_2$-*KRAS* 2$[OS^-]$ extraction probes. This suggests that the 1 nt and 2 nt mismatch fragments are not interfering with the annealing of target DNA to the probe.

The streptavidin-coated magnetic beads also experienced an increase in target capture Cq when performing extractions in the presence of a 20 nt complement. However, the target capture Cq also increased when performing extractions with 1 nt and 2 nt mismatch fragments spiked in the sample. This increase suggests that the biotinylated probe is annealing to the 1 and 2 nt mismatch fragment and, therefore, reducing the amount of target DNA that can be captured.

3.4.3 Optimization of the desorption step

Although there has been a significant amount of work performed to improve the loading efficiency of the ITO-DNA duplex to the MIL, few studies have evaluated the desorption step. Therefore, the desorption time and ionic strength of the desorption solution were optimized to improve the recovery of DNA from the $[P_{66614}^+][Mn(hfacac)_3^-]$, $[N_{888Bz}^+][Mn(hfacac)_3^-]$, and $[N_{888Bz}^+][Mn(hfacac)_2(Phtfacac)^-]$ MILs. As shown in Figure B5, an optimum desorption time of 4 min was achieved for the $[P_{66614}^+][Mn(hfacac)_3^-]$ and $[N_{888Bz}^+][Mn(hfacac)_2(Phtfacac)^-]$ MILs, and an optimum desorption time of 4 min and 8 min was achieved for the $[N_{888Bz}^+][Mn(hfacac)_3^-]$ MIL with the ITO and DTO probe, respectively. Less DNA was recovered after longer desorption times likely due to DNA adsorbing to the polypropylene tube.[40]

Therefore, 0.05% Tween 20 was added to the desorption solution in an effort to minimize adsorption. A 4 min desorption time was chosen as optimum due to the high amount of DNA recovered using all three MILs, while still maintaining a short desorption time. In addition, the presence of NaCl greatly promoted the desorption of DNA, as shown in Figure B6. The optimum concentration of NaCl was 100 mM for the $[P_{66614}^+][Mn(hfacac)_3^-]$ MIL, 200 mM for the $[N_{888Bz}^+][Mn(hfacac)_3^-]$ MIL, and 50 mM for the $[N_{888Bz}^+][Mn(hfacac)_2(Phtfacac)^-]$ MIL. There was no significant difference between the amount of DNA detected when ITO and DTO were used to extract DNA if desorbing at higher ionic strength. This suggests that electrostatic interactions between the ITO or DTO and the MIL may also play a role in the capture of the ITO/DTO-DNA duplex.

Recent studies have exploited the elevated temperatures required for PCR to desorb DNA from the MIL solvent during the reaction.[32,33,41] Adding DNA-enriched MIL to the PCR buffer is highly beneficial as it reduces the number of sample handling steps, allowing for higher sample throughput and minimizes the possibility of contamination. Interestingly, despite similar target capture Cqs being achieved with the DTO and ITO probes using 25−400 mM NaCl as a desorption solution, lower target capture Cqs and higher E_f were achieved using the ITOs when desorbing in 1x Sso Supermix, as shown in Figures B7 and B8.

3.4.4 Sequence-specific DNA extractions from complex matrices

Several reported sequence-specific DNA extraction procedures isolate total DNA prior to an extraction due to the complexity of the sample matrix.[20,42] However, this is often very time consuming, and an ideal sequence-specific DNA extraction should be capable of selectively extracting DNA from complex sample matrices. Previously, the ITO-MIL procedure has been applied towards bacterial cell lysate (1.53×10^8 *E. coli* cells),[29] 10-fold diluted plasma,[33] and plant cell lysate.[35] However, it has been unclear if either the ITO or DTO probe can extract more

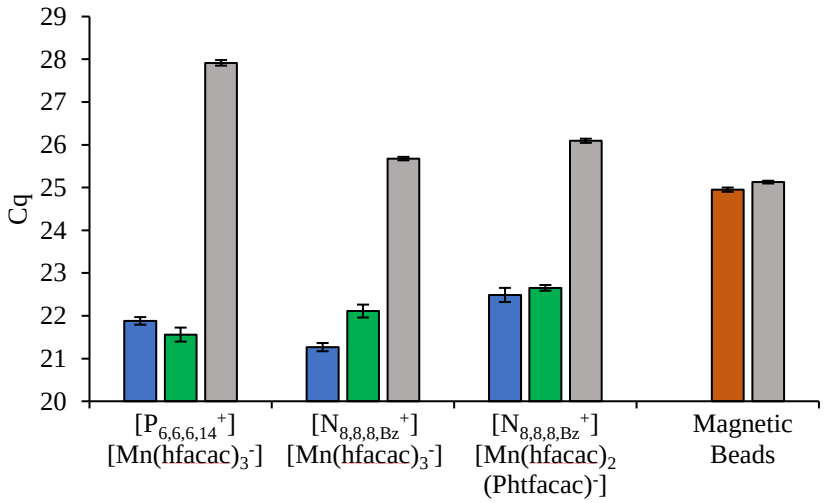

Figure 3.4 Target capture Cq associated with the static extraction using the (blue) $[ADIM^+]_2$-*KRAS* $2[Br^-]$ DTO, (green) highest loading ITO, (orange) biotinylated probe, and (grey) without a DNA extraction probe from 10-fold diluted plasma. ITO/DTO-MIL method: *KRAS* template concentration: 7.2×10^7 copies μL^{-1}, amount of $[ADIM^+]_2$-*KRAS* $2[Br^-]$ DTO relative to DNA: 5:1, amount of $[AOIM^+]$-*KRAS* $[PF_6^-]$ ITO relative to DNA: 10:1, sample volume: 50 µL, MIL volume: 1 µL; extraction time: 10 min, desorption time: 4 min, desorption volume: 50 µL. Dynabeads M−270 Steptavidin magnetic beads conditions: *KRAS* template concentration: 2×10^4 copies μL^{-1}, concentration of biotinylated probe: 332 fM, NaCl concentration: 25 mM, extraction time: 10 min; agitation rate: 250 rpm; desorption time: 10 min; desorption volume: 50 µL. (For interpretation of the references to colour in this figure legend, the reader is referred to the Web version of this article.)

DNA from complex matrices. When comparing the extraction of *KRAS* from 10-fold diluted plasma using the DTO or ITO probe, more DNA was detected using the $[AOIM^+]$-*KRAS* $[PF_6^-]$ ITO with the $[P_{66614}^+][Mn(hfacac)_3^-]$ MIL and the $[ADIM^+]_2$-*KRAS* $2[Br^-]$ DTO probe with the $[N_{888Bz}^+][Mn(hfacac)_3^-]$ MIL, as shown in Figure 3.4. There was no significant difference observed between the $[ADIM^+]_2$-*KRAS* $2[Br^-]$ DTO and $[ABzIM^+]$-*KRAS* $[Br^-]$ ITO probes with the $[N_{888Bz}^+][Mn(hfacac)_2(Phtfacac)^-]$ MIL in 10-fold diluted plasma. At femtomolar concentration-levels of target DNA, similar E_f was achieved using either the $[ADIM^+]_2$-*KRAS* $2[Br^-]$ DTO or $[ABzIM^+]$-*KRAS* $[Br^-]$ ITO probes with the $[N_{888Bz}^+][Mn(hfacac)_3^-]$ or $[N_{888Bz}^+][Mn(hfacac)_2(Phtfacac)^-]$ MILs, as shown in Figure 3.5. The $[AOIM^+]$-*KRAS* $[PF_6^-]$

ITO was capable of preconcentrating significantly more DNA from 10-fold diluted plasma compared to the $[ADIM^+]_2$-*KRAS* 2$[Br^-]$ DTO probe with the $[P_{66614}^+][Mn(hfacac)_3^-]$ MIL.

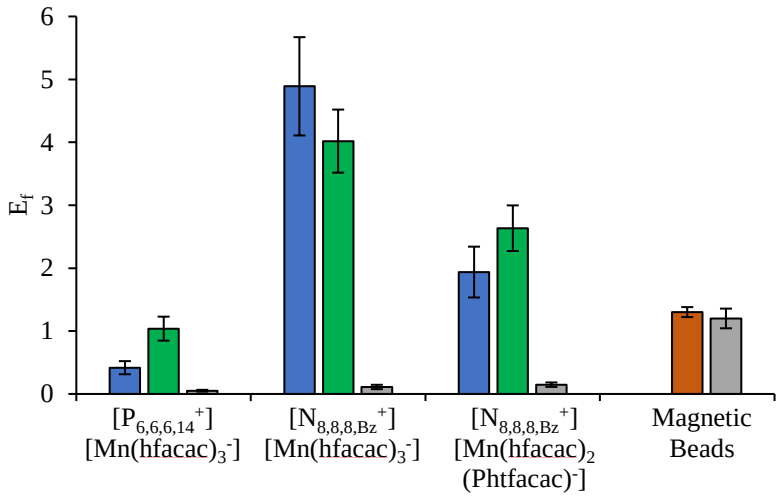

Figure 3.5 Enrichment factors from the dispersive extraction using the (blue) $[ADIM^+]_2$-*KRAS* 2$[Br^-]$ DTO, (green) highest loading ITO, (orange) biotinylated probe, and (grey) without a DNA extraction probe from 10-fold diluted plasma. $[P_{66614}^+][Mn(hfacac)_3^-]$ MIL conditions: amount of $[ADIM^+]_2$-*KRAS* 2$[Br^-]$ DTO relative to DNA: 5:1, amount of $[AOIM^+]$-*KRAS* $[PF_6^-]$ ITO relative to DNA: 10:1, NaCl concentration: 25 mM, sample volume: 1.0 mL, extraction time: 3 min $[N_{888Bz}^+][Mn(hfacac)_3^-]$ MIL conditions: amount of $[ADIM^+]_2$-*KRAS* 2$[Br^-]$ DTO relative to DNA: 5:1, amount of $[ABzIM^+]$-*KRAS* $[Br^-]$ relative to DNA: 10:1, NaCl concentration: 25 mM, sample volume: 1.0 mL, extraction time: 1 min $[N_{888Bz}^+][Mn(hfacac)_2(Phtfacac)^-]$ MIL conditions: amount of $[ADIM^+]_2$-*KRAS* 2$[Br^-]$ DTO relative to DNA: 5:1, amount of $[ABzIM^+]$-*KRAS* $[Br^-]$ relative to DNA: 10:1, NaCl concentration: 25 mM, sample volume: 1.0 mL, extraction time: 1 min. Dynabeads M−270 Steptavidin magnetic beads conditions: concentration of biotinylated probe: 332 fM; extraction time: 10 min; agitation rate: 250 rpm; desorption time: 10 min; desorption volume: 20 µL. (For interpretation of the references to colour in this figure legend, the reader is referred to the Web version of this article.)

Selective preconcentration of 2×10^2 and 2×10^3 copies μL^{-1} (0.33 and 3.3 fM, respectively) of *KRAS* from 10-fold diluted plasma was achieved using the ITO and DTO probes, as shown in Figure B9. However, based on the Student *t*-test there was no significant difference in E_f using the DTO or ITO at these concentrations suggesting that both probes function similarly at enriching low concentrations of DNA. When performing extractions of 2×10^2

copies μL^{-1} of *KRAS* from 10-fold diluted plasma, the $[N_{888Bz}^+][Mn(hfacac)_3^-]$ and $[N_{888Bz}^+][Mn(hfacac)_2(Phtfacac)^-]$ MILs exhibited slight preconcentration of DNA suggesting that the selectivity of the ITO/DTO-MIL method worsens as the concentration of target DNA decreases. Interestingly, extractions of either 7.2×10^7 or 2×10^4 copies μL^{-1} *KRAS* DNA from 10-fold diluted plasma using streptavidin-coated magnetic beads were not selective. It is possible that free biotin naturally found in plasma blocks binding sites on the beads or that the biotinylated probe is binding to plasma proteins.[43-45]

Previous studies have shown that imidazolium ILs that contain longer alkyl chain substituents (i.e., octyl chain length) interact more with proteins.[46] In the case of the ITO/DTO-procedure, the longer alkyl chains are used to improve loading of the probe-DNA duplex to the hydrophobic MIL; however, it is unclear if certain ITOs or DTOs strongly interact with plasma proteins instead of the MIL. Therefore, extractions from 10-fold diluted plasma were performed using the $[ADIM^+]_2$-*KRAS* $2[Br^-]$ and $[ABzIM^+]_2$-*KRAS* $2[Br^-]$ DTOs with the $[N_{888Bz}^+][Mn(hfacac)_3^-]$ MIL and the $[ADIM^+]_2$-*KRAS* $2[Br^-]$ and $[ADIM^+]_2$-*KRAS* $2[OS^-]$ DTOs with the $[P_{66614}^+][Mn(hfacac)_3^-]$ MIL. These DTOs were chosen because they exhibited similar loading efficiencies and, therefore, should extract similar amounts of DNA. As shown as Figure B10, the target capture Cqs associated with the extractions using the $[ADIM^+]_2$-*KRAS* $2[Br^-]$ and $[ABzIM^+]_2$-*KRAS* $2[Br^-]$ DTOs with the $[N_{888Bz}^+][Mn(hfacac)_3^-]$ and the $[ADIM^+]_2$-*KRAS* $2[Br^-]$ and$[ADIM^+]_2$-*KRAS* $2[OS^-]$ DTOs with the $[P_{66614}^+][Mn(hfacac)_3^-]$ MIL were within error. The target capture Cqs suggest that the different DTO probes suffer from similar matrix effects due to the plasma components.

Diluting the sample matrix can be beneficial as it decreases the concentration of PCR inhibitors and reduces the amount of protein aggregates. However, diluting the sample matrix

also decreases the concentration of DNA making it more challenging to detect low abundance mutations. Therefore, ITO/DTO-MIL extractions from 2-fold diluted plasma were investigated. Selective extractions from 2-fold diluted plasma were achieved for all three MILs, as shown in Figure B11. However, extractions using the DTO probe produced lower target capture Cqs compared to extractions using the ITO probes, possibly due to stronger interactions between the probe and hydrophobic MIL. The streptavidin-coated magnetic beads were capable of selective extraction in 2-fold diluted plasma whereas previously the extractions with and without the biotinylated probe in 10-fold diluted plasma were within error of one another. This may be linked to the significant amount of protein aggregation that occurs during the annealing step with 2-fold diluted plasma. Protein precipitation could limit the amount of biotinylated probe that interacts with soluble plasma proteins and allow for higher DNA recoveries.[43]

In most ctDNA sample preparation methods, ctDNA is extracted from plasma instead of whole blood due to the high probability of contaminating the sample with genomic DNA from circulating cells.[47,48] To ensure that plasma is cell-free, a lengthy double centrifugation step is required.[47,48] In addition, the process of generating plasma from blood removes circulating cell surface-bound DNA from analysis, which can aid cancer diagnosis and monitoring.[49] Therefore, the ITO/DTO-MIL method was applied towards the extraction of *KRAS* from 10-fold diluted whole blood to examine if selective extraction could be achieved. When performing ITO/DTO-MIL extractions from 10-fold diluted blood at picomolar levels of DNA, selective extraction was achieved using the $[P_{66614}^+][Mn(hfacac)_3^-]$ and $[N_{888Bz}^+][Mn(hfacac)_3^-]$ MILs, as shown in Figure 3.6. However, selective extraction could not be achieved using the $[ABzIM^+]$-*KRAS* $[Br^-]$ ITO with the $[N_{888Bz}^+][Mn(hfacac)_2(Phtfacac)^-]$ MIL or the magnetic beads. Selective extraction using the magnetic beads could only be achieved when diluting the blood 40-fold, as shown in

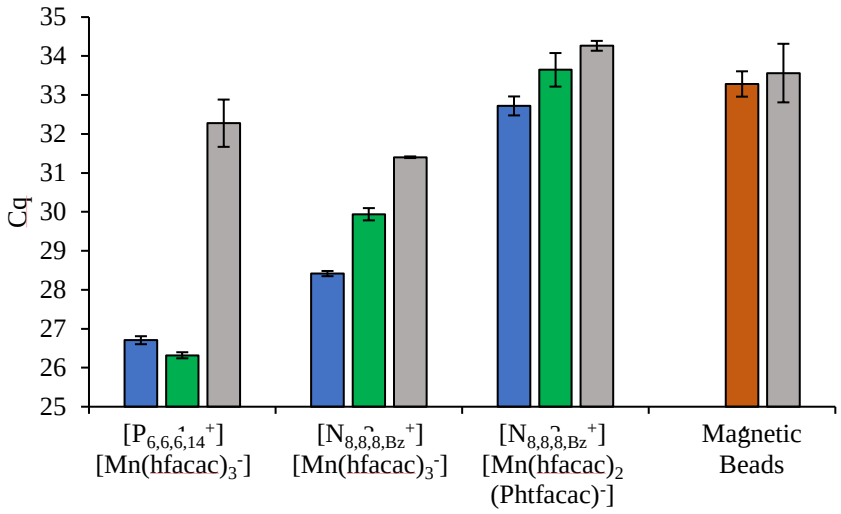

Figure 3.6 Target capture Cq obtained from static extraction using the (blue) $[ADIM^+]_2$-*KRAS* 2$[Br^-]$ DTO, (green) highest loading ITO, and (orange) biotinylated probe compared to extractions (grey) without a DNA extraction probe from 10-fold diluted blood. ITO/DTO-MIL method: *KRAS* template concentration: 7.2×10^7 copies μL^{-1}, amount of $[ADIM^+]_2$-*KRAS* 2$[Br^-]$ DTO relative to DNA: 5:1, amount of $[AOIM^+]$-*KRAS* $[PF_6^-]$ ITO relative to DNA: 10:1, sample volume: 50 µL, MIL volume: 1 µL; extraction time: 10 min, desorption time: 4 min, desorption volume: 50 µL. Dynabeads M−270 Steptavidin magnetic beads conditions: *KRAS* template concentration: 7.2×10^7 copies μL^{-1}, concentration of biotinylated probe: 7.2×10^8 copies μL^{-1}; extraction time: 10 min; agitation rate: 250 rpm; desorption time: 10 min; desorption volume: 50 µL. (For interpretation of the references to colour in this figure legend, the reader is referred to the Web version of this article.)

Figure B12. It was also possible to achieve selective extraction using the streptavidin-coated magnetic beads by proteinase K treatment at 56 °C for 15 min prior to annealing the probe to target DNA, as shown in Figure 3.7. In this procedure, the sample was also filtered to remove cellular debris and precipitated proteins before the magnetic beads were added. It was found that the $[N_{888Bz}^+][Mn(hfacac)_2(Phtfacac)^-]$ MIL was unable to selectively extract target DNA due to the saline solution used to dilute whole blood, as shown in Figure B13. Extractions from saline using the $[P_{66614}^+][Mn(hfacac)_3^-]$ or $[N_{888Bz}^+][Mn(hfacac)_3^-]$ MILs resulted in higher target capture Cqs when compared to extractions performed from pure water, possibly due to the higher ionic strength increasing the melting temperature of the target DNA. The ITO probes were

capable of extracting more DNA from saline compared to the DTO, but all extractions from saline with the $[P_{66614}^+][Mn(hfacac)_3^-]$ or $[N_{888Bz}^+][Mn(hfacac)_3^-]$ MILs were selective.

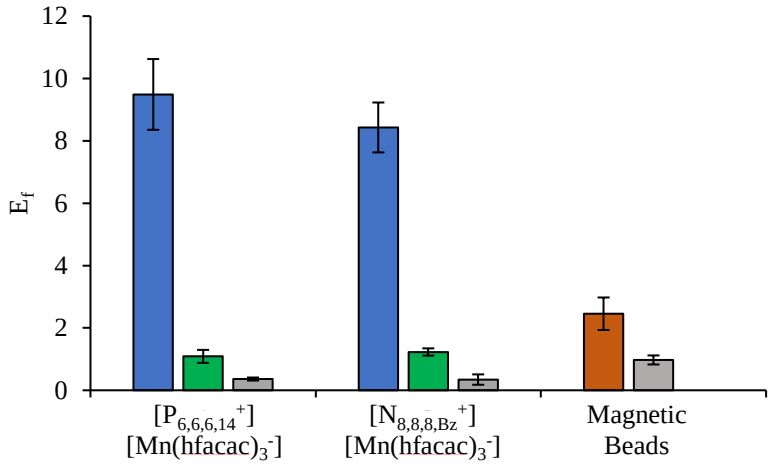

Figure 3.7. Enrichment factor produced from the dispersive extraction of *KRAS* target using the (blue) $[ADIM^+]_2$-*KRAS* 2$[Br^-]$ DTO, (green) highest loading ITO, and (orange) biotinylated probe compared to extractions (grey) without a DNA extraction probe from 10-fold diluted blood. $[P_{66614}^+][Mn(hfacac)_3^-]$ MIL conditions: amount of $[ADIM^+]_2$-*KRAS* 2$[Br^-]$ DTO relative to DNA: 5:1, amount of $[AOIM^+]$-*KRAS* $[PF_6^-]$ ITO relative to DNA: 10:1, NaCl concentration: 25 mM, sample volume: 1.0 mL, extraction time: 3 min $[N_{888Bz}^+][Mn(hfacac)_3^-]$ MIL conditions: amount of $[ADIM^+]_2$-*KRAS* 2$[Br^-]$ DTO relative to DNA: 5:1, amount of $[ABzIM^+]$-*KRAS* $[Br^-]$ relative to DNA: 10:1, NaCl concentration: 25 mM, sample volume: 1.0 mL, extraction time: 1 min. Dynabeads M−270 Steptavidin magnetic beads conditions: concentration of biotinylated probe: 332 fM, extraction time: 10 min; agitation rate: 250 rpm; desorption time: 10 min; desorption volume: 20 µL. (For interpretation of the references to colour in this figure legend, the reader is referred to the Web version of this article.)

When performing extractions from clinically-relevant concentrations of ctDNA, selective extraction using either the ITO or DTO probes was achieved with the $[P_{66614}^+][Mn(hfacac)_3^-]$ and $[N_{888Bz}^+][Mn(hfacac)_3^-]$ MILs, as shown in Figure 3.7. However, the DTO preconcentrated significantly more DNA compared to the ITO in whole blood matrices possibly due to stronger interactions between the probe and MIL during the extraction and washing steps. When performing extractions at 2×10^2 and 2×10^3 copies μL^{-1} (mutation abundance of 0.009% and 0.09%, respectively) with the $[P_{66614}^+][Mn(hfacac)_3^-]$ and $[N_{888Bz}^+][Mn(hfacac)_3^-]$ MILs,

selective preconcentration of target DNA could still be achieved using the $[ADIM^+]_2$-*KRAS* 2$[Br^-]$ DTO, as shown in Figure B14. However, extractions of 2×10^2 copies μL^{-1} *KRAS* from 10-fold diluted blood resulted in slight preconcentration when the DTO probe was not present, again suggesting that the DTO-MIL method is prone to coextraction under conditions of low target DNA concentration. This effect could possibly be limited by designing the MIL to further limit DNA extraction.

3.5 Conclusions

The ability of the ITO/DTO-MIL method to selectively extract DNA from 2-fold diluted plasma, 10-fold diluted plasma, and 10-fold diluted whole blood has been demonstrated. The desorption time and ionic strength of the desorption solution were optimized to ensure the maximum amount of DNA was desorbed from the MIL in a short amount of time (i.e., 4 min), with higher ionic strength significantly facilitating the desorption of DNA from the hydrophobic MIL. ITO probes were successful at extracting more DNA in saline compared to DTO probes, but DTO probes outperformed ITOs by extracting more DNA from complex biological matrices, including 2-fold diluted plasma and 10-fold diluted blood. However, there was no significant difference in enrichment factor when performing extractions from 10-fold diluted plasma with either the ITO or DTO. In comparison, commercially-available streptavidin-coated magnetic beads only exhibited selectivity in 2-fold diluted plasma and 40-fold diluted whole blood without labor-intensive sample clean-up steps. The DTO-MIL method represents a simple two-step extraction procedure to selectively preconcentrate low concentrations of DNA from increasingly complex matrices, suggesting that this method has the potential to be highly valuable in the field of ctDNA detection and analysis.

3.6 Declaration of competing interest

The authors declare that they have no known competing financial interests or personal relationships that could have appeared to influence the work reported in this paper.

3.7 Acknowledgements

J.L.A. acknowledges funding from the Chemical Measurement and Imaging Program at the National Science Foundation (CHE-1709372).

3.8 References

(1) Diehl, F.; Li, M.; Dressman, D.; He, Y.; Shen, D.; Szabo, S.; Diaz, L. A.; Goodman, S. N.; David, K. A.; Juhl, H.; et al. Detection and Quantification of Mutations in the Plasma of Patients with Colorectal Tumors. *Proc. Natl. Acad. Sci. U. S. A.* **2005**, *102* (45), 16368–16373.

(2) Fettke, H.; Kwan, E. M.; Azad, A. A. Cell-Free DNA in Cancer: Current Insights. *Cell. Oncol.* **2019**, *42* (1), 13–28.

(3) Ossandon, M. R.; Agrawal, L.; Bernhard, E. J.; Conley, B. A.; Dey, S. M.; Divi, R. L.; Guan, P.; Lively, T. G.; McKee, T. C.; Sorg, B. S.; et al. Circulating Tumor DNA Assays in Clinical Cancer Research. *J. Natl. Cancer Inst.* **2018**, *110* (9), 929–934.

(4) Newman, A. M.; Bratman, S. V.; To, J.; Wynne, J. F.; Eclov, N. C. W.; Modlin, L. A.; Liu, C. L.; Neal, J. W.; Wakelee, H. A.; Merritt, R. E.; et al. An Ultrasensitive Method for Quantitating Circulating Tumor DNA with Broad Patient Coverage. *Nat. Med.* **2014**, *20* (5), 548–554.

(5) Lito, P.; Solomon, M.; Li, L. S.; Hansen, R.; Rosen, N. Cancer Therapeutics: Allele-Specific Inhibitors Inactivate Mutant KRAS G12C by a Trapping Mechanism. *Science (80-.).* **2016**, *351* (6273), 604–608.

(6) Imamura, Y.; Morikawa, T.; Liao, X.; Lochhead, P.; Kuchiba, A.; Yamauchi, M.; Qian, Z. R.; Nishihara, R.; Meyerhardt, J. A.; Haigis, K. M.; et al. Specific Mutations in KRAS Codons 12 and 13, and Patient Prognosis in 1075 BRAF Wild-Type Colorectal Cancers. *Clin. Cancer Res.* **2012**, *18* (17), 4753–4763.

(7) Herreros-Villanueva, M.; Chen, C. C.; Yuan, S. S. F.; Liu, T. C.; Er, T. K. KRAS Mutations: Analytical Considerations. *Clin. Chim. Acta* **2014**, *431*, 211–220.

(8) Zinsky, R.; Bölükbas, S.; Bartsch, H.; Schirren, J.; Fisseler-Eckhoff, A. Analysis of KRAS Mutations of Exon 2 Codons 12 and 13 by SNaPshot Analysis in Comparison to Common DNA Sequencing. *Gastroenterol. Res. Pract.* **2010**, *2010*, 1–5.

(9) Rodda, A. E.; Parker, B. J.; Spencer, A.; Corrie, S. R. Extending Circulating Tumor DNA Analysis to Ultralow Abundance Mutations: Techniques and Challenges. *ACS Sensors* **2018**, *3* (3), 540–560.

(10) Don, R. H.; Cox, P. T.; Wainwright, B. J.; Baker, K.; Mattick, J. S. "Touchdown" PCR to Circumvent Spurious Priming during Gene Amplification. *Nucleic Acids Res.* **1991**, *19* (14), 4008.

(11) Huang, Q.; Wang, G. Y.; Huang, J. F.; Zhang, B.; Fu, W. L. High Sensitive Mutation Analysis on KRAS2 Gene Using LNA/DNA Chimeras as PCR Amplification Blockers of Wild-Type Alleles. *Mol. Cell. Probes* **2010**, *24* (6), 376–380.

(12) Dominguez, P. L.; Kolodney, M. S. Wild-Type Blocking Polymerase Chain Reaction for Detection of Single Nucleotide Minority Mutations from Clinical Specimens. *Oncogene* **2005**, *24* (45), 6830–6834.

(13) Huijsmans, C. J. J.; Poodt, J.; Savelkoul, P. H. M.; Hermans, M. H. A. Sensitive Detection and Quantification of the JAK2V617F Allele by Real-Time PCR: Blocking Wild-Type Amplification by Using a Peptide Nucleic Acid Oligonucleotide. *J. Mol. Diagnostics* **2011**, *13* (5), 558–564.

(14) You, Y.; Moreira, B. G.; Behlke, M. A.; Owczarzy, R. Design of LNA Probes That Improve Mismatch Discrimination. *Nucleic Acids Res.* **2006**, *34* (8), 1–11.

(15) Di Giusto, D. A. Strong Positional Preference in the Interaction of LNA Oligonucleotides with DNA Polymerase and Proofreading Exonuclease Activities: Implications for Genotyping Assays. *Nucleic Acids Res.* **2004**, *32* (3), 1–8.

(16) Li, J.; Wang, L.; Mamon, H.; Kulke, M. H.; Berbeco, R.; Makrigiorgos, G. M. Replacing PCR with COLD-PCR Enriches Variant DNA Sequences and Redefines the Sensitivity of Genetic Testing. *Nat. Med.* **2008**, *14* (5), 579–584.

(17) Milbury, C. A.; Li, J.; Makrigiorgos, G. M. Pcr-Based Methods for the Enrichment of Minority Alleles and Mutations. *Clin. Chem.* **2009**, *55* (4), 632–640.

(18) Al-Soud, W. A.; Jönsson, L. J.; Rådström, P. Identification and Characterization of Immunoglobulin G in Blood as a Major Inhibitor of Diagnostic PCR. *J. Clin. Microbiol.* **2000**, *38* (1), 345–350.

(19) Schrader, C.; Schielke, A.; Ellerbroek, L.; Johne, R. PCR Inhibitors - Occurrence, Properties and Removal. *J. Appl. Microbiol.* **2012**, *113* (5), 1014–1026.

(20) Guha, M.; Castellanos-Rizaldos, E.; Makrigiorgos, G. M. DISSECT Method Using PNA-LNA Clamp Improves Detection of EGFR T790m Mutation. *PLoS One* **2013**, *8* (6), 2–6.

(21) Taniguchi, K.; Uchida, J.; Nishino, K.; Kumagai, T.; Okuyama, T.; Okami, J.; Higashiyama, M.; Kodama, K.; Imamura, F.; Kato, K. Quantitative Detection of EGFR Mutations in Circulating Tumor DNA Derived from Lung Adenocarcinomas. *Clin. Cancer Res.* **2011**, *17* (24), 7808–7815.

(22) Michael Green, N. Avidin and Streptavidin. *Methods Enzymol.* **1990**, *184*, 51–67.

(23) Fan, Z. H.; Mangru, S.; Granzow, R.; Heaney, P.; Ho, W.; Dong, Q.; Kumar, R. Dynamic DNA Hybridization on a Chip Using Paramagnetic Beads. *Anal. Chem.* **1999**, *71* (21), 4851–4859.

(24) Leslie, D. C.; Li, J.; Strachan, B. C.; Begley, M. R.; Finkler, D.; Bazydlo, L. A. L.; Barker, N. S.; Haverstick, D. M.; Utz, M.; Landers, J. P. New Detection Modality for Label-Free Quantification of DNA in Biological Samples via Superparamagnetic Bead Aggregation. *J. Am. Chem. Soc.* **2012**, *134* (12), 5689–5696.

(25) Knob, R.; Hanson, R. L.; Tateoka, O. B.; Wood, R. L.; Guerrero-Arguero, I.; Robison, R. A.; Pitt, W. G.; Woolley, A. T. Sequence-Specific Sepsis-Related DNA Capture and Fluorescent Labeling in Monoliths Prepared by Single-Step Photopolymerization in Microfluidic Devices. *J. Chromatogr. A* **2018**, *1562*, 12–18.

(26) Knob, R.; Nelson, D. B.; Robison, R. A.; Woolley, A. T. Sequence-Specific DNA Solid-Phase Extraction in an on-Chip Monolith: Towards Detection of Antibiotic Resistance Genes. *J. Chromatogr. A* **2017**, *1523*, 309–315.

(27) Kelley, S. O. What Are Clinically Relevant Levels of Cellular and Biomolecular Analytes? *ACS Sensors* **2017**, *2* (2), 193–197.

(28) Maruyama, T.; Hosogi, T.; Goto, M. Sequence-Selective Extraction of Single-Stranded DNA Using DNA-Functionalized Reverse Micelles. *Chem. Commun.* **2007**, *7345* (43), 4450–4452.

(29) Clark, K. D.; Varona, M.; Anderson, J. L. Ion-Tagged Oligonucleotides Coupled with a Magnetic Liquid Support for the Sequence-Specific Capture of DNA. *Angew. Chemie - Int. Ed.* **2017**, *56* (26), 7630–7633.

(30) Hayashi, S.; Hamaguchi, H. O. Discovery of a Magnetic Ionic Liquid [Bmim]FeCl4. *Chem. Lett.* **2004**, *33* (12), 1590–1591.

(31) Clark, K. D.; Nacham, O.; Purslow, J. A.; Pierson, S. A.; Anderson, J. L. Magnetic Ionic Liquids in Analytical Chemistry: A Review. *Anal. Chim. Acta* **2016**, *934*, 9–21.

(32) Emaus, M. N.; Clark, K. D.; Hinners, P.; Anderson, J. L. Preconcentration of DNA Using Magnetic Ionic Liquids That Are Compatible with Real-Time PCR for Rapid Nucleic Acid Quantification. *Anal. Bioanal. Chem.* **2018**, *410* (17), 4135–4144.

(33) Emaus, M. N.; Varona, M.; Anderson, J. L. Sequence-Specific Preconcentration of a Mutation Prone KRAS Fragment from Plasma Using Ion-Tagged Oligonucleotides Coupled to QPCR Compatible Magnetic Ionic Liquid Solvents. *Anal. Chim. Acta* **2019**, *1068*, 1–10.

(34) Clark, K. D.; Zhu, C.; Anderson, J. L. Maximizing Ion-Tagged Oligonucleotide Loading on Magnetic Ionic Liquid Supports for the Sequence-Specific Extraction of Nucleic Acids. *Anal. Chem.* **2019**, *91* (9), 5945–5952.

(35) Marengo, A.; Emaus, M. N.; Bertea, C. M.; Bicchi, C.; Rubiolo, P.; Cagliero, C.; Anderson, J. L. Arabidopsis Thaliana ITS Sequence-Specific DNA Extraction by Ion-Tagged Oligonucleotides Coupled with a Magnetic Ionic Liquid. *Anal. Bioanal. Chem.* **2019**, *411* (25), 6583–6590.

(36) Nacham, O.; Clark, K. D.; Yu, H.; Anderson, J. L. Synthetic Strategies for Tailoring the Physicochemical and Magnetic Properties of Hydrophobic Magnetic Ionic Liquids. *Chem. Mater.* **2015**, *27* (3), 923–931.

(37) Pierson, S. A.; Nacham, O.; Clark, K. D.; Nan, H.; Mudryk, Y.; Anderson, J. L. Synthesis and Characterization of Low Viscosity Hexafluoroacetylacetonate-Based Hydrophobic Magnetic Ionic Liquids. *New J. Chem.* **2017**, *41* (13), 5498–5505.

(38) Farooq, M. Q.; Chand, D.; Odugbesi, G. A.; Varona, M.; Mudryk, Y.; Anderson, J. L. Investigating the Effect of Ligand and Cation on the Properties of Metal Fluorinated Acetylacetonate Based Magnetic Ionic Liquids. *New J. Chem.* **2019**, *43* (28), 11334–11341.

(39) Dias, R.; Mel'nikov, S.; Lindman, B.; Miguel, M. G. DNA Phase Behavior in the Presence of Oppositely Charged Surfactants. *Langmuir* **2000**, *16* (24), 9577–9583.

(40) Gaillard, C.; Strauss, F. Avoiding Adsorption of DNA to Polypropylene Tubes and Denaturation of Short DNA Fragments. *Tech. Tips Online* **1998**, *3* (1), 63–65.

(41) Clark, K. D.; Yamsek, M. M.; Nacham, O.; Anderson, J. L. Magnetic Ionic Liquids as PCR-Compatible Solvents for DNA Extraction from Biological Samples. *Chem. Commun.* **2015**, *51* (94), 16771–16773.

(42) Kidess, E.; Heirich, K.; Wiggin, M.; Vysotskaia, V.; Visser, B. C.; Marziali, A.; Wiedenmann, B.; Norton, J. A.; Lee, M.; Jeffrey, S. S.; et al. Mutation Profiling of Tumor DNA from Plasma and Tumor Tissue of Colorectal Cancer Patients with a Novel, High-Sensitivity Multiplexed Mutation Detection Platform. *Oncotarget* **2015**, *6* (4), 2549–2561.

(43) Sanghvi, R. S.; Lemons, R. M.; Baker, H.; Thoene, J. G. A Simple Method for Determination of Plasma and Urinary Biotin. *Clin. Chim. Acta* **1982**, *124* (1), 85–90.

(44) Mock, D. M.; DuBois, D. B. A Sequential, Solid-Phase Assay for Biotin in Physiologic Fluids That Correlates with Expected Biotin Status. *Anal. Biochem.* **1986**, *153* (2), 272–278.

(45) Piketty, M. L.; Polak, M.; Flechtner, I.; Gonzales-Briceño, L.; Souberbielle, J. C. False Biochemical Diagnosis of Hyperthyroidism in Streptavidin-Biotin-Based Immunoassays: The Problem of Biotin Intake and Related Interferences. *Clin. Chem. Lab. Med.* **2017**, *55* (6), 780–788.

(46) Pei, Y.; Wang, J.; Wu, K.; Xuan, X.; Lu, X. Ionic Liquid-Based Aqueous Two-Phase Extraction of Selected Proteins. *Sep. Purif. Technol.* **2009**, *64* (3), 288–295.

(47) El Messaoudi, S.; Rolet, F.; Mouliere, F.; Thierry, A. R. Circulating Cell Free DNA: Preanalytical Considerations. *Clin. Chim. Acta* **2013**, *424*, 222–230.

(48) Bronkhorst, A. J.; Aucamp, J.; Pretorius, P. J. Cell-Free DNA: Preanalytical Variables. *Clin. Chim. Acta* **2015**, *450*, 243–253.

(49) Skvortsova, T. E.; Rykova, E. Y.; Tamkovich, S. N.; Bryzgunova, O. E.; Starikov, A. V.; Kuznetsova, N. P.; Vlassov, V. V.; Laktionov, P. P. Cell-Free and Cell-Bound Circulating DNA in Breast Tumours: DNA Quantification and Analysis of Tumour-Related Gene Methylation. *Br. J. Cancer* **2006**, *94* (10), 1492–1495.

CHAPTER 4. MAGNETIC IONIC LIQUIDS AS SOLVENTS FOR RNA EXTRACTION AND PRESERVATION

Chenghui Zhu, Marcelino Varona and Jared L. Anderson

Department of Chemistry, Iowa State University, Ames, Iowa 50011, United States

Modified from a manuscript under review to *ACS Omega*

4.1 Abstract

Ribonucleic acid (RNA) is particularly sensitive to enzymatic degradation by endonucleases prior to sample analysis. In-field preservation has been a challenge for RNA sample preparation. Very recently, hydrophobic magnetic ionic liquid (MIL) has shown significant promise in the area of RNA extraction. In this study, MILs were synthesized and employed as solvents for the extraction and preservation of RNA in aqueous solution. RNA samples obtained from yeast cells were extracted and preserved by the trihexyl(tetradecyl) phosphonium tris(hexafluoroacetylaceto)cobaltate(II) ($[P_{66614}^+][Co(hfacac)_3^-]$) and trihexyl(tetradecyl) phosphonium tris(phenyltrifluoroacetylaceto)cobaltate(II) ($[P_{66614}^+][Co(Phtfacac)_3^-]$) MIL with a dispersion of the supporting media, polypropylene glycol, average Mn ~ 2000 (PPG-2000), at room temperature for up to 7 and 15 days period, respectively. High quality RNA treated with ribonuclease A (RNase A) was recovered from the tetra(1-octylimidazole)cobaltate(II) di(L-glutamate) ($[Co(OIM)_4^{2+}][Glu^-]_2$) and tetra(1-octylimidazole)cobaltate(II) di(L-aspartate) ($[Co(OIM)_4^{2+}][Asp^-]_2$) MILs after a 24 hour period at room temperature. Quantitative reverse transcription polymerase chain reaction (qRT-PCR) and agarose gel electrophoresis were used to determine the effect of RNA preservation. Furthermore, the preservation mechanism was investigated by exploring the partitioning of RNase A into the MIL using high-performance liquid chromatography.

4.2 Introduction

Ribonucleic acid (RNA) plays a prominent role in regulating gene expression and encoding proteins that are essential for the growth and survival of every living organism.[1-3] Because of its high biological relevance and significant role in gene expression, RNA has attracted notable research interest. However, messenger RNA (mRNA)[4] and small interfering RNA (siRNA)[5] are prone to degradation in a variety of ways including denaturation,[6] oxidization,[7] and nuclease cleavage.[8] For instance, mRNA is particularly prone to rapid degradation by ubiquitous ribonucleases (RNases).[4] In certain conditions, biological samples collected in the field may contain numerous compounds, such as RNase, which can degrade RNA instantly. These samples can only be handled by simple in-field treatments and require preservation before in-lab analysis.[9] Therefore, the isolation of RNA from contaminating RNases and subsequent preservation during sample preparation are critical steps in order to maximize the yield of pure RNA. Moreover, the isolated RNA must be sufficiently pure for analysis with biomolecular techniques such as the reverse transcription polymerase chain reaction (RT-PCR), quantitative RT-PCR (qRT-PCR), and Northern Blot analysis.[4,10-12]

A number of techniques have been developed that preserve RNA over time and protect it from endonuclease degradation *in vitro*. One of the most commonly used methods is diethylpyrocarbonate (DEPC) pretreatment, which can deactivate RNases by forming amide bonds between amino and carboxylic groups.[13,14] However, DEPC is unstable in aqueous solution and can easily react with carbon dioxide or ethanol,[15] which limits its use in certain applications. Other widely accepted methods include the paraffin-embedded tissue process and the formalin fixed paraffin-embedded tissues (FFPE).[2,16,17] FFPE is especially preferred in tissue sample preparation for downstream analysis involving the polymerase chain reaction (PCR). However, formalin can cross-react with proteins in the sample matrix,[18] leading to the inhibition

of reverse transcription for mRNA.[19] In addition, other methods such as lyophilization,[20] formamide protection,[21] and numerous RNase inhibitor treatments[22-24] have been applied for RNA preservation. Unfortunately, drawbacks to these preservation techniques include the requirements of specialized equipment, multiple tedious steps, or a high amount of energy. Because of the inherent limitations of current methods, it is important to explore the development of methods that effectively combine sample preparation and RNA preservation to minimize the risk of nuclease contamination and maximize the amount of recovered RNA for downstream analysis.

Recently, ionic liquid (IL)-based materials have been shown to exhibit encouraging compatibility in nucleic acid analysis.[25,26] ILs are organic molten salts that possess melting points at or below 100 °C. Because of their tunable cation and anion structures[27,28] and ability to interact with a variety of biomolecules,[29,30] ILs have demonstrated high potential as nucleic acid preservation and extraction solvents.[31-33] For instance, imidazolium[31] and choline-based[25,34] ILs have been previously reported in RNA preservation applications. They have been demonstrated to preserve RNA by either isolating the target nucleic acid from the sample matrix or by maintaining the stability of RNA within the IL.[35] Magnetic ionic liquids (MILs) are a subclass of ILs that incorporate paramagnetic centers in their chemical structures. Because of their ability to be manipulated by an external magnetic field and affinity for biological molecules such as DNA and RNA, MILs have drawn considerable research interest for nucleic acid extraction[36] and for applications requiring automatic operation.[37] In a previously published study,[38] several MILs with different chemical structures were demonstrated to simultaneously extract DNA from aqueous solutions while protecting DNA from deoxyribonuclease I (DNase I) degradation.

In order to stabilize RNA in a hydrophobic microenvironment and prevent degradation, several MILs were designed and synthesized in this study based on previously reported ILs.[35,38] The MILs were investigated for their ability to serve as RNA extraction and preservation media. The trihexyl(tetradecyl) phosphonium tris(hexafluoroacetylaceto)cobaltate(II) ($[P_{66614}^+][Co(hfacac)_3^-]$) and trihexyl(tetradecyl) phosphonium tris(phenyltrifluoroacetylaceto)cobaltate(II) ($[P_{66614}^+][Co(Phtfacac)_3^-]$) MILs were dispersed in polypropylene glycol (PPG), average Mn ≈ 2000 (PPG-2000). The MIL/PPG-2000 system was investigated for the capability of extracting and preserving yeast total RNA from aqueous solution which could subsequently be analyzed via the qRT-PCR. In addition, another two MILs, namely, tetra(1-octylimidazole)cobaltate(II) di(L-glutamate) ($[Co(OIM)_4^{2+}][Glu^-]_2$) and tetra(1-octylimidazole)cobaltate(II) di(L-aspartate) ($[Co(OIM)_4^{2+}][Asp^-]_2$) were capable of protecting yeast total RNA from RNase A degradation. Reversed-phase ion-pair liquid chromatography was used to investigate the RNase A extraction efficiency of the MILs to elucidate the preservation mechanism. Anion-exchange high-performance liquid chromatography (HPLC) and agarose gel electrophoresis were used to quantitatively evaluate the recovery efficiency of yeast total RNA. qRT-PCR was used to evaluate the structural integrity of mRNA from the preserved yeast total RNA.

4.3 Result and Discussion

4.3.1 Partitioning of RNA to MILs

MILs **1-3** (Table 4.1) were initially chosen for RNA extraction and preservation as they have been previously used for DNA extraction.[36,39] Two other MILs (**4** and **5**) incorporating aromatic moieties were also investigated. After a 60 min single-droplet extraction (SDE), the yeast total RNA extracted by the MILs was recovered by a liquid–liquid extraction (LLE) method using ethyl acetate and Tris-HCl/ ethylenediaminetetraacetic acid (EDTA) buffer prior to

Table 4.1 Chemical formula and structures of MILs **1-7** that were investigated in this study.

MIL	Chemical Formula	Structure
1	$[P_{66614}^{+}][Co(hfacac)_3^{-}]$	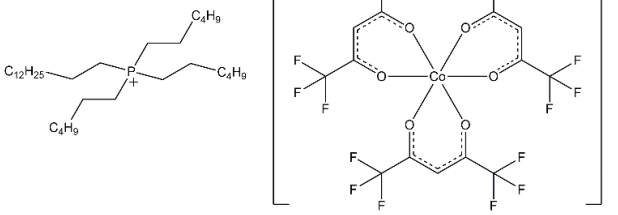
2	$[P_{66614}^{+}][Ni(hfacac)_3^{-}]$	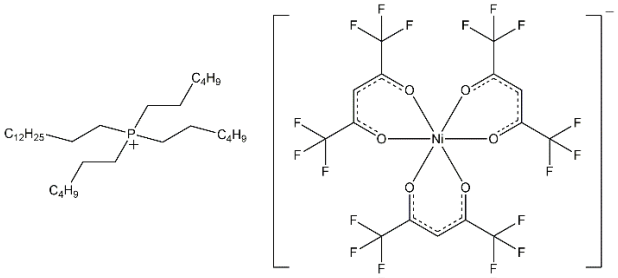
3	$[P_{66614}^{+}][Mn(hfacac)_3^{-}]$	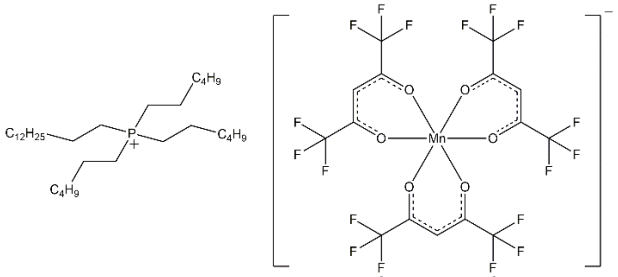
4	$[P_{66614}^{+}][Co(Phtfacac)_3^{-}]$	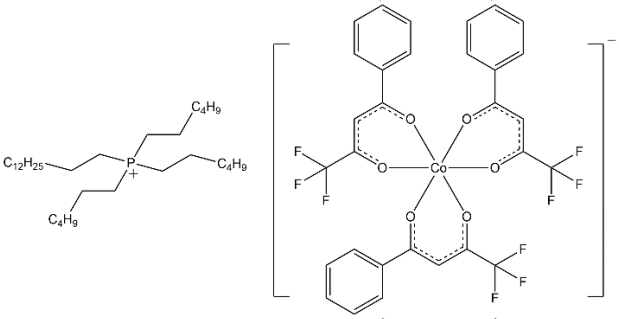
5	$[P_{66614}^{+}][Ni(Phtfacac)_3^{-}]$	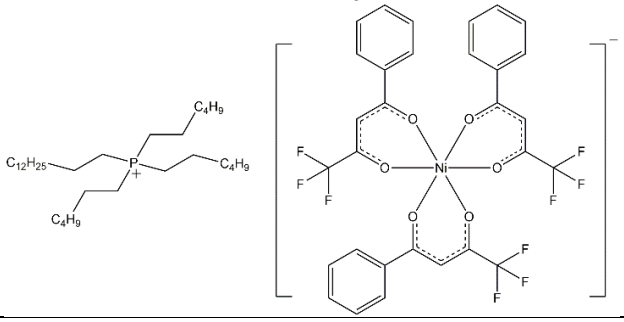

Table 4.1 (continued)

MIL	Chemical Formula	Structure
6	$[Co(OIM)_4^{2+}][Glu^-]_2$	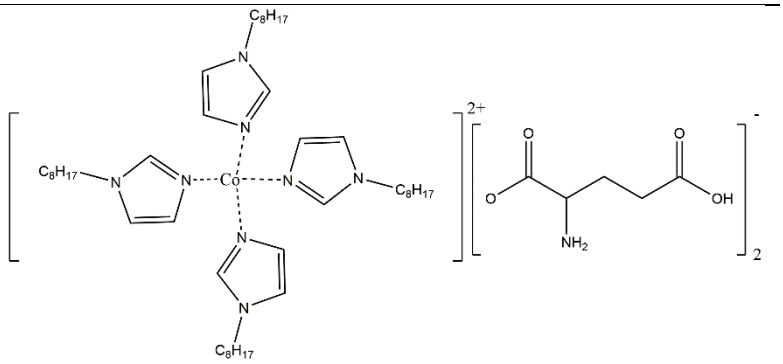
7	$[Co(OIM)_4^{2+}][Asp^-]_2$	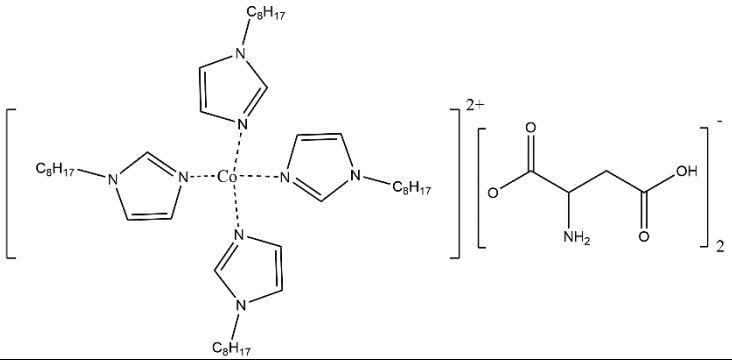

analysis. Different LLE buffer compositions were tested and optimized to maximize the recovery of RNA. Tris-HCl concentrations of 40, 80, 160, and 320 mM, EDTA concentrations of 1, 2, and 3 mM, and pH 7 and 8 were investigated for the RNA back-extraction. Consequently, a LLE buffer consisting of 160 mM Tris-HCl, 2 mM EDTA, and pH 8 was chosen as it afforded the highest RNA recovery. An external calibration curve for yeast total RNA was established and used to calculate the RNA concentration in aqueous solution (Figure C1 of Appendix C). The extraction efficiency (E_e) of MILs was determined by comparing the total RNA concentration before (C_{std}) and after (C_{ext}) extraction using Equation (4.1).

$$Extraction\ Efficiency\ (E_e\%) = \left(1 - \frac{C_{ext}}{C_{std}}\right) \times 100\% \quad \text{Equation (4.1)}$$

As shown in Figure C2, MIL **4** exhibited the highest E_e (72.79 ± 5.66%) of MILs **1-5,** close to double the E_e of MIL **1** (39.34 ± 2.65%) though they have the same metal center and cation in their chemical structures. In addition, MIL **5** exhibited an E_e (33.12 ± 3.64%) higher than that of MIL **2** (21.02 ± 2.68%). The reason for this dramatic increase in the E_e could be due to the aromatic moieties in MILs **4** and **5**, which may interact via π-π stacking interaction with the exposed bases in RNA.[40] A positive control and a no reverse transcriptase (NRT) control were performed together. As shown in Figure 4.1, mRNA recovered from MILs **1-3** produced complementary DNA (cDNA), indicating intact mRNA. Subsequently, the cycle of quantification (Cq) values generated by qRT-PCR were compared with the positive control (33.03). The Cq value is related to the amount of cDNA and each decrease of one Cq value represents a 2-fold increase in the mass of nucleic acid. MIL **1** and **3** did not show a significant increase in the Cq value (MIL **1**: 34.00, MIL **2**: 36.31, MIL **3**: 34.13), suggesting only limited RNA loss during the extraction and recovery process. As an example, mRNA recovered from MIL **1** produced approximately 49% less cDNA than the positive control. The nonamplified NRT control ensured that there was no false-positive amplification caused by leftover cDNA sequences in the total yeast RNA. Based on these experiments, MILs **1**, **4**, and **5** were chosen to further examine their preservation ability.

Initially, an identical RNA extraction procedure using MILs **1**, **4** and **5** was performed with a RNA aqueous solution containing 500 ng yeast total RNA. The biphasic mixtures were stored for another 6 h before recovery. In addition, another 500 ng of yeast total RNA was directly stored for 6 h at -20 °C and used as a positive control. As shown in Figure 4.2, neither qRT-PCR or agarose gel electrophoresis showed a significant amount of RNA recovered from MIL **5**. However, a portion of mRNA was recovered from MIL **1**, as demonstrated by a Cq value

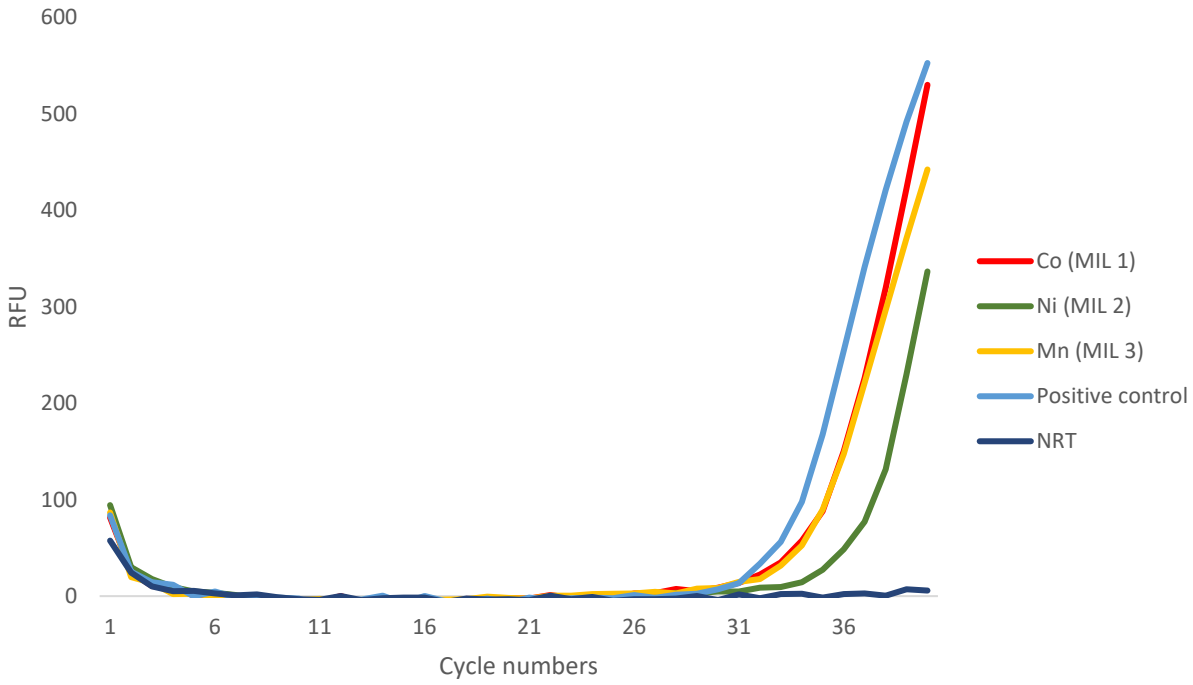

Figure 4.1 Representative qRT-PCR amplification of cDNA following extraction of 100 ng of RNA with 5 µL of MILs **1-3** and LLE recovery. Positive control: recovery of 100 ng of RNA by LLE.

of 38.82. MIL **4** afforded a higher mRNA recovery producing a Cq value of 34.86, approximately 16-times greater than MIL **1**. Agarose gel electrophoresis also indicated that MIL **4** exhibited a superior ability to preserve extracted RNA from degradation compared to the other two MILs. Comparing the results shown in Figure 4.2 to Figure C2, the MIL with a higher extraction efficiency produced a lower Cq value, except for MIL **5**. Surprisingly, MIL **5** produced the highest Cq value (no amplification in 40 cycles) and no bright cDNA band was observed in the agarose gel, suggesting that the metal center in the MIL structure may play a role in extraction as well as recovery of nucleic acid.[41] In addition, the amount of RNA recovered from MILs **1**, **4**, and **5** was no better than the positive control (29.11). The yeast total RNA recovered from MILs **1**, **4**, and **5** was not able to be detected by either HPLC or qRT-PCR after preservation at room temperature for 24 h (Figure C3). While these results are encouraging,

additional conditions must be explored to increase the stability and preservation time of RNA in MILs.

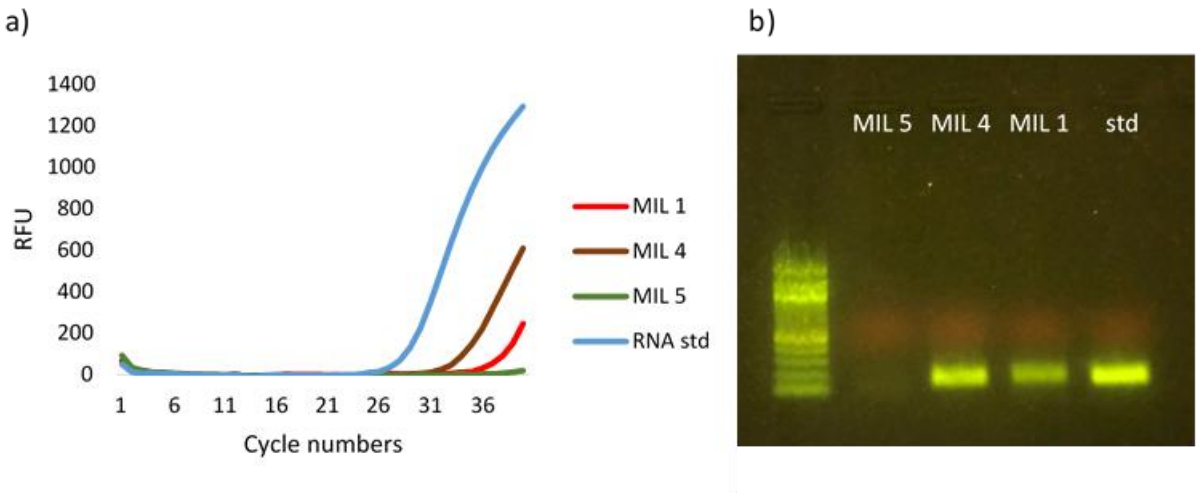

Figure 4.2 a) Representative qRT-PCR amplification of cDNA following preservation of 500 ng of RNA for 6 hours. b) Agarose gel electrophoresis of cDNA after qRT-PCR amplification (left lane: 100 bp DNA ladder, New England BioLabs).

4.3.2 Degradation of RNA under Various Conditions

To further investigate the preservation process of RNA in MILs, MIL **4** was chosen to examine additional conditions as it possessed the highest E_e of the MILs previously tested. Initially, sodium dodecyl sulfate (SDS) was incorporated in the yeast total RNA standard solution based on previous studies and commonly used RNA preservation methods.[8,17] Consequently, SDS increased the stability of yeast total RNA extracted by MIL **4**. RNA could be recovered and detected by qRT-PCR after a 1-day preservation period, as shown in Table 4.2. However, the RNA still suffered from degradation after a 3-day storage period as no amplification was detected by qRT-PCR. In addition, as RNA can be degraded at a relatively faster rate in aqueous solution than in an anhydrous environment,[16] the presence of water is considered an essential component during RNA degradation. Therefore, removing water from the biphasic mixture after the extraction process by directly pipetting out was also investigated.

As shown in Table 4.2, the amount of recovered RNA from MIL **4** dramatically increased when compared to the previous experiment where water remained in contact with MIL after extraction. In addition, other methods of water removal such as applying vacuum did not significantly affect the amount of RNA recovered. In comparison, Table 4.2 reveals that no amplification was detected for the negative control where RNA was directly stored in aqueous solution at room temperature for a period of 1 day. A possible explanation of this observation may be that the extracted nucleic acid remains on the surface of the MIL. The contact between RNA and water leads to an increase in the degradation rate. Another possible explanation was considered that the degradation of RNA in the aqueous phase may shift the equilibrium in the biphasic system and cause more RNA to be degraded. Although removal of water can increase the preservation time and improve stability, RNA directly preserved by the MIL cannot be detected by the qRT-PCR after a 3-day preservation period (Table 4.2).

Table 4.2 Comparison of the RNA preservation conditions of using 0.1% SDS and the separation of MIL **4** from the aqueous phase.

0.1% SDS	Aqueous phase	Preservation time (days)	Cq value
✓	✓ (remained)	1	36.45
✓	✓ (remained)	3	no amplification
×	× (separated)	1	27.76
×	× (separated)	3	no amplification
✓	× (separated)	1	33.06
×	✓ (remained)	1	no amplification

4.3.3 PPG-2000 Enhances Preservation of RNA in MILs

A number of polymers such as polyethylene glycol (PEG), PPG, and polyvinylpyrrolidone (PVP) have been used to vary the partitioning of various compounds including nucleic acid and proteins between the phases in a two-phase system.[42] In order to increase the preservation time of RNA, PPG-2000 was introduced as a hydrophobic supporting

solvent for RNA preservation. More specifically, MIL **4** was dissolved in PPG-2000 in a 1:5 (v:v) ratio before the yeast total RNA extraction process. LLE using ethyl acetate and Tris-HCl/EDTA buffer was no longer effective because of the presence of PPG-2000. Thus, an ethanol precipitation method was used to recover the yeast total RNA from the MIL/PPG-2000 phase. As a result, the amount of RNA recovered from MIL **4**/PPG-2000 increased dramatically. A direct comparison of the amount of yeast total RNA recovered from MIL/PPG-2000 revealed a 4.92 times higher amount of RNA recovered from the MIL, as shown in Figure C4. To study the effect of PPG-2000, an additional experiment was performed using the same procedure with PPG-2000 but without MILs. As shown in Figure C5, the PPG-2000 had a very limited effect on extraction efficiency of yeast total RNA, confirming its role as a supporting medium for MIL-based extraction. Furthermore, the recovery was determined using Equation (4.2) using the HPLC peak area of recovered RNA (A_{re}), RNA standard (A_{std}), the volume of resuspended DEPC-treated water (V_w), and RNA standard (V_{std}). Although the recovery of RNA varied from MIL **1** (0.66% RNA was recovered after 3 days) and MIL **4** (1.00% RNA was recovered after 3 days), the preservation time had a significant increase after applying PPG-2000. As shown in Figure 4.3, preserved RNA could still be detected by the qRT-PCR and agarose gel electrophoresis after a 15-day preservation period. In contrast, the RNA directly stored in water was completely degraded after 7 days.

$$Recovery\ (\%) = \frac{A_{re} \times V_w}{A_{std} \times V_{std}} \times 100\% \quad \text{Equation (4.2)}$$

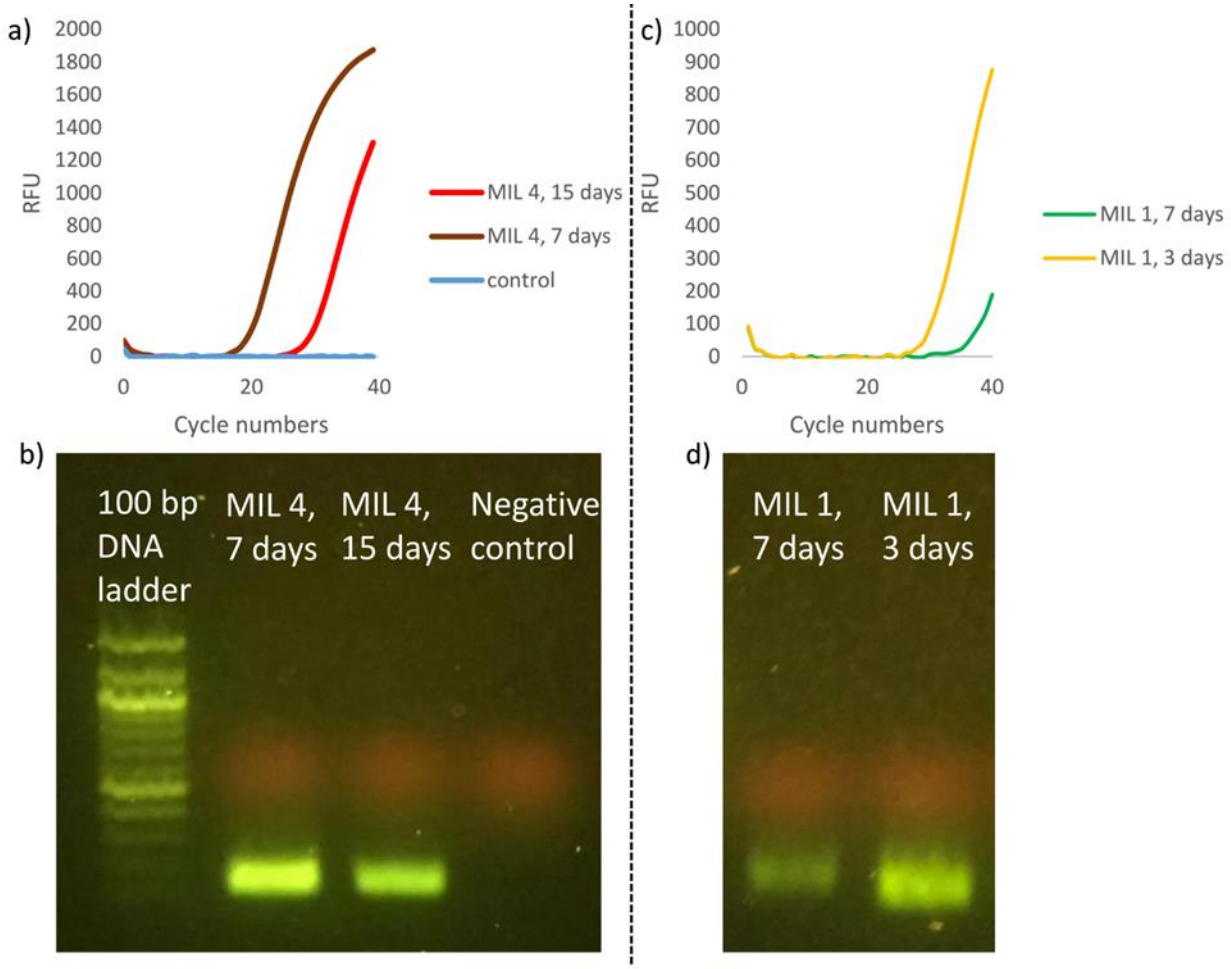

Figure 4.3 qRT-PCR amplification and agarose gel electrophoresis of cDNA after preserving 5 µg of RNA in MIL **4**/PPG-2000 for 7 and 15 days (a, b), MIL **1**/PPG-2000 for 3 and 7 days (c, d).

4.3.4 RNA Preservation against RNase A

As mentioned previously, nucleic acid preservation in the presence of endonucleases is a significant challenge during sample preparation. In particular, ubiquitous RNases can degrade RNA instantly. To determine if MIL/PPG-2000 could prevent RNA from endonuclease degradation, RNase A was introduced into the system before extraction. As shown in Figure C6, no RNA was recovered from either MIL **1**/PPG-2000 or MIL **4**/PPG-2000 in the presence of RNase A.

In order to reduce the degradation caused by RNase A, optimized conditions were tested. Consequently, no amplification was observed by qRT-PCR after a 1-h incubation of RNase A followed by a 1-h extraction of yeast total RNA though the experimental conditions for RNA preservation up to 15 days period were applied. Furthermore, the addition of 0.1% SDS solution did not improve RNA preservation, as shown in Figure C6.

Inspired by the work of Freire and co-workers[35] which incorporated amino acids in the chemical structure of ILs, MIL **6** and **7** were synthesized and investigated. The extraction and preservation steps were performed using the experimental conditions previously described with an additional step of spiking RNase A into the MIL/PPG-2000 system. Consequently, a significant amount of RNA was recovered from both MIL **6**/PPG-2000 (22.01% recovery) and MIL **7**/PPG-2000 (12.61% recovery), as shown in Figure 4.4. Although the qRT-PCR results in Figure C7 revealed high Cq values which should represent a low amount of cDNA, these values from the experiments could be due to MIL moieties in the RNA precipitate inhibiting the qPCR amplification rather than insufficient preservation. To test this assumption, agarose gel electrophoresis experiments were performed by directly loading recovered RNA samples. The agarose gel electrophoresis results in Figure 4.5 demonstrated the preservation of RNA. Bands can be observed even without performing an amplification step, indicating a high quantity of RNA recovery.

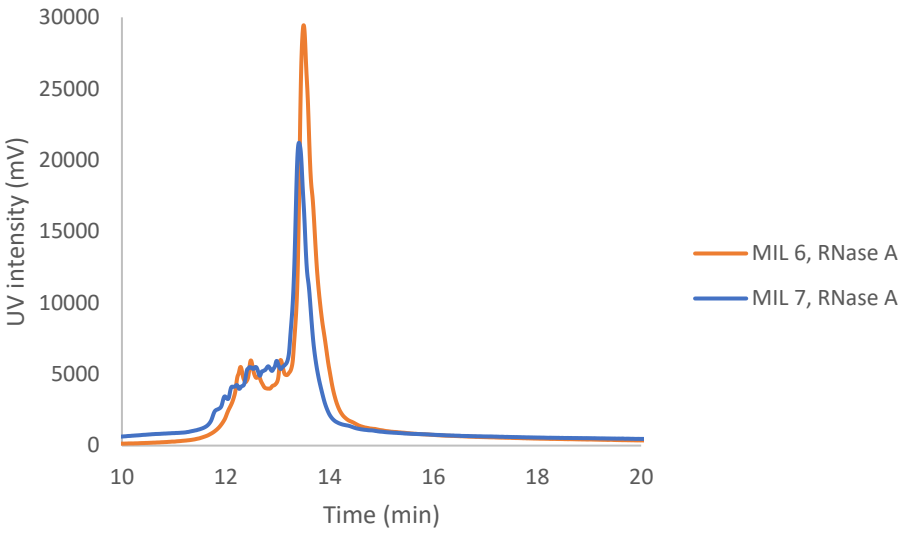

Figure 4.4 HPLC quantification of 5 µg of RNA recovered from MIL **6**/PPG-2000 spiked with 4 µg RNase A (orange) and MIL **7**/PPG-2000 spiked with 4 µg RNase A (blue).

Because some ILs may play a role in the preservation of nucleic acids by destabilizing endonucleases,[43] the partitioning of RNase A to MILs was further investigated by reversed-phase ion-pair liquid chromatography. MILs **1**, **4**, **6**, and **7** were tested because of their advanced preservation ability of yeast total RNA. As shown in Figure C8, the amounts of RNase A extracted by MILs was not significant at first but had a slowly increase within 4 h. This suggests that the mechanism of RNA preservation is mainly due to the RNA-MIL interaction. However, the endonuclease destabilization by the MILs may promote the preservation as well if the extraction time increased. Compared with other MILs, MIL **6** and **7** exhibited a superior ability in protecting RNA from RNase A degradation. Furthermore, the recovered RNA can be detected by agarose gel electrophoresis even after 24 h incubation in the presence of RNase A (Figure 4.5).

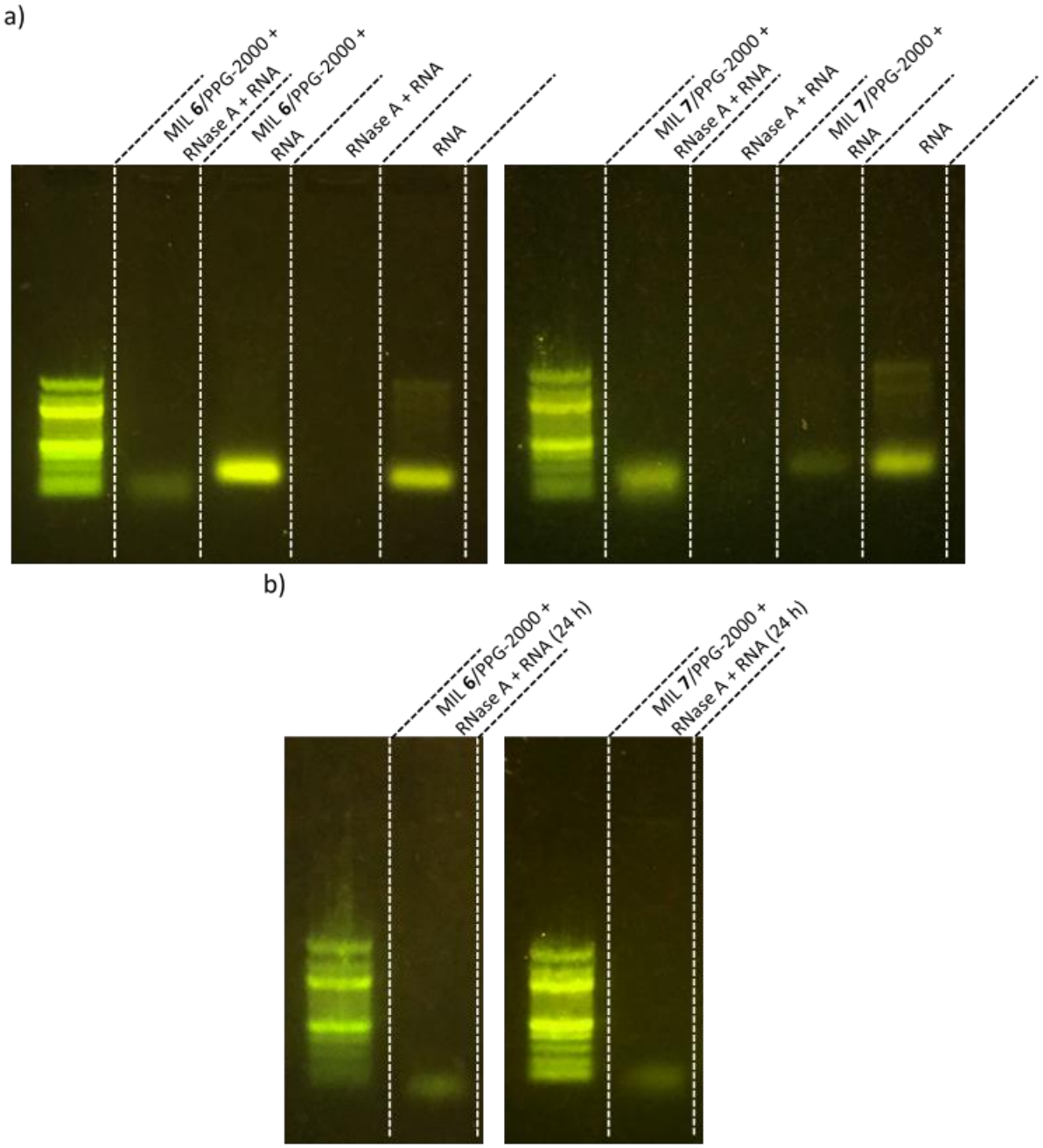

Figure 4.5 Effect of RNase A on RNA preservation within a) MIL **6**/PPG-2000 for 2 hours and MIL **7**/PPG-2000 for 2 hours. b) MIL **6**/PPG-2000 for 24 hours and MIL **7**/PPG-2000 for 24 hours. Left lane of each agarose gel: 100 bp DNA ladder (New England BioLabs).

4.4 Experimental Section

4.4.1 Reagents and Materials

LC-MS grade acetonitrile (≥ 99.9%), hexane, mixture of isomers (≥ 98.5%), methanol (≥ 99.8%), chloroform (≥ 99.8%), isoamyl alcohol (≥ 98%), ethyl acetate (≥ 99.5%), water (DEPC-treated and sterile filtered), trifluoroacetic acid (99%), EDTA (99.4 - 100.06%), poly(propylene glycol) (PPG, average Mn ≈ 2000), liquified phenol (≥ 89.0%), cobalt(II) chloride (97%), silver nitrate (≥ 99.0%), sodium dodecyl sulfate (99%), magnesium chloride (99.0 - 102.0%), L-glutamic acid, L-aspartic acid, yeast synthetic drop-out medium, Amberlite IRN78 hydroxide form, and acid-wash glass beads were purchased from Sigma Aldrich (St. Louis, MO, USA). Ethyl ether (≥ 99%) was purchased from Avantor (Center Valley, PA, USA). 1,1,1,5,5,5-Hexafluoroacetylacetone (99%), 4,4,4-trifluoro-1-phenyl-1,3-butanedione (99%), glycerol (99+%), and nickel(II) chloride (98%) were purchased from Acros Organics (Morris, NJ, USA). Tris(hydroxymethyl)aminomethane (ultra pure) and tris(hydroxymethyl)aminomethane hydrochloride (≥ 99.0%) were purchased from RPI (Mount Prospect, IL, USA). Sodium hydroxide, glucose (dextrose anhydrous), agarose, sodium chloride, sodium hydroxide, sodium acetate, dimethylsulfoxide (DMSO), acetic acid, and ammonium hydroxide were purchased from Fisher Scientific (Fair Lawn, NJ, USA). The SsoAdvanced Universal SYBR Green Supermix was purchased from Bio-Rad Laboratories (Hercules, CA, USA). Manganese(II) chloride tetrahydrate (98.0 - 101.0%) was purchased from Alfa Aesar (Ward Hill, MA, USA). Ethanol (200 proof) was purchased from Decon Labs, Inc. (King of Prussia, PA, USA). Octylimidazole (98%) was purchased from IOLITEC (Tuscaloosa, AL, USA). The Difco yeast nitrogen base w/o amino acid was purchased from Becton Dickinson (Sparks, MD, USA). RQ1 RNase-Free DNase I was purchased from Promega (Madison, WI,

USA). The SuperScript III Reverse Transcriptase Kit and SYBR Safe DNA gel stain were purchased from Invitrogen (Carlsbad, CA, USA). RNase A (from bovine pancreas) was purchased from Roche (Mannheim, Germany). All primers were purchased from Integrated DNA Technologies (Coralville, IA, USA).

4.4.2 MIL Synthesis

The chemical structures of all MILs that were examined in this study are shown in Table 4.1. Among them, the $[P_{66614}^+][Co(hfacac)_3^-]$, $[P_{66614}^+][Ni(hfacac)_3^-]$, $[P_{66614}^+][Mn(hfacac)_3^-]$, $[P_{66614}^+][Co(Phtfacac)_3^-]$, and $[P_{66614}^+][Ni(Phtfacac)_3^-]$ MILs were synthesized according to the previously published procedures.[37,44] The $[Co(OIM)_4^{2+}][Cl^-]_2$ salt was synthesized based on the previously published procedures.[45,46] Each equivalent of the salt was dissolved in methanol, and an anion-exchange reaction was performed in a column filled with 4-6 equiv of the Amberlite IRN78 resin in the hydroxide form. The eluent was reacted with 2.2 equiv of glutamic acid or aspartic acid at room temperature overnight to obtain the $[Co(OIM)_4^{2+}][Glu^-]_2$ and $[Co(OIM)_4^{2+}][Asp^-]_2$ MIL solutions, respectively. The residual neutral amino acid was crystallized in cold acetonitrile and removed by filtration.

The $[P_{66614}^+][Co(hfacac)_3^-]$, $[P_{66614}^+][Ni(hfacac)_3^-]$, $[P_{66614}^+][Mn(hfacac)_3^-]$, $[P_{66614}^+][Co(Phtfacac)_3^-]$, and $[P_{66614}^+][Ni(Phtfacac)_3^-]$ MILs were synthesized by reacting 10 mmol of ammonium hydroxide with 10 mmol of hexafluoroacetylacetone or 4,4,4-trifluoro1-phenyl-1,3-butanedione. Subsequently, 3.3 mmol of cobalt(II) chloride hexahydrate, nickel(II) chloride hexahydrate, or manganese(II) chloride tetrahydrate were added and reacted for 24 h at room temperature. The $[NH_4^+][M(hfacac)_3^-]$ and $[NH_4^+][M(Phtfacac)_3^-]$ salt products were washed with water several times and subsequently reacted with 1 mmol of purified $[P_{66614}^+][Cl^-]$ in methanol for 24 h at room temperature. The MIL products in diethyl ether solution were washed with deionized water and dried at 50 °C overnight under reduced pressure.

4.4.3 Yeast Total RNA Preparation

The total RNA and mRNA samples were both obtained from yeast cells (BY4735). The first generation of yeast cells was transferred into a 100 mL volume of the liquid medium (0.67% yeast nitrogen base, 0.2% synthetic dropout medium, and 2% glucose) and incubated at 300 rpm for approximately 2 days at 30 °C until OD_{600} > 1.0 (the optical density of the yeast cell suspension measured at 600 nm). After incubation, the yeast cell suspension was transferred into two separate 50 mL centrifuge tubes and centrifuged at 3700 rpm for 5 min at 4 °C. The precipitated cells were washed with DEPC-treated water and centrifuged under the previously described condition. The washed cells were then resuspended in 3 mL (1 volume) RNA extraction buffer which consisted of 50 mM Tris-HCl, 10 mM EDTA, and 0.1 M NaCl, at pH 7.5 with 5% SDS. One volume of denaturing buffer (phenol (pH 4): chloroform: isoamyl alcohol, v/v/v = 49.5:49.5:1) was added to the resuspended cells along with 1 g of acid-washed glass beads. The mixture was incubated at room temperature for 6 min and vortexed at high speed for 2 min. The suspension was centrifuged, and the supernatant carefully transferred to a new tube. Another volume of denaturing buffer was added and vortexed at high speed for 2 min. After centrifugation, the supernatant was carefully transferred to a new tube. The supernatant was extracted with one volume of denaturing buffer and centrifuged before transferring to another new tube. Subsequently, the chloroform: isoamyl alcohol (v/v = 24:1) buffer was added, and the tubes were vortexed at high speed for 2 min to remove the residual phenol in the supernatant. For each volume of RNA solution, a 0.1 volume of 3 M sodium acetate (pH 5.2) and 3 volumes of iced ethanol stored at -20 °C were added to the aqueous layer. The suspension was incubated at -20 °C for at least 1 h to precipitate the nucleic acid. The precipitate was washed with 70% ethanol after centrifugation and resuspended in DEPC-treated water. The obtained yeast total RNA was further treated with DNase I in 1× Reaction Buffer (New England BioLabs) for 30 min

at 37 °C to remove genomic DNA. DNase I was inactivated by an addition of 2 mM EGTA at 65 °C for 10 min subsequently, and the solution was stored at -80 °C. Eventually, the concentration of the yeast total RNA solution was analyzed using a NanoDrop Spectrophotometer (Thermo 2000c).

4.4.4 qRT-PCR Conditions

The reverse transcription reaction was performed using a SuperScript III Reverse Transcriptase Kit (Invitrogen). The reaction mix consisted of 4 µL of 5× First-Strand Buffer, 1 µL of 10 µM reverse primer (5'-TAC CGG CAG ATT CCA AAC CC-3'), 1 µL of 0.1 M DTT, 1 µL of 10 mM dNTP, 1 µL of SuperScript III RT (200 U/µL), RNA sample solution, and Milli-Q water to yield a 20 µL reaction mix. The thermal protocol for all reaction mixes was as follows: 65 °C for 5 min, 4 °C for 5 min, 45 °C for 60 min, 70 °C for 15 min, and hold at 4 °C at the end. After the reverse transcription reaction, 1-2 µL of the solution was subjected to a qPCR reaction mix which consisted of 10 µL of SsoAdvanced Universal SYBR Green Supermix (2×), 2.6 µL of 50 mM $MgCl_2$, 1 µL of DMSO, 0.6 µL of 10 µM forward primer (5'-GAA ATG CAA ACC GCT GCT CA-3'), 0.6 µL of 10 µM reverse primer, and 3.2-4.2 µL of Milli-Q water (20 µL for each reaction mix). The thermal cycling protocol for the qPCR was as follows: an initial denaturation step of 5 min at 95.0 °C followed by 40 cycles of 10 s at 95.0 °C and 30 s at 64.0 °C.

4.4.5 Agarose Gel Electrophoresis Conditions

A 0.8% agarose gel containing 5% SYBR Safe DNA Gel Stain (10,000×) was used for agarose gel electrophoresis. A volume of 20 µL of either the cDNA generated by reverse transcription or the RNA was pretreated with 4 µL of 30% glycerol before loading on the gel. Agarose gel electrophoresis was carried out for 30 min at 125 V with 1× TAE buffer.

4.4.6 LLE and Recovery of the RNA Sample

A 5 µL volume of MIL was added directly to the RNA sample solution, and the mixture was incubated without stirring at room temperature for approximately 60 min. The aqueous phase was then separated and prepared for HPLC injection to determine the extraction efficiency of RNA, while the MIL phase was separated and dissolved in 25 µL of ethyl acetate. The RNA in the MIL phase was recovered into the aqueous phase by adding 25 µL of DEPC-treated water or 25 µL of LLE buffer (160 mM Tris-HCl, 2 mM EDTA, pH 8), and the biphasic mixture was vortexed for 1 min. A 12 µL volume of the aqueous phase was subjected to qRT-PCR. The generated and amplified cDNA was further analyzed by agarose gel electrophoresis. A positive control was performed using the same procedure without the MIL present.

4.4.7 Preservation of RNA within MILs

A 2 µg mass of RNA in aqueous solution or 0.1 % SDS solution was extracted by 5 µL of MIL for approximately 60 min. Two different preservation conditions were investigated: (1) the biphasic mixture was directly stored at room temperature or -20 °C and (2) the aqueous phase was carefully removed before the MIL phase was stored at room temperature or -20 °C. Subsequently, the remaining total RNA was recovered by LLE, as previously described, and analyzed by qRT-PCR. Additionally, to increase the preservation time, a 5 µL volume of MIL was dissolved in 25 µL of PPG-2000 before the extraction and preservation of a 5 µg mass of RNA aqueous solution. The aqueous phase was carefully removed subsequently, and the MIL/PPG-2000 phase was stored at room temperature or -20 °C for 7- to 15-day preservation period. Afterward, 150 µL of iced ethanol and 5 µL of 3 M sodium acetate (pH 5.2) was added to precipitate the remaining RNA. The solution was kept at -20 °C for 1 to 2 h and centrifuged at 15,000 rpm for at least 10 min. After carefully removing the supernatant, the RNA was

resuspended with DEPC-treated water followed by downstream analysis by HPLC, qRT-PCR, or agarose gel electrophoresis.

4.4.8 Preservation of RNA from RNase A

The RNA preservation experiments were performed by the previously described methods with the addition of RNase A. A 5 µL volume of MIL was initially dissolved in 25 µL of PPG-2000, followed by 4 µL of 1 µg/µL RNase A solution being spiked with MIL/PPG-2000. After an incubation time of 60 min, the aqueous phase was removed, and 5 µg of RNA sample solution was added and incubated for 60 min. The aqueous phase was carefully removed, and total RNA was recovered by ethanol precipitation and resuspended in DEPC-treated water. A negative control was performed using the same procedure without MILs.

4.4.9 Partitioning Behavior of RNA and MILs

The standard RNA solution used in these experiments was a diluted 10 ppm yeast total RNA solution. SDE was performed with 1 µL of MIL and 50 µL of standard solution to determine the partitioning behavior. After 1-h extraction, the residual aqueous solution was analyzed by anion-exchange HPLC using a Shimadzu LC-20AT HPLC chromatograph (Columbia, MD, USA) with a multiwavelength UV-vis detector and separated on a 35 × 4.6 mm i.d. × 2.5 µm TSKgel DEAE-NPR anion exchange column with a 5 × 4.6 mm i.d. × 5 µm TSKgel DEAE-NPR guard column (Tosoh Bioscience, King of Prussia, PA). Mobile phase A consisted of 20 mM Tris-HCl (pH 7) and mobile phase B consisted of 1 M NaCl and 20 mM Tris-HCl (pH 7). RNA was detected at 260 nm and the amount of RNA was determined using an external calibration curve. Gradient elution was performed with the following program: 0% B from 0 to 2 min, increased from 0 to 5% B from 2 to 9 min, increased to 50% B from 9 to 10 min, increased to 100% B from 10 to 15 min, held at 100% B from 15 to 20 min, decreased from 100 to 0% from 20 to 22 min, and held at 0% from 22 to 30 min.

4.4.10 Partitioning Behavior of RNase A and MILs

A 100 µL volume of 1 µg/µL RNase A solution was extracted by 1 µL of MILs using the same SDE method described in the previous experiments. After 1-h extraction, the residual aqueous solution was injected onto a Shimadzu LC-20AT HPLC with a multiwavelength UV-vis detector and separated by a 50 × 4.6 mm i.d. × 2.7 µm Poroshell 120 EC-C18 reverse phase column (Agilent, Santa Clara, CA, USA). Mobile phase A consisted of 0.1% TFA/H_2O, and mobile phase B consisted of 0.07% TFA/ACN. Gradient elution was performed with the following program: increased from 5 B to 100% B from 0 to 20 min, held at 100% B from 20 to 30 min, and decreased from 100 to 5% B from 30 to 40 min.

4.5 Conclusions

In this study, hydrophobic MILs were prepared and applied as solvents to extract and preserve yeast total RNA from aqueous solution. RNA was able to be preserved for a period of 15 days to facilitate recovery using the $[P_{66614}^+][Co(hfacac)_3^-]$ and $[P_{66614}^+][Co(Phtfacac)_3^-]$ MILs with the aid of an additional dispersion of PPG-2000. Although the recovery was relatively low, the recovered RNA was able to be analyzed by HPLC, qRT-PCR, and agarose gel electrophoresis. In addition, the $[Co(OIM)_4^{2+}][Glu^-]_2$ and $[Co(OIM)_4^{2+}][Asp^-]_2$ MILs demonstrated the capability of extracting and protecting yeast total RNA from RNase A degradation simultaneously, as determined by HPLC and agarose gel electrophoresis. The extraction efficiency of RNase A was found to be lower than RNA, suggesting that the MIL solvent provides an anhydrous microenvironment to prevent RNA from interacting with RNase A. This study offers a new method for RNA preservation and can be highly beneficial for in-field biological sample preparation and storage. Ongoing studies are focused on improving the recovery, in-depth study of preservation mechanism, alleviating qRT-PCR inhibition caused by MIL moieties, and further increasing the preservation time in the presence of RNase A.

4.6 Acknowledgements

The authors acknowledge funding from Chemical Measurement and Imaging Program at the National Science Foundation (Grant No. CHE-1709372). The author certify that they have no affiliations with or involvement in any organization or entity with any financial interest in the subject matter or materials discussed in this manuscript.

4.7 References

(1) Valadi, H.; Ekström, K.; Bossios, A.; Sjöstrand, M.; Lee, J. J.; Lötvall, J. O. Exosome-Mediated Transfer of MRNAs and MicroRNAs Is a Novel Mechanism of Genetic Exchange between Cells. *Nat. Cell Biol.* **2007**, *9* (6), 654–659.

(2) Wang, F.; Flanagan, J.; Su, N.; Wang, L. C.; Bui, S.; Nielson, A.; Wu, X.; Vo, H. T.; Ma, X. J.; Luo, Y. RNAscope: A Novel in Situ RNA Analysis Platform for Formalin-Fixed, Paraffin-Embedded Tissues. *J. Mol. Diagnostics* **2012**, *14* (1), 22–29.

(3) Head, I. M.; Saunders, J. R.; Pickup, R. W. Microbial Evolution, Diversity, and Ecology: A Decade of Ribosomal RNA Analysis of Uncultivated Microorganisms. *Microb. Ecol.* **1998**, *35* (1), 1–21.

(4) Condon, C. Maturation and Degradation of RNA in Bacteria. *Curr. Opin. Microbiol.* **2007**, *10* (3), 271–278.

(5) Behlke, M. A. Progress towards in Vivo Use of SiRNAs. *Mol. Ther.* **2006**, *13* (4), 644–670.

(6) Strauss, J. H.; Kelly, R. B.; Sinsheimer, R. L. Denaturation of RNA with Dimethyl Sulfoxide. *Biopolymers* **1968**, *6* (6), 793–807.

(7) Kong, Q.; Lin, C. L. G. Oxidative Damage to RNA: Mechanisms, Consequences, and Diseases. *Cell. Mol. Life Sci.* **2010**, *67* (11), 1817–1829.

(8) Mendelsohn, S. L.; Young, D. A. Efficacy of Sodium Dodecyl Sulfate, Diethyl Pyrocarbonate, Proteinase K and Heparin Using a Sensitive Ribonuclease Assay. *Biochim. Biophys. Acta* **1978**, *519*, 461–473.

(9) Murphy, M. A.; Waits, L. P.; Kendall, K. C.; Wasser, S. K.; Higbee, J. A.; Bogden, R. An Evaluation of Long-Term Preservation Methods for Brown Bear (Ursus Arctos) Faecal DNA Samples. *Conserv. Genet.* **2002**, *3* (4), 435–440.

(10) Zhiguo, W.; Baofeng, Y. *MicroRNA Expression Detection Methods*; **2010**; Vol. 91.

(11) Smith, M. T.; Wilding, K. M.; Hunt, J. M.; Bennett, A. M.; Bundy, B. C. The Emerging Age of Cell-Free Synthetic Biology. *FEBS Lett.* **2014**, *588* (17), 2755–2761.

(12) Hatzimanikatis, V.; Choe, L. H.; Lee, K. H. Proteomics: Theoretical and Experimental Considerations. *Biotechnol. Prog.* **1999**, *15* (3), 312–318.

(13) Wolf, B.; Lesnaw, J. A.; Reichmann, M. E. A Mechanism of the Irreversible Inactivation of Bovine Pancreatic Ribonuclease by Diethylpyrocarbonate: A General Reaction of Diethylpyrocarbonate with Proteins. *Eur. J. Biochem.* **1970**, *13* (3), 519–525.

(14) Fedorcsák, I.; Ehrenberg, L. Effects of Diethyl Pyrocarbonate and Methyl Methanesulfonate on Nucleic Acids and Nucleases. *Acta Chemica Scandinavica*. **1966**, pp 107–112.

(15) Pearse, A. G. E.; Polak, J. M.; Adams, C.; Kendall, P. A. Diethylpyrocarbonate, a Vapour-Phase Fixative for Immunofluorescence Studies on Polypeptide Hormones. *Histochem. J.* **1974**, *6* (3), 347–352.

(16) Farragher, S. M.; Tanney, A.; Kennedy, R. D.; Paul Harkin, D. RNA Expression Analysis from Formalin Fixed Paraffin Embedded Tissues. *Histochem. Cell Biol.* **2008**, *130* (3), 435–445.

(17) Koopmans, M.; Monroe, S. S.; Coffield, L. M.; Zaki, S. R. Optimization of Extraction and PCR Amplification of RNA Extracts from Paraffin-Embedded Tissue in Different Fixatives. *J. Virol. Methods* **1993**, *43* (2), 189–204.

(18) Park, Y. N.; Abe, K.; Li, H.; Hsuih, T.; Thung, S. N.; Zhang, D. Y. Detection of Hepatitis C Virus RNA Using Ligation-Dependent Polymerase Chain Reaction in Formalin-Fixed, Paraffin-Embedded Liver Tissues. *Am. J. Pathol.* **1996**, *149* (5), 1485–1491.

(19) McGhee, J. D.; von Hippel, P. H. Formaldehyde as a Probe of DNA Structure. 3. Equilibrium Denaturation of DNA and Synthetic Polynucleotides. *Biochemistry* **1977**, *16* (15), 3267–3276.

(20) Naddeo, M.; Vitagliano, L.; Russo, A.; Gotte, G.; D'Alessio, G.; Sorrentino, S. Interactions of the Cytotoxic RNase A Dimers with the Cytosolic Ribonuclease Inhibitor. *FEBS Lett.* **2005**, *579* (12), 2663–2668.

(21) Chomczynski, P. Solubilzation in Formamide Protects RNA from Degradation. *Nucleic Acids Res.* **1992**, *20* (14), 3791–3792.

(22) Russo, A.; Acharya, K. R.; Shapiro, R. Small Molecule Inhibitors of RNase A and Related Enzymes. *Methods Enzymol.* **2001**, *341* (1992), 629–648.

(23) Jenkins, J. L.; Shapiro, R. Identification of Small-Molecule Inhibitors of Human Angiogenin and Characterization of Their Binding Interactions Guided by Computational Docking. *Biochemistry* **2003**, *42* (22), 6674–6687.

(24) Earl, C. C.; Smith, M. T.; Lease, R. A.; Bundy, B. C. Polyvinylsulfonic Acid: A Low-Cost Rnase Inhibitor for Enhanced RNA Preservation and Cell-Free Protein Translation. *Bioengineered* **2018**, *9* (1), 90–97.

(25) Pedro, A. Q.; Pereira, P.; Quental, M. J.; Carvalho, A. P.; Santos, S. M.; Queiroz, J. A.; Sousa, F.; Freire, M. G. Cholinium-Based Good's Buffers Ionic Liquids as Remarkable Stabilizers and Recyclable Preservation Media for Recombinant Small RNAs. *ACS Sustain. Chem. Eng.* **2018**, *6* (12), 16645–16656.

(26) Mondal, D.; Sharma, M.; Mukesh, C.; Gupta, V.; Prasad, K. Improved Solubility of DNA in Recyclable and Reusable Bio-Based Deep Eutectic Solvents with Long-Term Structural and Chemical Stability. *Chem. Commun.* **2013**, *49* (83), 9606–9608.

(27) Brown, P.; Butts, C. P.; Eastoe, J.; Padrón Hernández, E.; Machado, F. L. D. A.; De Oliveira, R. J. Dication Magnetic Ionic Liquids with Tuneable Heteroanions. *Chem. Commun.* **2013**, *49* (27), 2765–2767.

(28) Santos, E.; Albo, J.; Irabien, A. Magnetic Ionic Liquids: Synthesis, Properties and Applications. *RSC Adv.* **2014**, *4* (75), 40008–40018.

(29) Fujita, K.; MacFarlane, D. R.; Forsyth, M. Protein Solubilising and Stabilising Ionic Liquids. *Chem. Commun.* **2005**, *70* (38), 4804–4806.

(30) Chandran, A.; Ghoshdastidar, D.; Senapati, S. Groove Binding Mechanism of Ionic Liquids: A Key Factor in Long-Term Stability of DNA in Hydrated Ionic Liquids? *J. Am. Chem. Soc.* **2012**, *134* (50), 20330–20339.

(31) Benedetto, A.; Ballone, P. Room Temperature Ionic Liquids Meet Biomolecules: A Microscopic View of Structure and Dynamics. *ACS Sustain. Chem. Eng.* **2016**, *4* (2), 392–412.

(32) Taha, M.; E Silva, F. A.; Quental, M. V.; Ventura, S. P. M.; Freire, M. G.; Coutinho, J. A. P. Good's Buffers as a Basis for Developing Self-Buffering and Biocompatible Ionic Liquids for Biological Research. *Green Chem.* **2014**, *16* (6), 3149–3159.

(33) Marsh, K. N.; Boxall, J. A.; Lichtenthaler, R. Room Temperature Ionic Liquids and Their Mixtures - A Review. *Fluid Phase Equilib.* **2004**, *219* (1), 93–98.

(34) Mazid, R. R.; Divisekera, U.; Yang, W.; Ranganathan, V.; Macfarlane, D. R.; Cortez-Jugo, C.; Cheng, W. Biological Stability and Activity of SiRNA in Ionic Liquids. *Chem. Commun.* **2014**, *50* (88), 13457–13460.

(35) Quental, M. V.; Pedro, A. Q.; Pereira, P.; Sharma, M.; Queiroz, J. A.; Coutinho, J. A. P.; Sousa, F.; Freire, M. G. Integrated Extraction-Preservation Strategies for RNA Using Biobased Ionic Liquids. *ACS Sustain. Chem. Eng.* **2019**, *7* (10), 9439–9448.

(36) Clark, K. D.; Nacham, O.; Yu, H.; Li, T.; Yamsek, M. M.; Ronning, D. R.; Anderson, J. L. Extraction of DNA by Magnetic Ionic Liquids: Tunable Solvents for Rapid and Selective DNA Analysis. *Anal. Chem.* **2015**, *87* (3), 1552–1559.

(37) Pierson, S. A.; Nacham, O.; Clark, K. D.; Nan, H.; Mudryk, Y.; Anderson, J. L. Synthesis and Characterization of Low Viscosity Hexafluoroacetylacetonate-Based Hydrophobic Magnetic Ionic Liquids. *New J. Chem.* **2017**, *41* (13), 5498–5505.

(38) Clark, K. D.; Sorensen, M.; Nacham, O.; Anderson, J. L. Preservation of DNA in Nuclease-Rich Samples Using Magnetic Ionic Liquids. *RSC Adv.* **2016**, *6* (46), 39846–39851.

(39) Nacham, O.; Clark, K. D.; Varona, M.; Anderson, J. L. Selective and Efficient RNA Analysis by Solid-Phase Microextraction. *Anal. Chem.* **2017**, *89* (20), 10661–10666.

(40) Yu, C.; Chan, K. H.; Wong, K. M.; Yam, V. W. Single-Stranded Nucleic Acid-Induced Helical Self-Assembly of Alkynylplatinum (II) Terpyridyl Complexes. *Proc. Natl. Acad. Sci. U. S. A.* **2006**, *103* (52), 1–6.

(41) Reddy, P. R.; Radhika, M.; Manjula, P. Synthesis and Characterization of Mixed Ligand Complexes of Zn(II) and Co(II) with Amino Acids: Relevance to Zinc Binding Sites in Zinc Fingers. *J. Chem. Sci.* **2005**, *117* (3), 239–246.

(42) Zaslavsky, B. Y.; Ferreira, L. A.; Darling, A. L.; Uversky, V. N. The Solvent Side of Proteinaceous Membrane-Less Organelles in Light of Aqueous Two-Phase Systems. *Int. J. Biol. Macromol.* **2018**, *117*, 1224–1251.

(43) Constantinescu, D.; Weingärtner, H.; Herrmann, C. Protein Denaturation by Ionic Liquids and the Hofmeister Series: A Case Study of Aqueous Solutions of Ribonuclease A. *Angew. Chemie - Int. Ed.* **2007**, *46* (46), 8887–8889.

(44) Farooq, M. Q.; Chand, D.; Odugbesi, G. A.; Varona, M.; Mudryk, Y.; Anderson, J. L. Investigating the Effect of Ligand and Cation on the Properties of Metal Fluorinated Acetylacetonate Based Magnetic Ionic Liquids. *New J. Chem.* **2019**, *43* (28), 11334–11341.

(45) Chand, D.; Farooq, M. Q.; Pathak, A. K.; Li, J.; Smith, E. A.; Anderson, J. L. Magnetic Ionic Liquids Based on Transition Metal Complexes with N-Alkylimidazole Ligands. *New J. Chem.* **2019**, *43* (1), 20–23.

(46) Goodrich, B. F.; De La Fuente, J. C.; Gurkan, B. E.; Zadigian, D. J.; Price, E. A.; Huang, Y.; Brennecke, J. F. Experimental Measurements of Amine-Functionalized Anion-Tethered Ionic Liquids with Carbon Dioxide. *Ind. Eng. Chem. Res.* **2011**, *50* (1), 111–118.

CHAPTER 5. GENERAL CONCLUSIONS

This thesis summarized the application of ILs and MILs in nucleic acid analysis. ILs and MILs in this study were investigated to improve the efficiency of DNA/RNA analysis and overcome drawbacks to conventional methods. They demonstrate the superior capability for biological sample preparation and analysis.

Chapter 2 introduces a method using ITO or DTO probes loading to MIL supports to extract and enrich specific DNA sequences from interfering sequences. A series of ITO/DTO probes with various hydrophobic and fluorophilic functional groups in the cation and anion moieties were investigated for the sequence-specific extraction with the $[P_{66614}^{+}][Mn(hfacac)_3^{-}]$ and $[P_{66614}^{+}][Mn(Phtfacac)_3^{-}]$ MIL supports. The DTO with two alkyl groups (C_8) performed the best loading ability with MIL among other probes. Furthermore, the DTO-MIL system was demonstrated that is more efficient of extracting target DNA from solutions containing single nucleotide variants than a commercial magnetic bead-based approach.

Chapter 3 optimizes the ITO/DTO-MIL method and expends it to more complex sample matrices including diluted plasma and diluted blood. Various DTO probes, MILs, extraction, and desorption conditions were studied to maximize the efficiency of this method. The target DNA sequences can be captured even at femtomolar level by $[ADIM^{+}]_2$-*KRAS* 2$[Br^{-}]$ DTO and $[ABzIM^{+}]$-*KRAS* $[Br^{-}]$ ITO in the presence of interfering biomolecules. The improved sequence-specific extraction method can be potential in the field of low-amount DNA detection.

Chapter 4 describes a use of MIL solvents to extract and preserve RNA from aqueous solution. The $[P_{66614}^{+}][Co(hfacac)_3^{-}]$ and $[P_{66614}^{+}][Co(Phtfacac)_3^{-}]$ MILs were able to preserve RNA for a period of 15 days at room temperature. In addition, RNA was protected from RNase A degradation within the $[Co(OIM)_4^{2+}][Glu^{-}]_2$ and $[Co(OIM)_4^{2+}][Asp^{-}]_2$ MILs. The advantages

of this novel method include simplifying the extraction and preservation procedures and minimizing the risk of nuclease contamination, which make it highly beneficial for in-field biological sample preparation and storage.

APPENDIX A. SUPPLEMENTAL INFORMATION ACCOMPANYING CHAPTER 2

Synthesis of magnetic ionic liquids

First, 30 mL of ethanol (200 proof) were used to dissolve 10 mmol of ammonium hydroxide in a 100 mL round flask. The flask was sealed with a rubber septum and 10 mmol of hexafluoroacetylacetone (hfacac) or 4,4,4-trifluoro-1-phenyl-1,3-butanedione ($PhCF_3acac$) were added dropwise to the mixture using a syringe. After the white vapor settled, 3.3 mmol of $MnCl_2 \cdot 4H_2O$ were added and the reaction was stirred at room temperature overnight. Next, the solvent was evaporated in vacuo and 10 mL of diethyl ether were used to dissolve the crude reaction products. The solution was then passed through filter paper if precipitation happened, transferred into a separatory funnel, and the crude products were washed with 20 mL aliquots of deionized water 5 to 10 times until the aqueous fraction yielded no precipitate upon addition of $AgNO_3$ solution. Next, the diethyl ether was evaporated in vacuo and the metal salt was dried at 50 °C overnight under reduced pressure. For each 1 mmol of metal salt, 1 mmol of trihexyl(tetradecyl)phosphonium chloride ($[P_{66614}^+][Cl^-]$) was added and the mixture was dissolved with approximately 30 mL of methanol. The reaction mixture was stirred at room temperature overnight. After evaporating the solvent, the products were redissolved in diethyl ether and transferred into a separatory funnel, washed with 20 mL of deionized water 5 to 10 times, and tested with $AgNO_3$ solution until the aqueous fractions yielded no visible precipitate. The diethyl ether phase was evaporated in vacuo and dried at 50 °C overnight under reduced pressure to yield a viscous orange $[P_{66614}^+][Mn(hfacac)_3^-]$ or brownish orange $[P_{66614}^+][Mn(Phtfacac)_3^-]$ liquid that was immiscible with water and responded to application of a magnetic field.

Synthesis of imidazolium-based ion tags

The synthesis and characterization of the allyl-bearing ion tag moieties was undertaken as previously reported with slight modifications where necessary.[1] Briefly, the 1-allyl-3-hexadecylimidazolium bromide ($[AHIM^+][Br^-]$) and 1-allyl-3-decylimidazolium bromide ($[ADIM^+][Br^-]$) salts were synthesized by reacting allylimidazole with the corresponding alkyl halide in 1:1.2 molar ratio in acetonitrile under reflux for 48 h. The solvent was evaporated *in vacuo* and the crude product washed with 5×20 mL aliquots of hexane. The product was then dried overnight in a vacuum oven at 40 °C.

The imidazolium salts with bis[(trifluoromethyl)sulfonyl]imide ($[NTf_2^-]$), perfluorobutanesulfonate ($[PFBS^-]$), and octylsulfate ($[OS^-]$) anions were prepared by metathesis reactions as described previously.[1] Briefly, a 1:1.2 mole ratio of imidazolium salt (bromide form) to $LiNTf_2$, KPFBS, or NaOS were dissolved in water and stirred at room temperature for 16 h. The hydrophobic ionic liquid underwent phase separation for the $[NTf_2^-]$ and $[PFBS^-]$ analogs and was isolated, washed with water several times, and dried in a vacuum oven set to 60 °C. Since the product with $[OS^-]$ anion did not phase separate, the reaction solution was slowly removed by rotovap and the resulting precipitate dissolved in dichloromethane. The DCM layer was washed with 5 mL aliquots of water until the aqueous phase yielded no precipitate from addition of $AgNO_3$.

LC-TOFMS Characterization of ITOs/DTO

The characterization of ITOs/DTO was performed using LC-TOFMS as previously reported.1 The modified oligos were separated using an Agilent Technologies 50 mm × 2.1 mm i.d. × 1.8 μm particle Zorbax Extend-C18 column that was equilibrated for 9 min at 0.2 mL min^{-1}. A mobile phase composition of 95:5 A:B was employed, with mobile phase A consisting of 5 mM triethylammonium acetate (pH 7.4) and mobile phase B as acetonitrile. The following

gradient elution program was used: 5 % B from 0-5 min, increase to 19.4 % B from 5 to 17 min, increase to 35 % B from 17 to 18 min, hold at 35 % B from 18 to 20 min, decrease to 5 % B from 20 to 21 min. LC eluent was diverted to waste for the first 8 min of the method. The nebulizing gas was set to 35 psi and the flow of the drying (N_2) gas was 9 L min^{-1} with a temperature of 350 °C. The capillary voltage was 4000 V. Spectra were acquired from 100-3000 m/z at 1 Hz.

Melt curve conditions

Melting point analysis was performed using the melt curve function on a Bio-Rad CFX96 Touch Real-Time PCR Detection System (Hercules, CA, USA). A 20 µL solution consisting of 10 µL of SsoAdvanced Universal SYBR Green Supermix (2x), 5 µL of 100 mM NaCl, 0.5 nmol of ITO or DTO, and 0.5 nmol of the DNA complement was prepared in a PCR tube. For measuring melt curves of ITOs/DTOs and mismatched sequences, the DNA complement was replaced by 0.5 nmol of a DNA sequence with 1 or 2 mismatched bases. The temperature program was initiated at 90.0 °C for 5 min, was cooled at max ramp to 20.0 °C for 10 min, and then the temperature was increased by 0.5 °C every 5 s to 95.0 °C. Melting points were assigned using the CFX Manager software.

Magnetic bead-based DNA extraction from samples containing single and double nucleotide variants

Streptavidin-coated magnetic beads and biotinylated oligonucleotide probes were used to capture DNA targets according to the manufacturer's instructions. To each tube, 16.9 fmol of biotinylated probe, 0.169 fmol of 261 bp target DNA, and either 0.169 fmol of a 20 mer complementary to the oligo probe, a 20 mer with 1 mismatched base, or a 20 mer with 2 mismatched bases were added. The final volume of the sample was 50 µL with a final NaCl concentration of 25 mM. All qPCR tubes were heated at 90 °C for 5 min and cooled to 4 °C for 5

min. Next, approximately 0.13 μg of prewashed M-270 Dynabeads (washing buffer: 10mM Tris-HCl pH = 7.5, 2 M NaCl, 1 mM EDTA) were added to the tube and all samples subjected to light shaking (60 rpm) for 10 min. After washing with deionized water three times, target DNA was desorbed from the magnetic beads with deionized water heated at 90 °C for 10 min and collected for qPCR amplification.

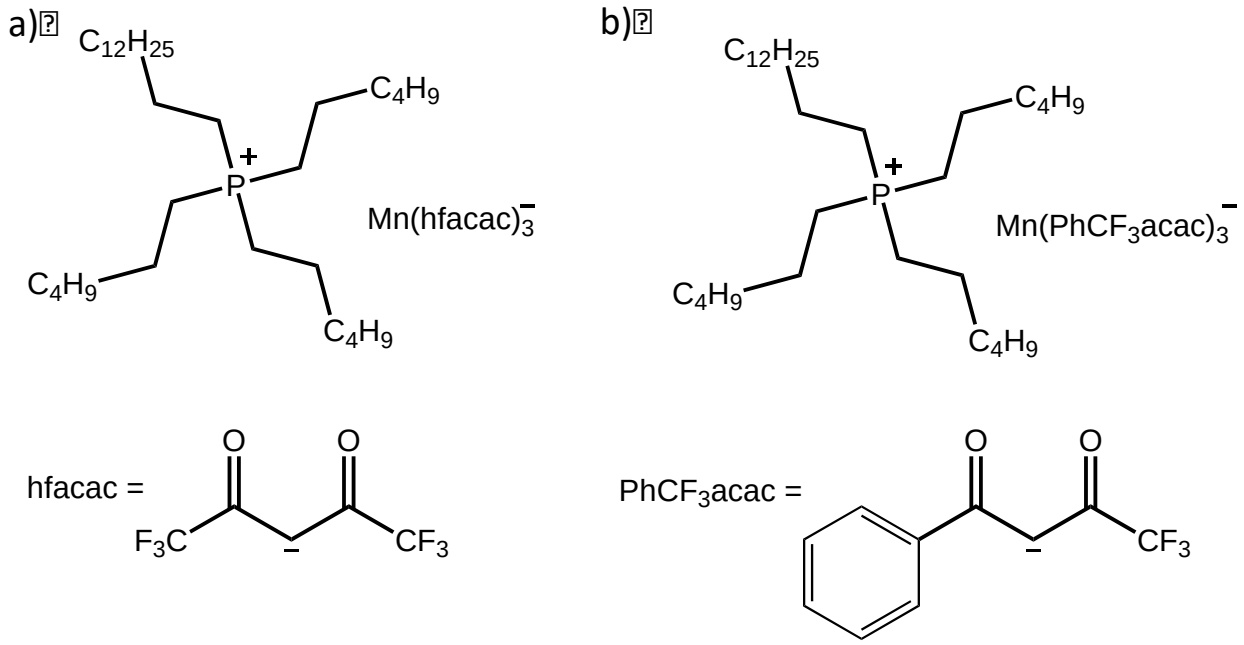

Figure A1. Chemical structures of the magnetic ionic liquid (MIL) supports used in this study.

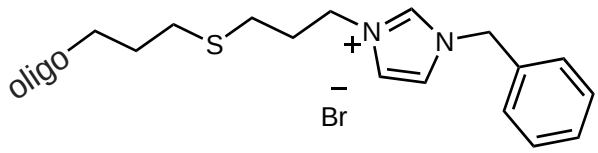

Figure A2. Chemical structure of the [ABzIM+][Br-]-ITO.

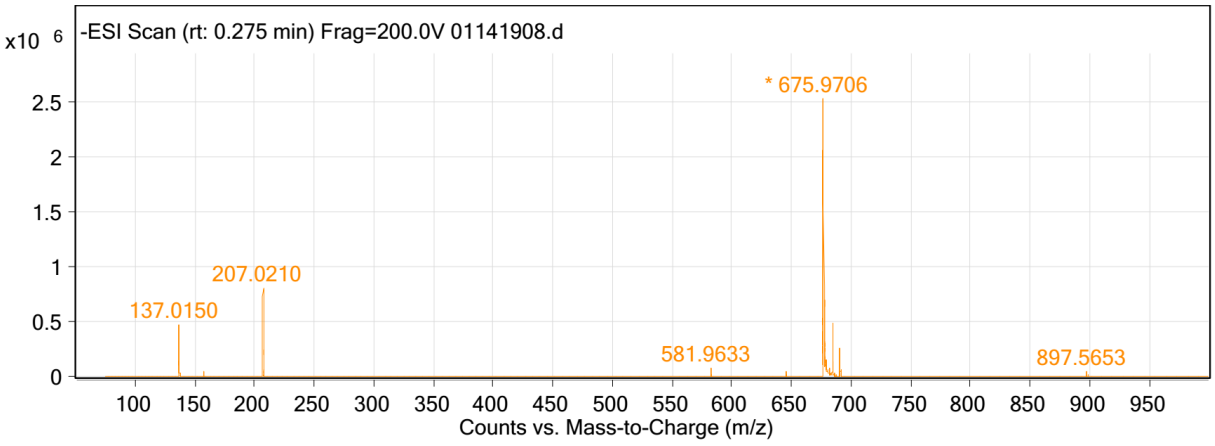

Figure A3. Mass spectrum (negative mode) of the $[P_{66614}^{+}][Mn(hfacac)_3^{-}]$ MIL.

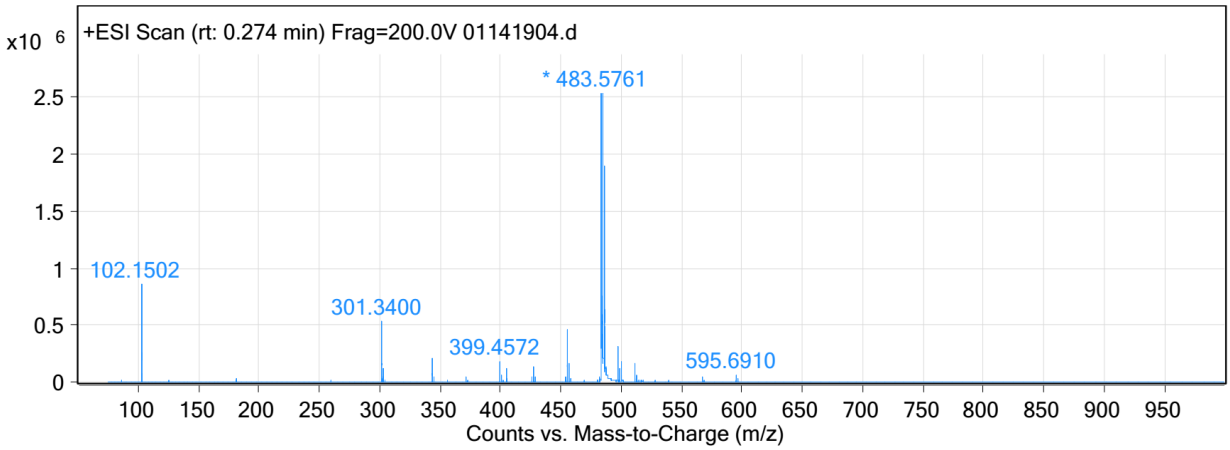

Figure A4. Mass spectrum (positive mode) of the $[P_{66614}^{+}][Mn(hfacac)_3^{-}]$ MIL.

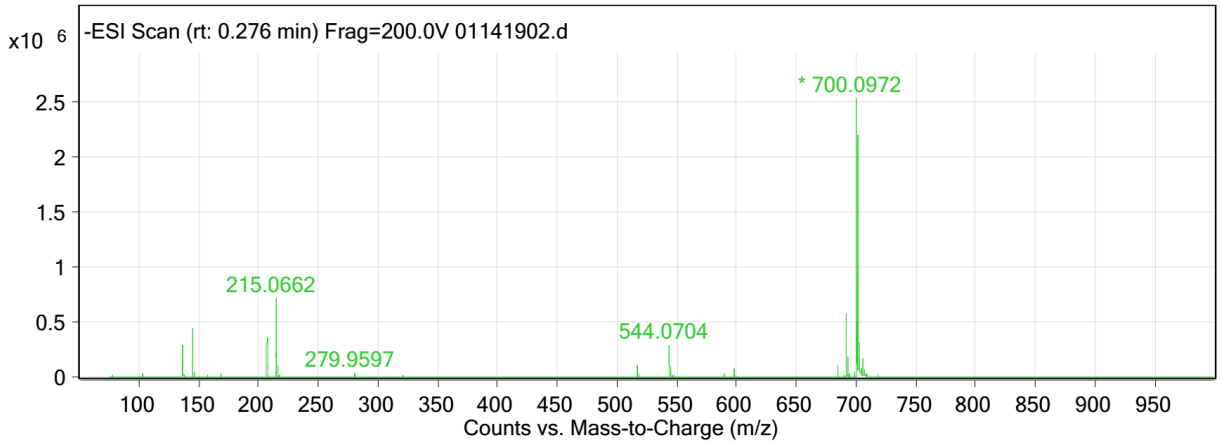

Figure A5. Mass spectrum (negative mode) of the $[P_{66614}^{+}][Mn(Phtfacac)_3^{-}]$ MIL.

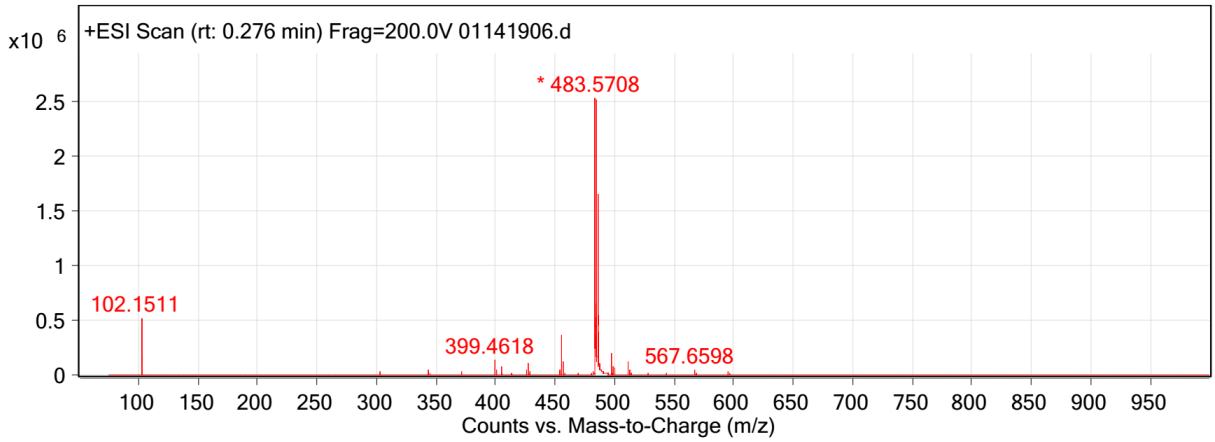

Figure A6. Mass spectrum (positive mode) of the $[P_{66614}^{+}][Mn(Phtfacac)_3^{-}]$ MIL.

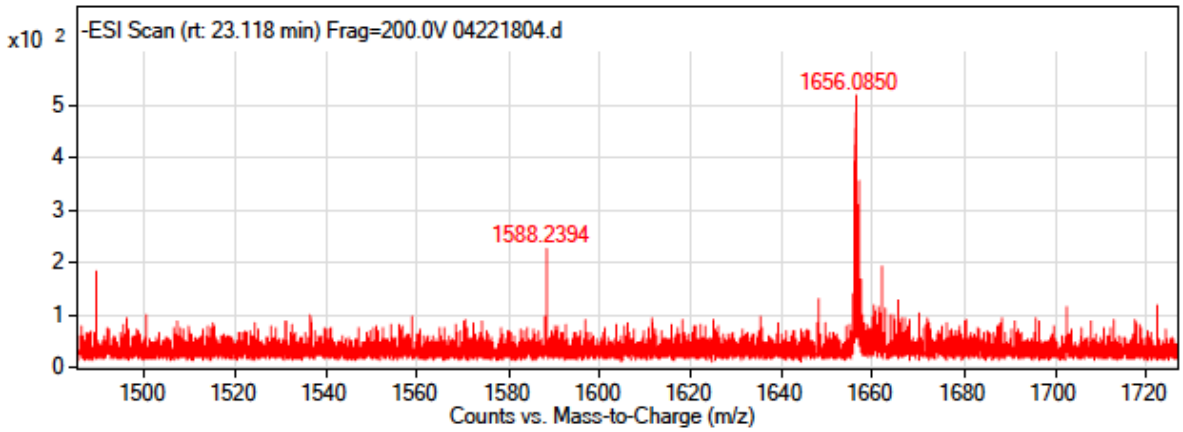

Figure A7. Mass spectrum (negative mode) of the $[AOIM]_2[Br]$-DTO.

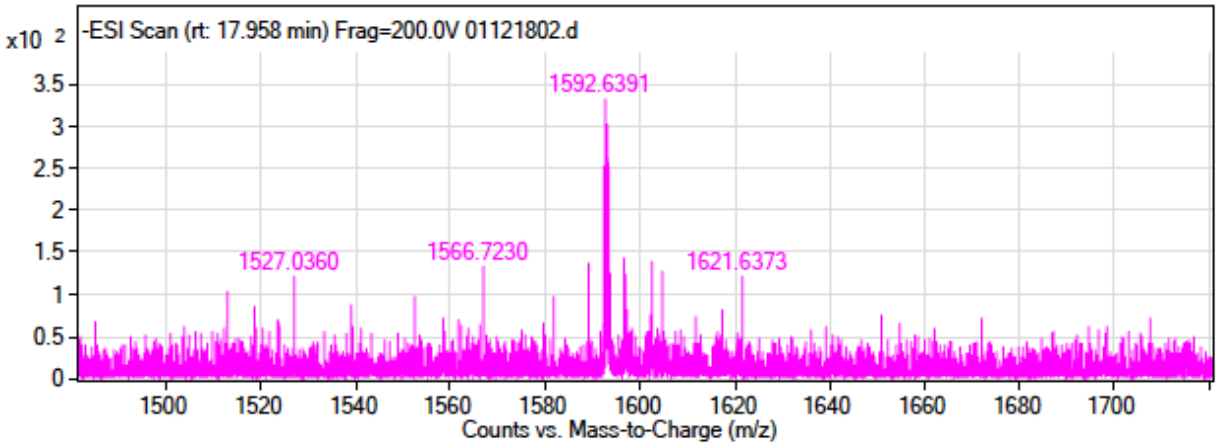

Figure A8. Mass spectrum (negative mode) of the [ADIM][Br]-ITO.

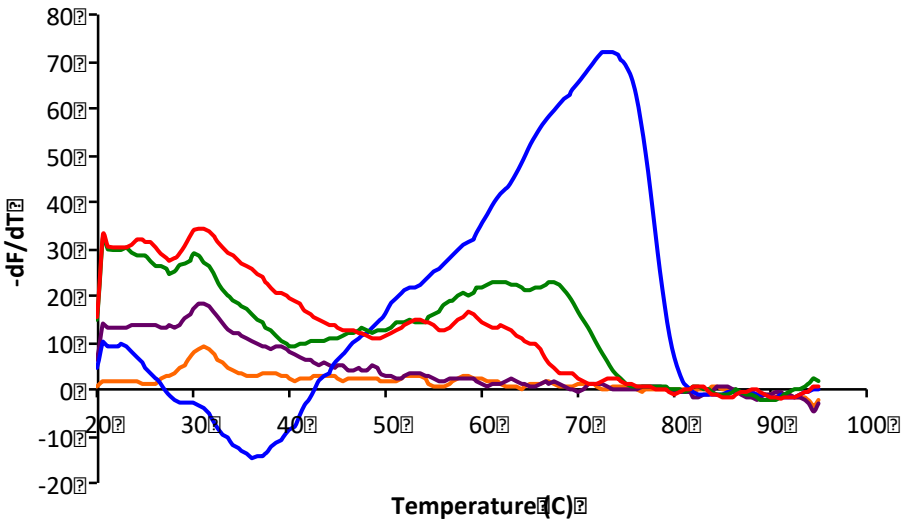

Figure A9. Melt curves for the $[AOIM^+]_2[Br^-]$ DTO probe and complementary DNA (blue), 1 nt mismatch (green), 2 nt mismatch (red), random sequence with no matching bases (purple), and DTO alone (orange).

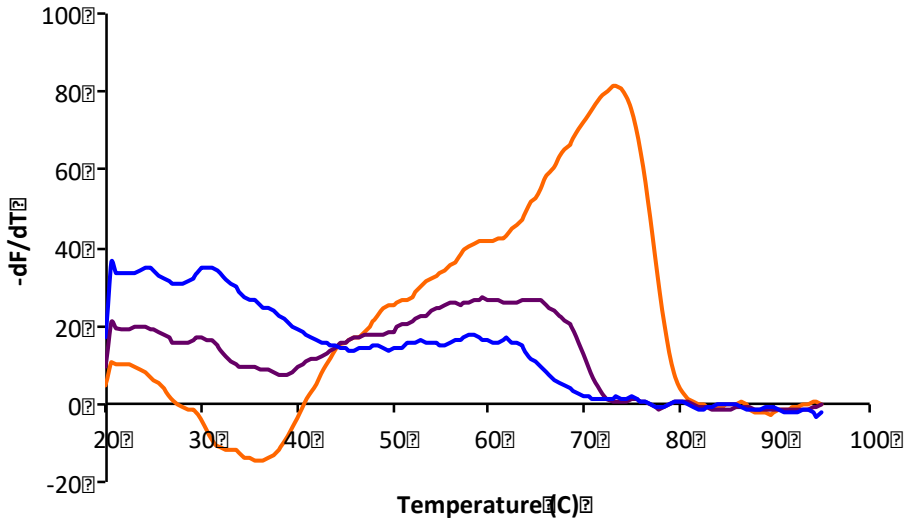

Figure A10. Melt curves for [AOIM$^+$][Br$^-$] ITO probe and complementary DNA (orange), 1 nt mismatch (purple), and 2 nt mismatch (blue) sequences.

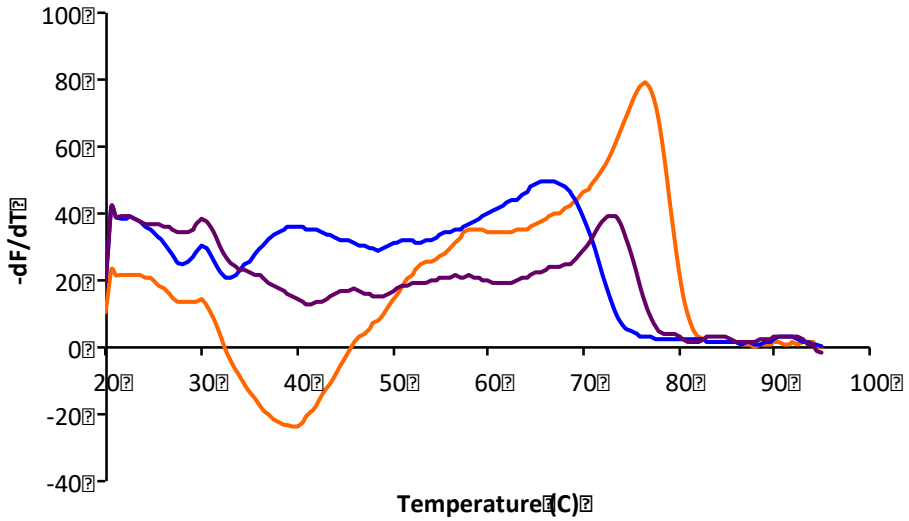

Figure A11. Melt curves for unmodified oligonucleotide probe and complementary DNA (orange), 1 nt mismatch (purple), and 2 nt mismatch (blue) sequences.

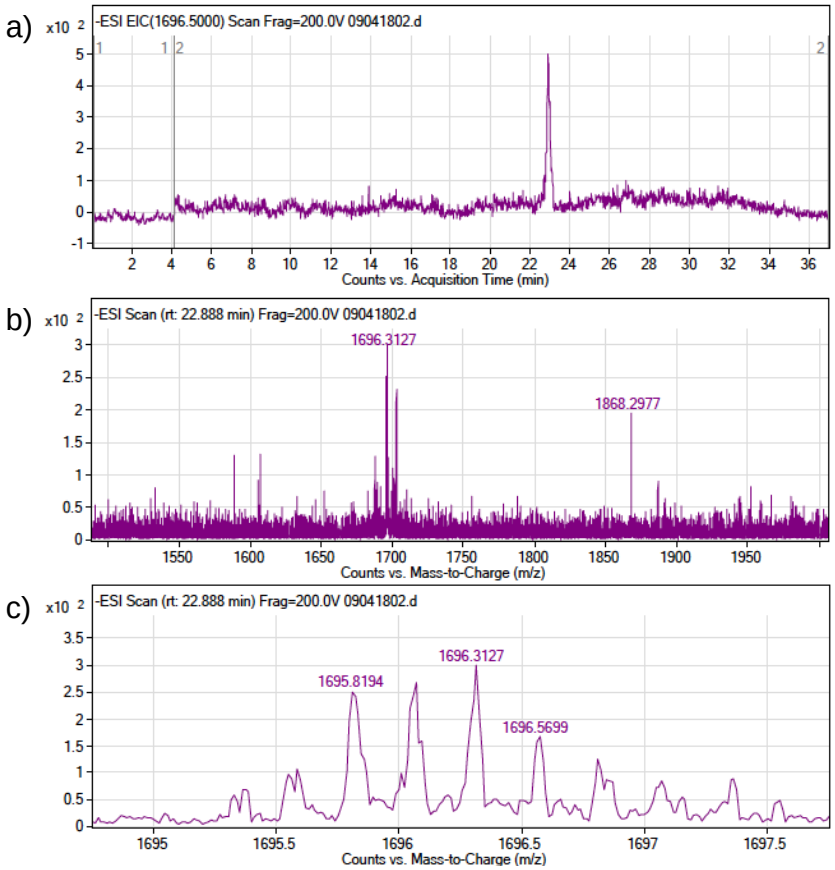

Figure A12. Panel (a) shows the extracted ion chromatogram of the KRAS [AOIM$^+$][Br$^-$]-DTO with the mass spectrum (negative mode) shown in (b). Panel (c) shows the isotope distribution for the KRAS DTO.

Table A1. Single- and double-stranded DNA loading efficiencies for the [ABzIM$^+$][Br$^-$]-ITO and the [AOIM$^+$][Br$^-$]-ITO on MIL supports.

MIL support	Target Extraction Efficiency (%, n = 3)				
	ABzIM-tagged oligo (n=3)	ssDNA complement (n=3)	Duplex (ABzIM-ITO +complement, n=3)	Duplex (AOIM-ITO +complement, n=3)	Duplex (unmodified oligo +complement, n=3)
[P_{66614}^+] [$Mn(hfacac)^{3-}$]	20 ± 7	12 ± 5	25 ± 5	25 ± 3	2 ± 2
[P_{66614}^+] [$Mn(CF_3Phacac)^{3-}$]	30 ± 4	27 ± 6	40 ± 3	20 ± 5	>1 ± 1

[a] Conditions: concentration of oligo/duplex: 8 ng μL^{-1}; MIL volume: 1 μL; sample volume: 50 μL; extraction time: 10 min; quantification method: anion-exchange HPLC with UV detection at 260 nm.

Table A2. Optimization of probe:target ratio for the DTO extraction system coupled with qPCR.

Target amount (fmol)	DTO amount (fmol)	DTO:target mole ratio	DTO:MIL (fmol μL^{-1})	Cq [a]
16.9	845	50:1	845	26.79
16.9	338	20:1	338	27.16
16.9	169	10:1	169	23.63
0.169	1.69	10:1	1.69	38.02
0.169	0.845	5:1	0.845	33.99
0.169	0.338	2:1	0.338	34.53
0.169	0.169	1:1	0.169	34.97

[a] Conditions: amount of target DNA: 0.169 fmol; MIL volume: 1 µL; sample volume: 50 µL; extraction time: 10 min; desorption time: 10 min at 90 °C quantification method: qPCR.

References

(1) Clark, K. D.; Varona, M.; Anderson, J. L. Ion-Tagged Oligonucleotides Coupled with a Magnetic Liquid Support for the Sequence-Specific Capture of DNA. *Angew. Chemie - Int. Ed.* **2017**, *56* (26), 7630–7633.

APPENDIX B. SUPPLEMENTAL INFORMATION ACCOMPANYING CHAPTER 3

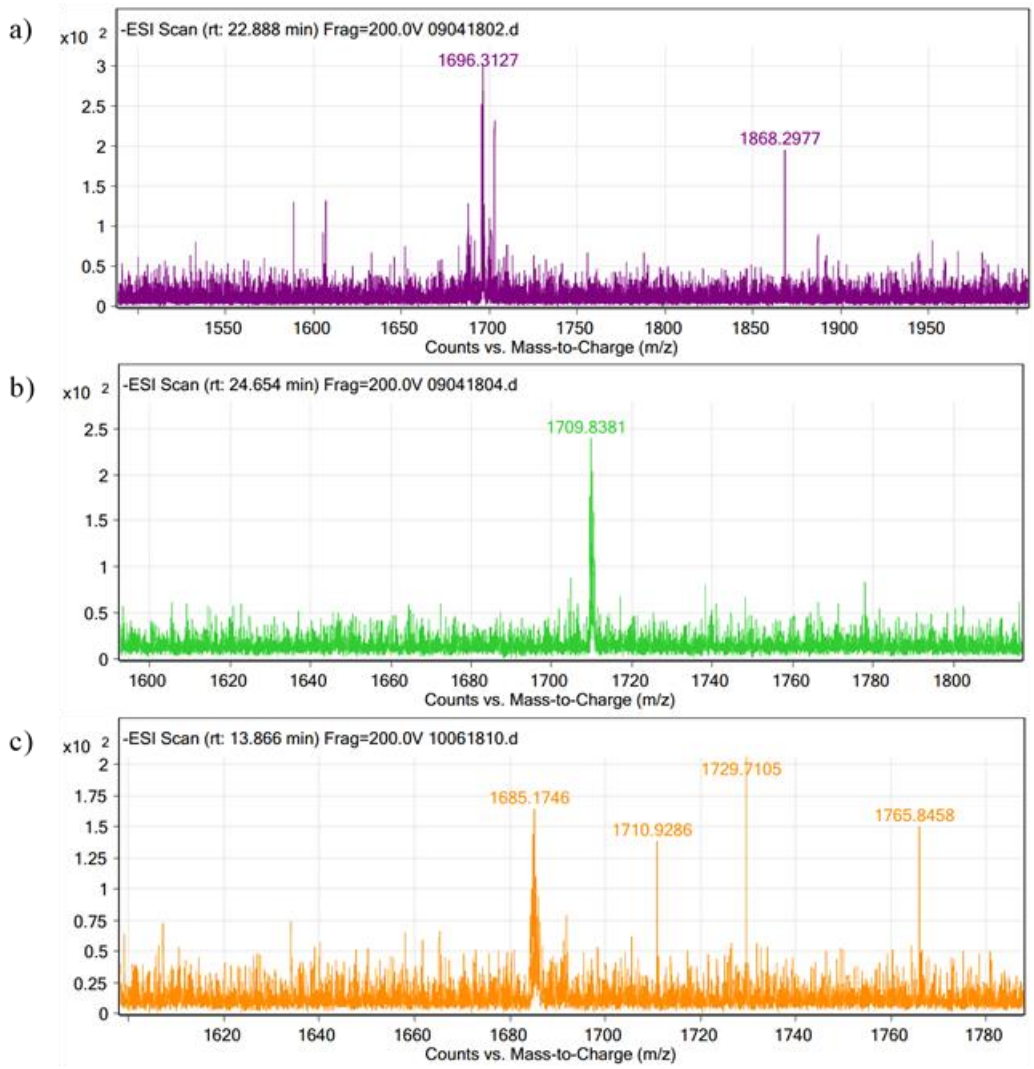

Figure B1. Mass spectra (negative ion mode) of the (a) $[AOIM^+]_2$-*KRAS*, (b) $[ADIM^+]_2$-*KRAS*, and (c) $[ABzIM^+]_2$-*KRAS* DTOs.

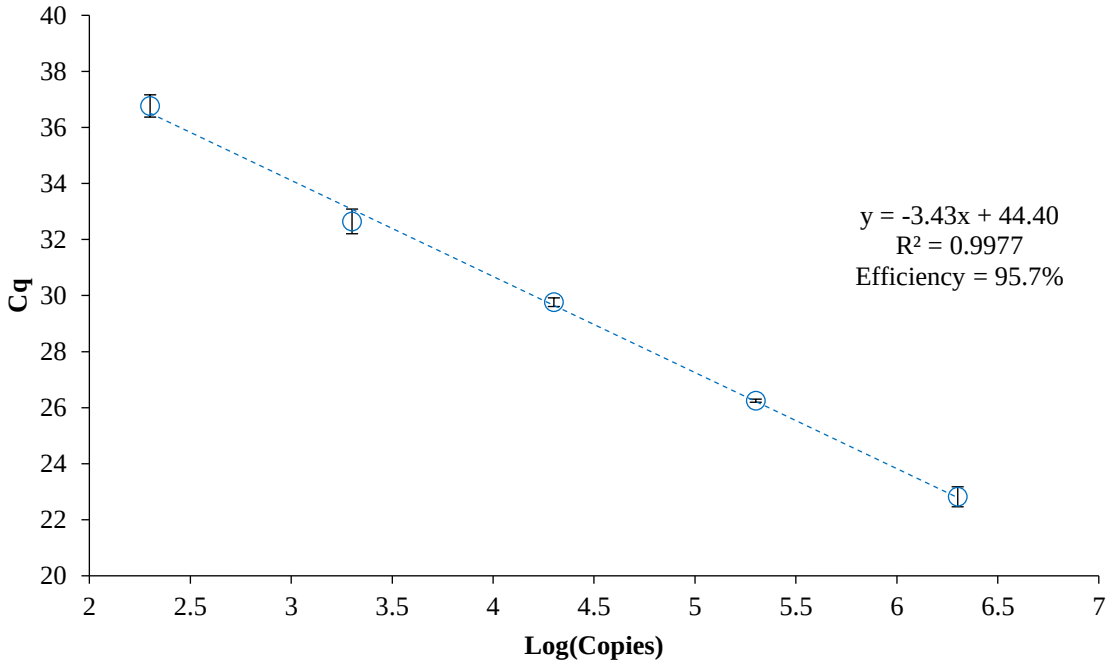

Figure B2. Five-point standard curve consisting of 10-fold dilutions of *KRAS* using qPCR.

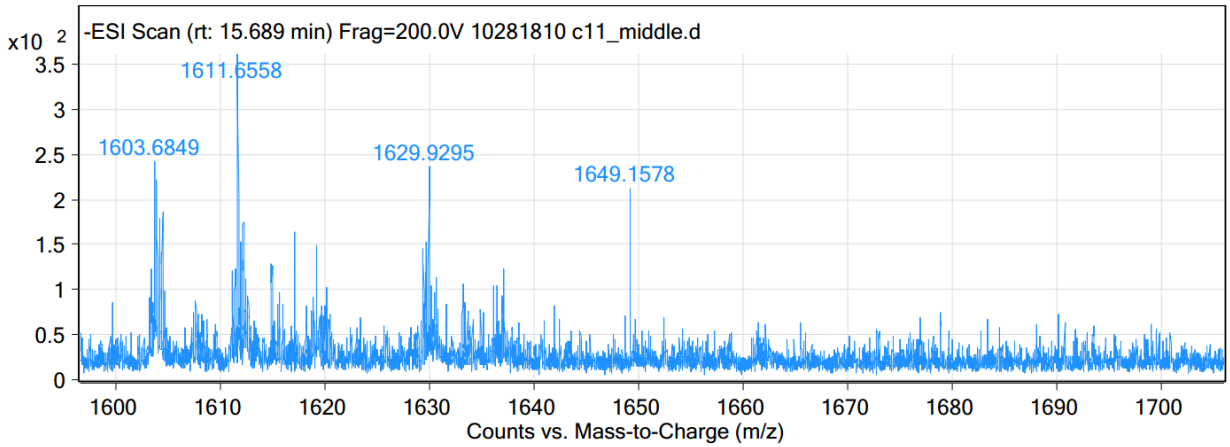

Figure B3. Mass spectrum (negative ion mode) of the reaction product from attempts to synthesize an undecylimidazolium-modified DTO.

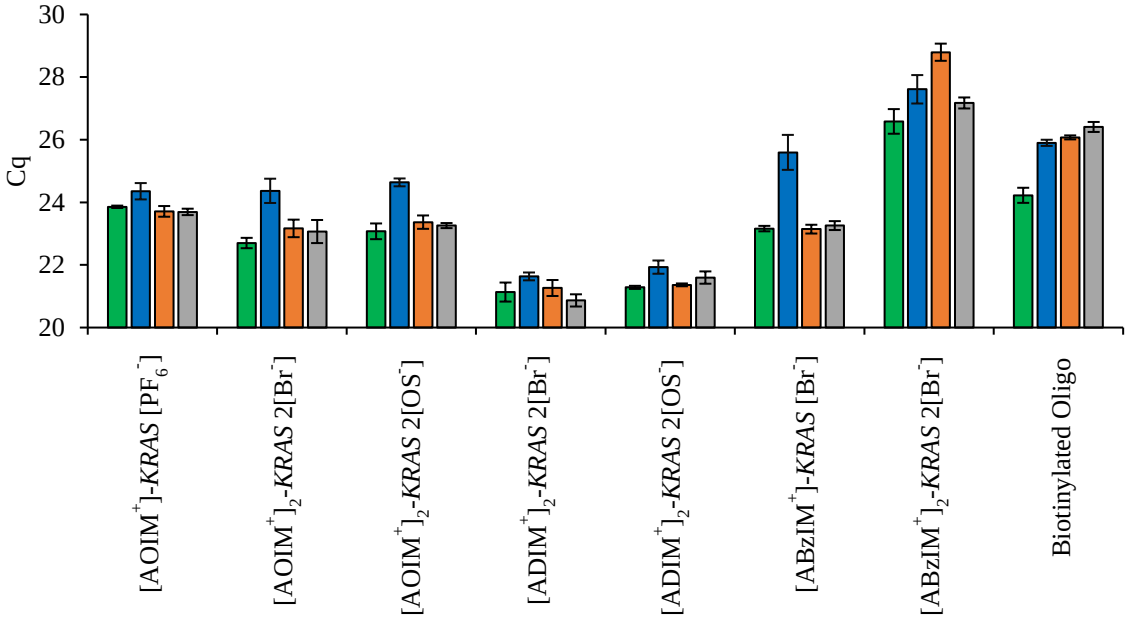

Figure B4. qPCR results for sequence-specific extraction of *KRAS* from (green) pure water and in the presence of a 20 nt (blue) complementary fragment, (yellow) 1 nt mismatch fragment, and (grey) 2 nt mismatch. *KRAS* template concentration: 7.2×10^{7} copies μL^{-1}, amount of $[ADIM^{+}]_2$-*KRAS* 2$[Br^{-}]$ DTO relative to DNA: 5:1, amount of $[AOIM^{+}]$-*KRAS* $[PF_6^{-}]$ ITO relative to DNA: 10:1, sample volume: 50 µL, MIL volume: 1 µL; extraction time: 10 min, desorption time: 4 min, desorption volume: 50 µL.

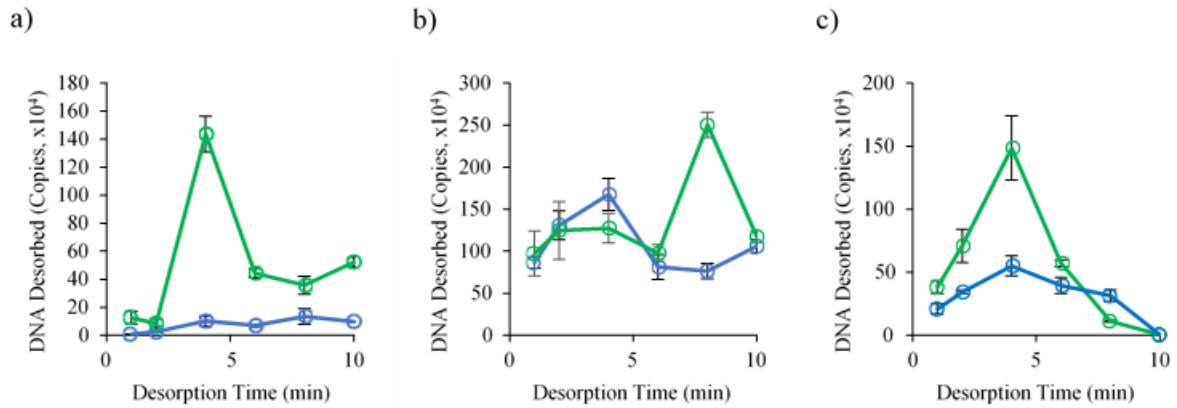

Figure B5. Amount of DNA desorbed over time after performing the static extraction of *KRAS* using the (blue) $[ADIM^{+}]_2$-*KRAS* 2$[Br^{-}]$ DTO and (green) highest loading ITO probe while desorbing in different concentrations of NaCl with the (a) $[P_{66614}^{+}][Mn(hfacac)_3^{-}]$, (b) $[N_{888Bz}^{+}][Mn(hfacac)_3^{-}]$, and (c) $[N_{888Bz}^{+}][Mn(hfacac)_2(Phtfacac)^{-}]$ MILs. *KRAS* template concentration: 7.2×10^{7} copies μL^{-1}, amount of $[ADIM^{+}]_2$-*KRAS* 2$[Br^{-}]$ DTO relative to DNA: 5:1, amount of $[AOIM^{+}]$-*KRAS* $[PF_6^{-}]$ ITO relative to DNA: 10:1, sample volume: 50 µL, MIL volume: 1 µL; extraction time: 10 min, desorption time: 4 min, desorption volume: 50 µL.

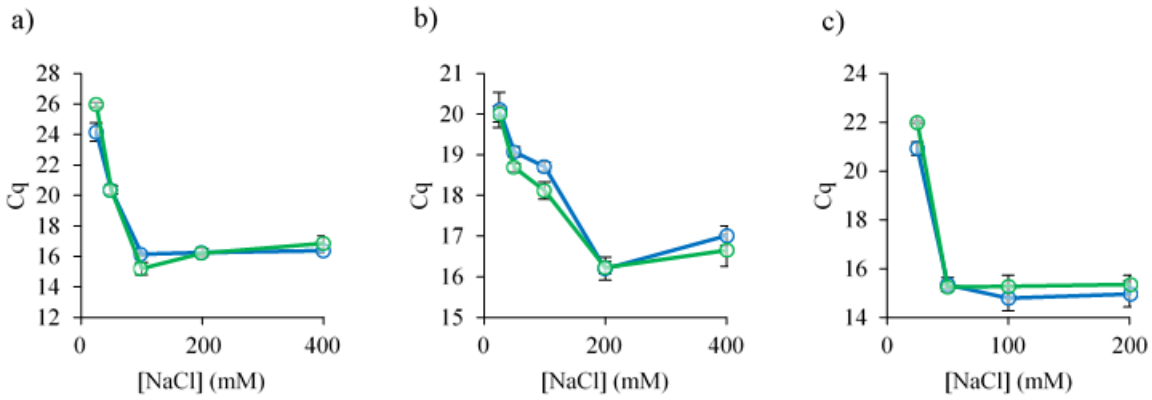

Figure B6. Cq values resulting from the static extraction of *KRAS* using the (blue) $[ADIM^+]_2$-*KRAS* 2$[Br^-]$ DTO and (green) highest loading ITO probe while desorbing in different concentrations of NaCl with the (a) $[P_{66614}^+][Mn(hfacac)_3^-]$, (b) $[N_{888Bz}^+][Mn(hfacac)_3^-]$, and (c) $[N_{888Bz}^+][Mn(hfacac)_2(Phtfacac)^-]$ MILs. *KRAS* template concentration: 7.2×10^7 copies μL^{-1}, amount of $[ADIM^+]_2$-*KRAS* 2$[Br^-]$ DTO relative to DNA: 5:1, amount of $[AOIM^+]$-*KRAS* $[PF_6^-]$ ITO relative to DNA: 10:1, sample volume: 50 µL, MIL volume: 1 µL; extraction time: 10 min, desorption time: 4 min, desorption volume: 50 µL.

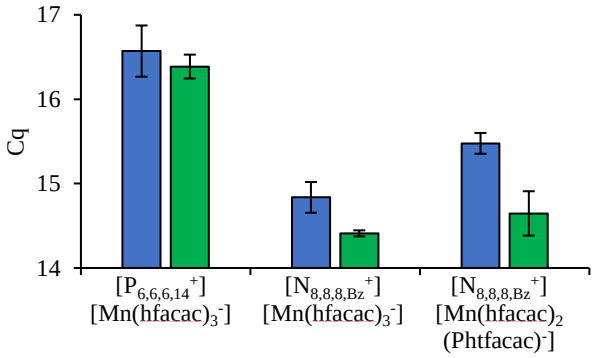

Figure B7. Target capture Cq values with the desorption of target DNA when desorbing into the qPCR buffer using the (blue) DTO and (green) ITO probes. *KRAS* template concentration: 7.2×10^7 copies μL^{-1}, amount of $[ADIM^+]_2$-*KRAS* 2$[Br^-]$ DTO relative to DNA: 5:1, amount of $[AOIM^+]$-*KRAS* $[PF_6^-]$ ITO relative to DNA: 10:1, sample volume: 50 µL, MIL volume: 1 µL; extraction time: 10 min, desorption time: 4 min, desorption volume: 50 µL.

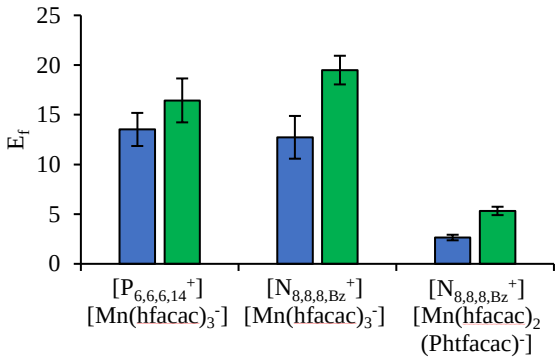

Figure B8. Enrichment factors (E_f) associated with the dispersive extraction of target *KRAS* with the desorption of target DNA with the (blue) DTO and (green) ITO probes. $[P_{66614}^+][Mn(hfacac)_3^-]$ MIL conditions: KRAS template concentration: 2×10^4 copies μL^{-1}, amount of $[ADIM^+]_2$-*KRAS* 2$[Br^-]$ DTO relative to DNA: 5:1, amount of $[AOIM^+]$-*KRAS* $[PF_6^-]$ ITO relative to DNA: 10:1, NaCl concentration: 25 mM, sample volume: 1.0 mL, MIL volume: 8 µL; extraction time: 3 min. $[N_{888Bz}^+][Mn(hfacac)_3^-]$ MIL conditions: KRAS template concentration: 2×10^4 copies μL^{-1}, amount of $[ADIM^+]_2$-*KRAS* 2$[Br^-]$ DTO relative to DNA: 5:1, amount of $[ABzIM^+]$-*KRAS* $[Br^-]$ relative to DNA: 10:1, NaCl concentration: 25 mM, sample volume: 1.0 mL, MIL volume: 6 µL: extraction time: 1 min. $[N_{888Bz}^+][Mn(hfacac)_2(Phtfacac)^-]$ MIL conditions: KRAS template concentration: 2×10^4 copies μL^{-1}, amount of $[ADIM^+]_2$-*KRAS* 2$[Br^-]$ DTO relative to DNA: 5:1, amount of $[ABzIM^+]$-*KRAS* $[Br^-]$ relative to DNA: 10:1, NaCl concentration: 25 mM, sample volume: 1.0 mL, MIL volume: 4 µL; extraction time: 1 min.

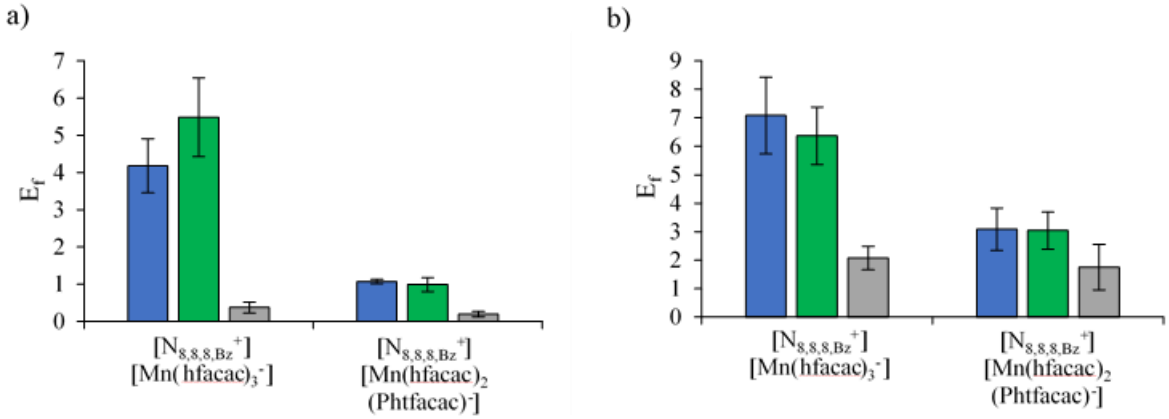

Figure B9. Enrichment factors (E_f) resulting from the DLLME of (a) 2×10^3 and (b) 2×10^2 copies μL^{-1} *KRAS* using the (blue) $[ADIM^+]_2$-*KRAS* 2$[Br^-]$ DTO, (green) $[ABzIM^+]$-*KRAS* $[Br^-]$ ITO, and (grey) negative control without the probe from 10-fold diluted plasma. $[N_{888Bz}^+][Mn(hfacac)_3^-]$ MIL conditions: amount of DTO relative to DNA: 5:1, amount of ITO relative to DNA: 10:1, NaCl concentration: 25 mM, sample volume: 1.0 mL, MIL volume: 6 µL: extraction time: 1 min. $[N_{888Bz}^+][Mn(hfacac)_2(Phtfacac)^-]$ MIL conditions: amount of DTO relative to DNA: 5:1, amount of ITO relative to DNA: 10:1, NaCl concentration: 25 mM, sample volume: 1.0 mL, MIL volume: 4 µL; extraction time: 1 min.

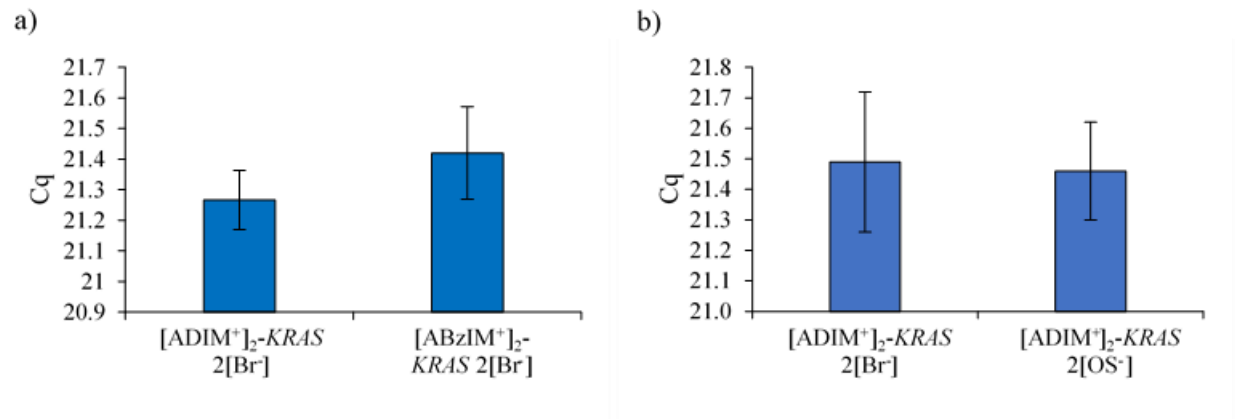

Figure B10. Target capture Cq obtained from the capture of target DNA using the (a) $[ADIM^+]_2$-*KRAS* 2$[Br^-]$ and $[ABzIM^+]_2$-*KRAS* 2$[Br^-]$ DTOs with the $[N_{888Bz}{}^+][Mn(hfacac)_3{}^-]$ MIL and (b) $[ADIM^+]_2$-*KRAS* 2$[Br^-]$ and $[ADIM^+]_2$-*KRAS* 2$[OS^-]$ DTOs with the $[P_{66614}{}^+][Mn(hfacac)_3{}^-]$ MIL from 10-fold diluted plasma. ITO/DTO-MIL method: KRAS template concentration: 7.2×10^7 copies μL^{-1}, amount of DTO relative to DNA: 5:1, sample volume: 50 µL, MIL volume: 1 µL; extraction time: 10 min, desorption time: 4 min, desorption volume: 50 µL.

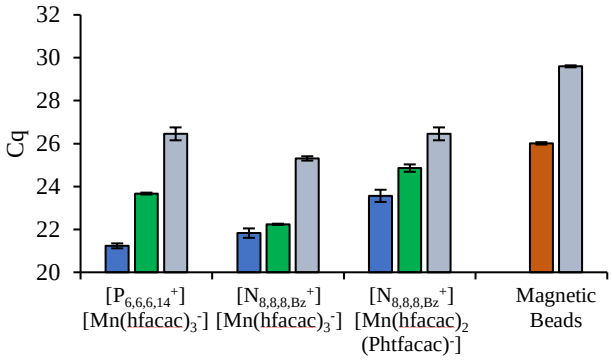

Figure B11. Target capture Cqs from the extraction of target DNA with the (blue) $[ADIM^+]_2$-*KRAS* 2$[Br^-]$ DTO, (green) ITO, (orange) biotinylated probe, and (grey) without a DNA extraction probe from 2-fold diluted plasma. ITO/DTO-MIL method: *KRAS* template concentration: 7.2×10^7 copies μL^{-1}, amount of $[ADIM^+]_2$-*KRAS* 2$[Br^-]$ DTO relative to DNA: 5:1, amount of $[AOIM^+]$-*KRAS* $[PF_6{}^-]$ ITO relative to DNA: 10:1, sample volume: 50 µL, MIL volume: 1 µL; extraction time: 10 min, desorption time: 4 min, desorption volume: 50 µL. Dynabeads M-270 Steptavidin magnetic beads conditions: *KRAS* template concentration: 7.2×10^7 copies μL^{-1}, concentration of biotinylated probe: 7.2×10^8 copies μL^{-1}, NaCl concentration: 25 mM, mass of magnetic beads: 10 µg; sample volume: 1.0 mL; extraction time: 10 min; agitation rate: 250 rpm; desorption time: 10 min; desorption volume: 20 µL.

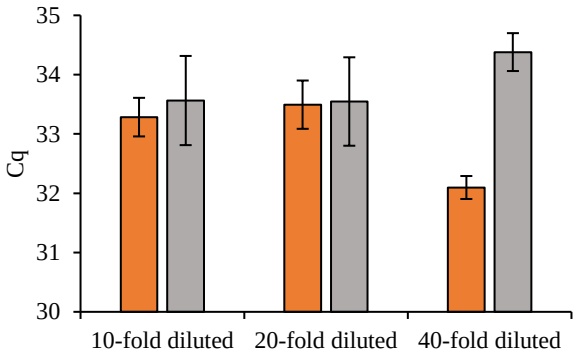

Figure B12. Target capture Cq values associated with the extraction of target *KRAS* from different concentrations of 10, 20, and 40-fold diluted whole blood using streptavidin-coated magnetic beads (orange) with and (grey) without a biotinylated probe. *KRAS* template concentration: 2×10^4 copies μL^{-1}, concentration of biotinylated probe: 332 fM, NaCl concentration: 25 mM, mass of magnetic beads: 10 µg; sample volume: 1.0 mL; extraction time: 10 min; agitation rate: 250 rpm; desorption time: 10 min; desorption volume: 20 µL.

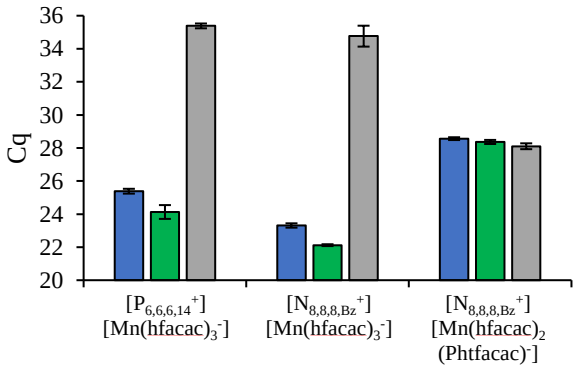

Figure B13. Target capture Cq values associated with the static extraction of *KRAS* using the (blue) DTO, (green) ITO, and (grey) without the probe from saline (154 mM). *KRAS* template concentration: 7.2×10^7 copies μL^{-1}, amount of $[ADIM^+]_2$-*KRAS* 2$[Br^-]$ DTO relative to DNA: 5:1, amount of $[AOIM^+]$-*KRAS* $[PF_6^-]$ ITO relative to DNA: 10:1, sample volume: 50 µL, MIL volume: 1 µL; extraction time: 10 min, desorption time: 4 min, desorption volume: 50 µL.

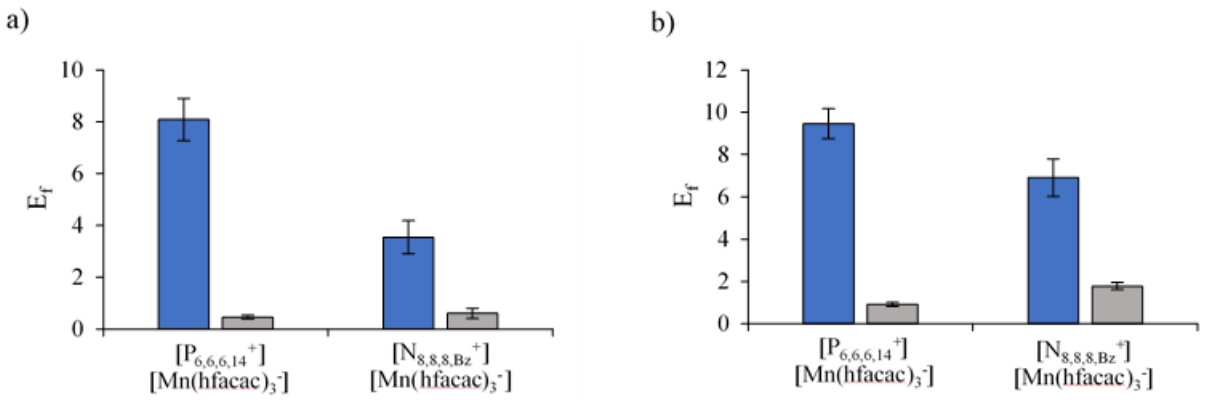

Figure B14. Enrichment factors (E_f) from the DLLME of (a) 2×10^3 and (b) 2×10^2 copies μL^{-1} *KRAS* using the (blue) DTO along with the extraction (grey) without any extraction probe from 10-fold diluted blood. $[P_{66614}^+][Mn(hfacac)_3^-]$ MIL conditions: amount of $[ADIM^+]$-*KRAS* $2[Br^-]$ DTO relative to DNA: 5:1, NaCl concentration: 25 mM, sample volume: 1.0 mL, MIL volume: 8 µL; extraction time: 3 min. $[N_{888Bz}^+][Mn(hfacac)_3^-]$ MIL conditions: amount of $[ADIM^+]_2$-*KRAS* $2[Br^-]$ DTO relative to DNA: 5:1, amount of $[ABzIM^+]$-*KRAS* $[Br^-]$ relative to DNA: 10:1, NaCl concentration: 25 mM, sample volume: 1.0 mL, MIL volume: 6 µL: extraction time: 1 min.

APPENDIX C. SUPPLEMENTAL INFORMATION ACCOMPANYING CHAPTER 4

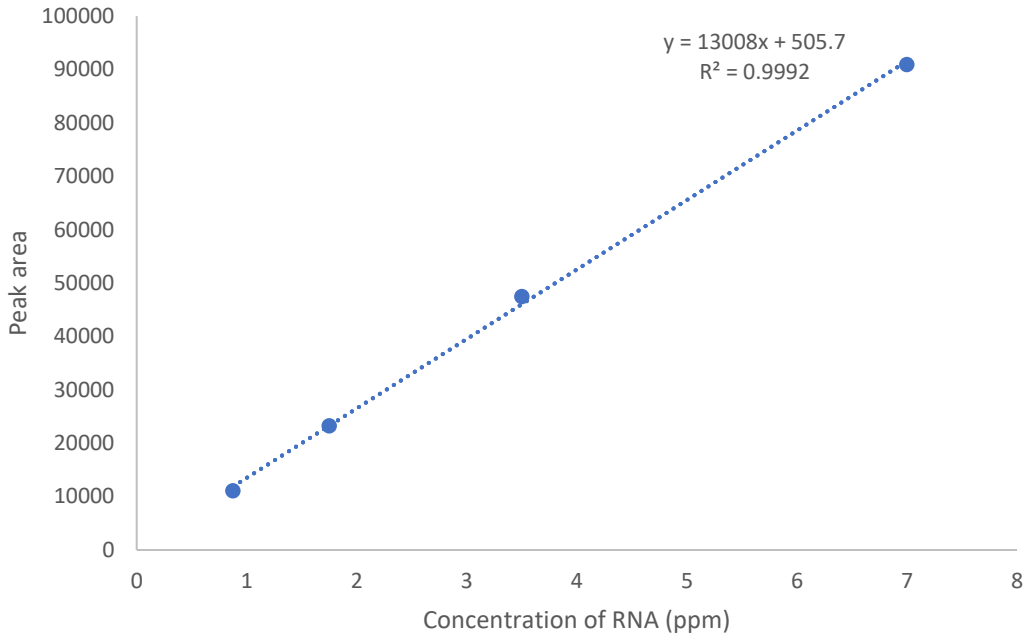

Intercept ± confidence limits	Slope ± confidence limits	Number of calibration levels	Linear concentration	Determination coefficient (R^2)	Standard deviation of the regression	Detection limit
506 ± 1073	13008 ± 266	3	0.875 ppm - 7 ppm	0.9992	590	0.19 ppm

Figure C1. Calibration curve of yeast total RNA in aqueous solution by anion-exchange HPLC.

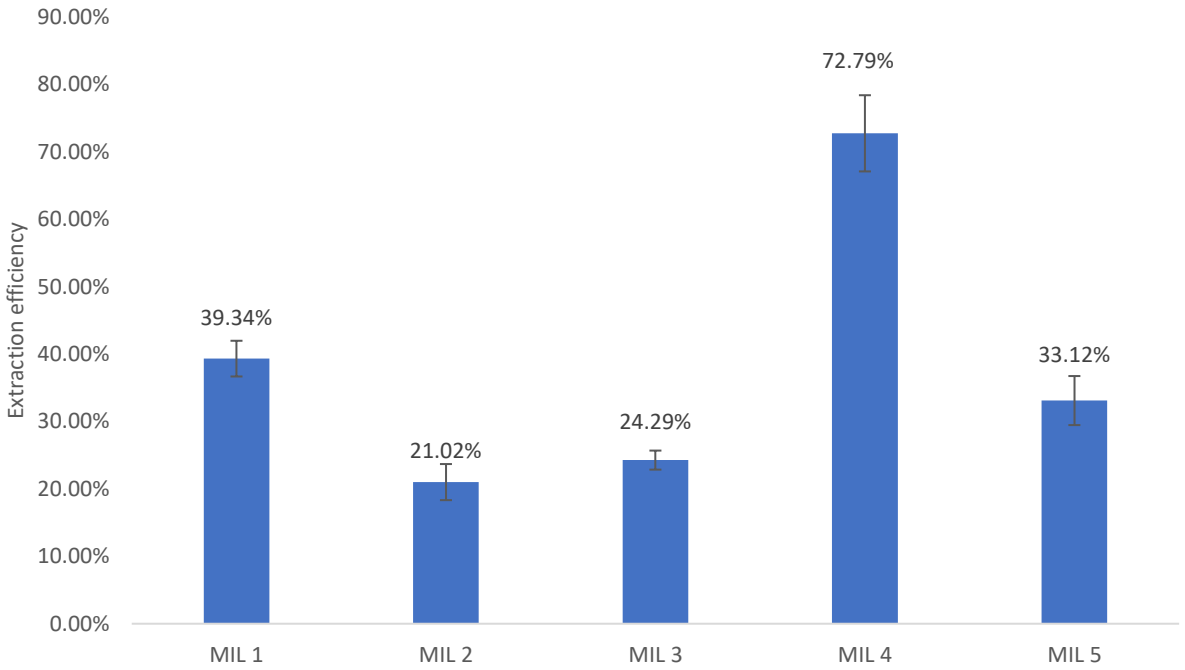

Figure C2. Extraction efficiency of yeast total RNA using different MILs. Number of replicates = 3. MIL **1**: 39.34% ± 2.65%, MIL **2**: 21.02% ± 2.68%, MIL **3**: 24.29% ± 1.41%, MIL **4**: 72.79% ± 5.66%, and MIL **5**: 33.12% ± 3.64%.

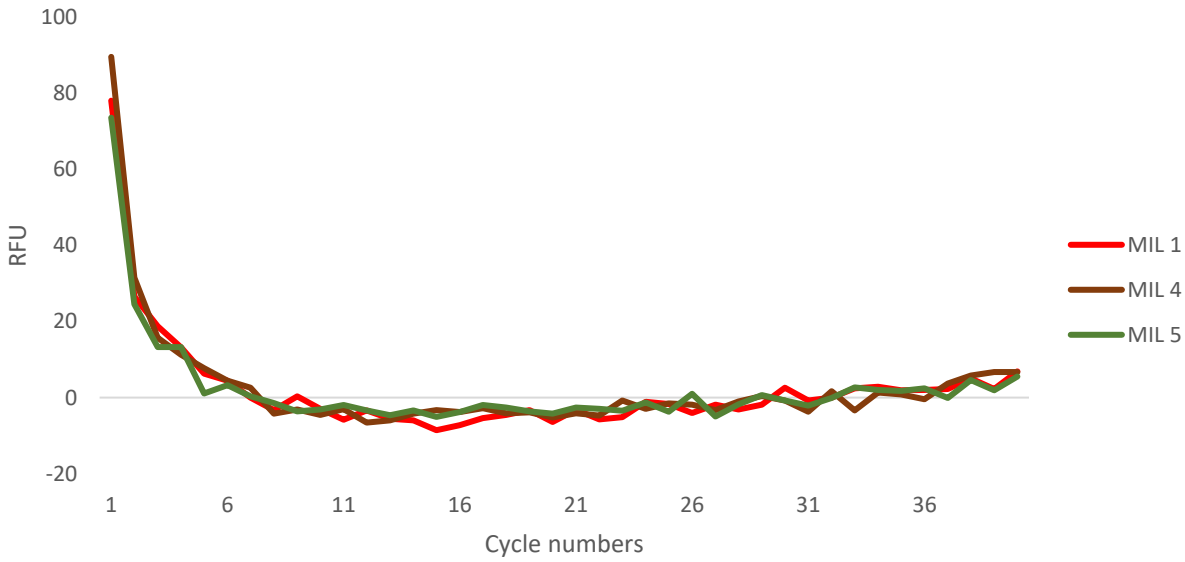

Figure C3. cDNA amplification following preservation of 500 ng of RNA by MIL **1** (red), MIL **4** (brown), and MIL **5** (green) for 24 hours. No amplification was detected in 40 cycles.

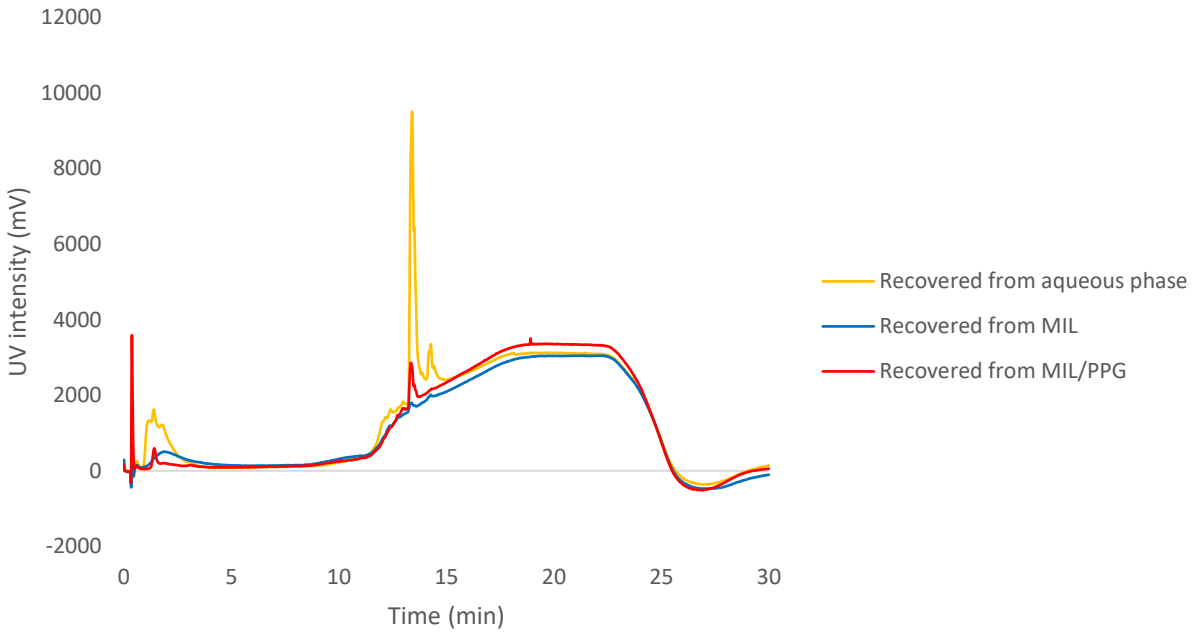

Figure C4. Recovery of 400 ng RNA from aqueous phase (yellow), MIL phase (blue), and MIL/PPG-2000 phase (red). RNA was precipitated by ethanol at -20 °C and resuspended in DEPC treated water before being analyzed by HPLC.

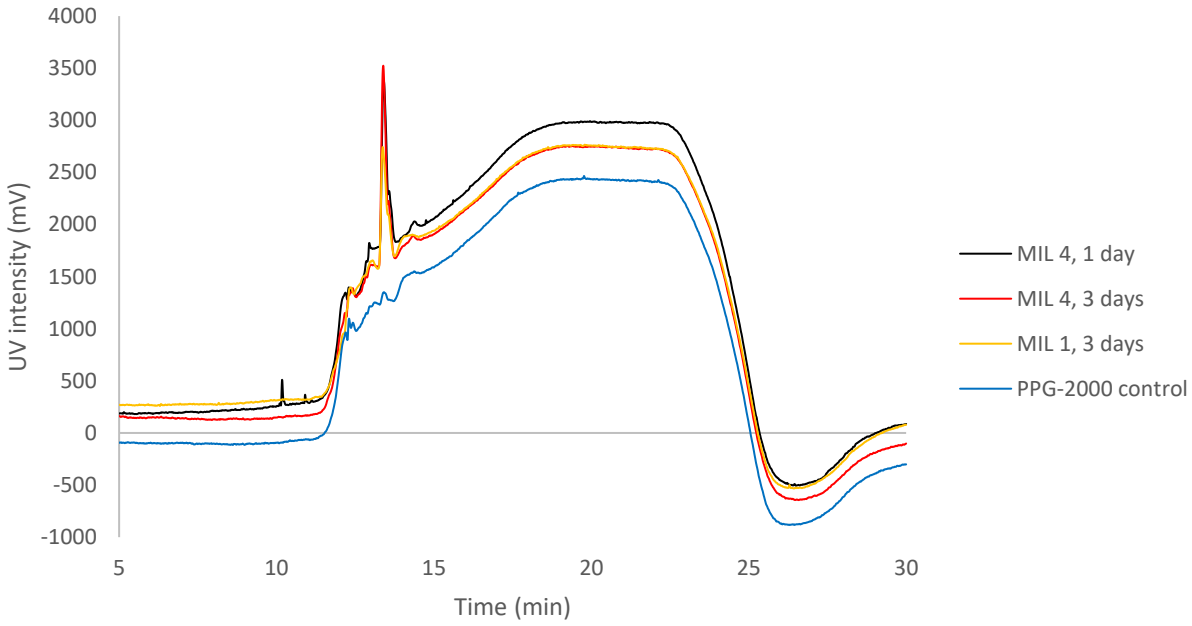

Figure C5. Recovery of 5 μg RNA from MIL **4**/PPG-2000 for 1 day (black), MIL **4**/PPG-2000 for 3 days (red), MIL **1**/PPG-2000 for 3 days (yellow), and PPG-2000 for 3 days (blue).

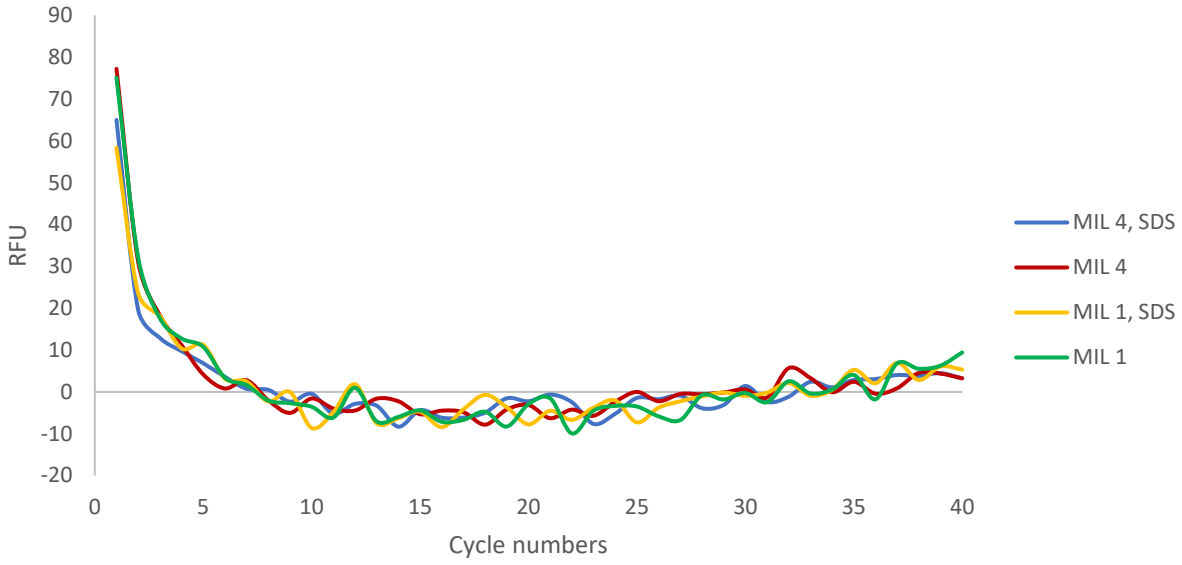

Figure C6. cDNA amplification following preservation of 2 µg of RNA with RNase A present for 1 hour. RNA in 0.1% SDS solution was preserved by MIL **4** (blue) and MIL **1** (yellow). RNA in water solution was preserved by MIL **4** (red) and MIL **1** (green). No amplification was detected in 40 cycles.

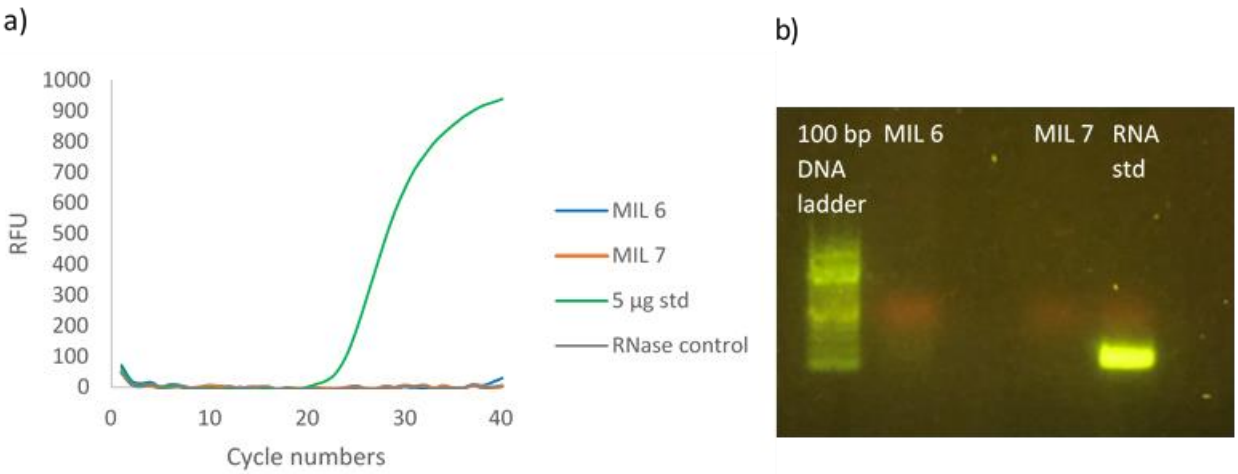

Figure C7. a) cDNA amplification following preservation of 5 µg of RNA with RNase A present for 2 hours. RNA was recovered from MIL **6**/PPG-2000 (blue), MIL **7**/PPG-2000 (orange), and water spiking with RNase A (gray). No amplification was detected in 40 cycles. cDNA amplification of 5 µg of RNA (green). b) Agarose gel electrophoresis of cDNA after amplification.

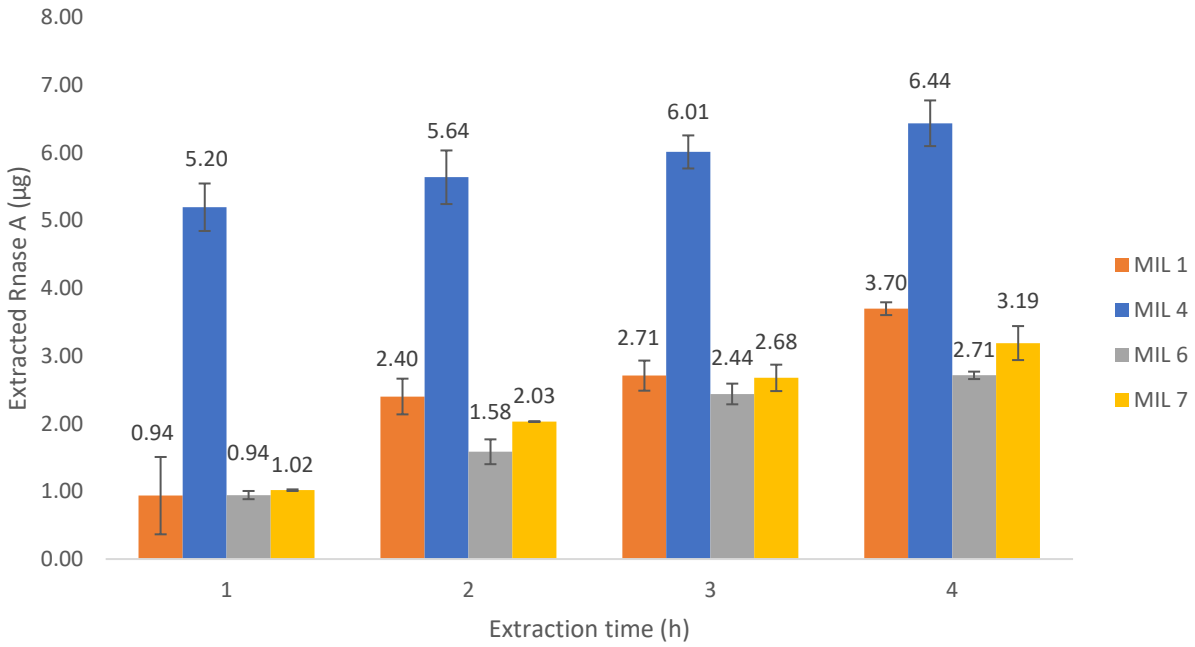

Figure C8. Static extraction of 24 µg RNase A using different MILs within 4 hours. Number of replicates = 3. The mass (µg) of RNase A was extracted by MIL **1** (orange), MIL **4** (blue), MIL **6** (gray), and MIL **7** (yellow) in 4 hours.